

Aus der II. Medizinische Klinik
der Medizinischen Fakultät Mannheim
(Direktor: Prof. Dr. med. Matthias Ebert)

PRRX1 expression and functions in hepatocellular carcinoma

Inauguraldissertation
zur Erlangung des Doctor scientiarum humanarum (Dr. sc. hum.)
der
Medizinischen Fakultät Mannheim
der Ruprecht-Karls-Universität
zu
Heidelberg

vorgelegt von
Weronika Piorońska

aus
Kościan, Polen
2021

Dekan: Prof. Dr. med. Sergij Goerd
Referent: Prof. Dr. rer. nat. Steven Dooley

TABLE OF CONTENTS

ABBREVIATIONS.....	1
1. INTRODUCTION	4
1.1 The Liver	4
1.1.1 The physiologic anatomy of the liver.....	4
1.1.2 Functions	5
1.2 Hepatocellular carcinoma (HCC).....	6
1.2.1 Etiology, risk factors and pathogenesis.....	6
1.2.1.1 Molecular pathogenesis/signatures of HCC.....	9
1.2.1.2 Alterations in metabolism.....	10
1.2.2 Diagnosis	11
1.2.3 Staging systems	12
1.2.4 Treatment	12
1.3 TGF-β signaling	13
1.3.1 TGF- β in liver disease.....	14
1.3.2 TGF- β in liver cancer	14
1.3.2.1 TGF- β and EMT.....	15
1.4 Paired related homeobox 1 (PRRX1)	16
1.4.1 General functions of <i>PRRX1</i>	17
1.4.2 <i>PRRX1</i> in cancer	17
1.4.3 <i>PRRX1</i> in liver cancer.....	18
2 AIMS OF THE STUDY	20
2.1 Regulation of <i>PRRX1</i>.....	20
2.2 Functions of <i>PRRX1</i>.....	20
3 MATERIALS AND METHODS	21
3.1 Materials.....	21
3.1.1 Equipment and consumables.....	21
3.1.2 Reagents	24
3.1.3 Buffers	27
3.1.4 Antibodies	28
3.1.5 Gene primer sequences used for qPCR	29

3.1.6	Bioinformatics platforms and analytical tools	31
3.2	Methods.....	32
3.2.1	Bioinformatics	32
3.2.1.1	Collection of liver cancer microarray datasets	32
3.2.1.2	Correlation of deregulated genes in HCC with <i>PRRX1</i>	32
3.2.1.3	Clinicopathological parameters.....	32
3.2.1.4	Pathway analyses and gene ontology	33
3.2.2	Cell Biology	33
3.2.2.1	Cell culture.....	33
3.2.2.2	Knockdown of <i>PRRX1</i>	34
3.2.2.3	Western blot	35
3.2.2.4	Migration scratch assay	35
3.2.2.5	Proliferation assay	36
3.2.2.6	Clonogenic assay	36
3.2.2.7	Apoptosis assay.....	37
3.2.2.8	Glucose consumption and lactate output.....	37
3.2.2.9	Analysis of metabolites in cells	38
3.2.2.10	ATP determination assay.....	39
3.2.3	Molecular Biology	40
3.2.3.1	RNA isolation and cDNA synthesis.....	40
3.2.3.2	Quantitative polymerase chain reaction.....	40
3.2.4	Statistical analyses	41
4	RESULTS.....	42
4.1	<i>PRRX1</i> expression in HCC.....	42
4.1.1	<i>PRRX1</i> is frequently upregulated in HCC	42
4.1.2	Expression patterns of <i>PRRX1</i> in HCC cell lines	43
4.1.3	Correlation of <i>PRRX1</i> with <i>TGF-β</i> isoforms and receptors	46
4.1.4	<i>TGF-β</i> regulates <i>PRRX1</i> expression	48
4.2	<i>PRRX1</i> functions in HCC	50
4.2.1	<i>In silico</i> analysis of <i>PRRX1</i> related genes	50
4.2.2	Correlation with clinicopathological variables.....	52
4.2.3	<i>ZEB1</i> and <i>ZEB2</i> as novel transcription factors related to <i>PRRX1</i>	53
4.2.4	Influence of <i>PRRX1</i> on migration and the expression of EMT markers in HCC	59

4.2.5	Cell proliferation.....	60
4.2.6	Cell clonogenicity.....	62
4.2.7	<i>PRRX1</i> and cell death.....	62
4.3	<i>PRRX1</i> and liver cancer cell metabolism	63
4.3.1	Inverse correlation with metabolic pathways.....	63
4.3.2	<i>PRRX1</i> , glycolysis and the TCA cycle	67
4.3.2.1	Gene expression level	67
4.3.2.2	Role in glucose consumption and lactate output	73
4.3.2.3	Alteration of metabolites in sugar metabolism and the TCA cycle	74
4.3.2.4	Alterations of ATP level	78
4.3.3	<i>PRRX1</i> and fatty acid metabolism	79
4.3.3.1	Gene expression level	79
4.3.3.2	Total fatty acid / metabolites	80
5	DISCUSSION	84
5.1	<i>PRRX1</i> expression in HCC.....	84
5.2	TGF- β as regulator of <i>PRRX1</i> expression	85
5.3	The functions of <i>PRRX1</i> in HCC.....	85
6	SUMMARY	90
7	REFERENCES.....	91
8	RESUME	103
9	ACKNOWLEDGEMENTS	106

ABBREVIATIONS

ACACA/B	acetyl-CoA carboxylase alpha/beta
ACOX2	acyl-CoA oxidase 2
ACSL5	acyl-CoA synthetase long chain family member 5
AFP	alpha fetoprotein
APS	ammonium persulfate
ATP	adenosine triphosphate
BCLC	Barcelona clinic liver cancer
BSA	bovine serum albumin
CCC	cholangiocarcinoma
CDH1/2	cadherin 1/2
CPT2	carnitine palmitoyltransferase 2
DAVID	The Database for Annotation, Visualization and Integrated Discovery
DMEM	Dulbecco's modified eagle medium
DMSO	dimethyl sulfoxide
dNTP	deoxynucleoside triphosphates
DPBS	Dulbecco's phosphate buffered saline
ECM	extracellular matrix
EGF	epithelial growth factor
EMT	epithelial-to-mesenchymal transition
FASN	fatty acid synthase
FBS	fetal bovine serum
FH	fumarate hydratase
GAPDH	glyceraldehyde 3-phosphate dehydrogenase
GC/MS	Gas chromatography/Mass spectrometry
GLS1	glutaminase 1
GLUT1/2	glucose transporter 1/2
GO	gene ontology
GOT1/2	glutamic-oxaloacetic transaminases 1/2
GPT1/2	glutamate-pyruvate transaminases 1/2
GSEA	gene set enrichment analysis
HBSS	Hank's balanced saltsSolution
HBV	hepatitis B virus

HCC	hepatocellular carcinoma
HCV	hepatitis C virus
HGF	hepatocyte growth factor
HK1/2	hexokinase 1/2
HSC	hepatic stellate cells
IDH3A/B	isocitrate dehydrogenases 3A/B
IGF	insulin like growth factor
KEGG	Kyoto Encyclopedia of Genes and Genomes
LDHA/B	lactate dehydrogenase A/B
MDH1	malate dehydrogenase 1
mRNA	messenger RNA
MTT	thiazolyl blue tetrazolium bromide
NAFLD	non-alcoholic fatty liver disease
NASH	non-alcoholic steatohepatitis
NCBI GEO	National Center for Biotechnology Information Gene Expression Omnibus
o/n	overnight
OGDH	oxoglutarate dehydrogenase
OS	overall survival
PCK1	phosphoenolpyruvate carboxykinase 1
PDHX	pyruvate dehydrogenase complex
PPAR γ	peroxisome proliferator activated receptor gamma
PPIA	peptidylprolyl isomerase a
PRRX1a/b	paired-related homeobox 1 a/b
qPCR	quantitative polymerase chain reaction
SDHA/B/C/D	succinate dehydrogenase complex flavoprotein subunits A/B/C/D
SDS	sodium dodecyl sulfate
siRNA	small interfering RNA
SLC1A5	transmembrane sodium
SNAI1/2	snail family transcriptional repressor 1/2
STAT	signal transducer and activator of transcription
SUCLG1/2	uccinate-CoA ligase GDP/ADP-forming subunit 1/2
TBS	tris-buffered saline
TBST	tris-buffered saline with Tween 20
TCA	tricarboxylic acid cycle

TCGA	The Cancer Genome Atlas
TEMED	N,N,N',N'-tetramethylethylenediamine
TGF- β 1/2/3	transforming growth factor beta receptor 1/2/3
TGFBR1/2/3	transforming growth factor beta 1/2/4
TNM	tumour-node-metastasis classification
TP53	tumor protein P53
TWIST1/2	twist family BHLH transcription factor 1/2
VEGF	vascular endothelial growth factor
VIM	vimentin
WB	western blot
ZEB1/2	zinc finger E-box-binding homeobox 1/2

1. INTRODUCTION

1.1 The Liver

The liver is the largest internal organ in the human body with a width of about 15 cm. Depending on gender and body size, the weight of a liver ranges between 1.3 to 1.7 kg, which also makes it the heaviest internal organ. This organ is located in the right part of the abdomen (Abdel-Misih & Bloomston, 2010) and has a plethora of essential functions (Trefts, Gannon, & Wasserman, 2017), such as:

- the metabolism of fats, carbohydrates and proteins
- synthesis of plasma proteins (e.g., albumin and clotting factors)
- storage of glucose, especially in the form of glycogen and fats
- metabolism of vitamins and minerals
- bile production and excretion
- detoxification and removal of xenobiotics

The mentioned crucial tasks of the liver can be efficiently accomplished due to its unique architecture described in the following section.

1.1.1 The physiologic anatomy of the liver

The liver in healthy state is a reddish-brown, wedge-shaped organ. It is divided into two lobes, a large right lobe and a small left lobe by the attachment of the falciform ligament. Two further lobes are located on the visceral surface of liver. The liver is connected to two blood vessels termed the hepatic artery and the portal vein. The hepatic artery delivers oxygenized blood from the aorta, while the portal vein delivers nutrient-rich blood from the digestive tract, spleen and pancreas. The lobes of the liver are built up by lobules that are shaped like a hexagonal plate and consist of the portal triad, hepatocytes and a central vein, which is located in the centre of the lobule (Trefts et al., 2017). In the periphery of the lobules are ducts for bile. The external fibrous layer that envelopes the liver lobules is called Glisson's capsule. At the level of the liver lobules, the hepatic artery and the portal vein divide into small capillaries called the liver sinusoids. These sinusoids run parallel to the hepatocytes, the main cell type in the liver, and culminate into the central vein. Besides the hepatocytes, which constitute the main cell population, the liver also consist of several other cell types, including the cholangiocytes, Kupffer cells (also known as stellate macrophages), hepatic stellate

cells (HSCs), and liver sinusoidal endothelial cells (Pineiro-Carrero & Pineiro, 2004). The cholangiocytes are the second group of the epithelial cell population of the liver and are key linings of the bile duct lumen. The crucial physiologic function of cholangiocytes is modification of hepatic canalicular bile being transported along the biliary tree (Maroni et al., 2015). Kupffer cells, which are the resident macrophage population of the liver, recognize multiple stimuli from pathogens and trigger subsequent immune responses. HSCs are located inside the space of Disse (a small area between the sinusoids and hepatocytes) in the liver and are a cell population that can exist in two states, in a quiescent or in an activated state (Shang, Hosseini, Liu, Kisseleva, & Brenner, 2018). HSCs store lipid droplets and the majority of vitamin A in the human body in the quiescent state (Pineiro-Carrero & Pineiro, 2004). Liver sinusoidal endothelial cells play important roles in the liver physiology. Those cells mediate the filtration and allow the liver to have a scavenger functions. Moreover, those cells have immunological functions (Shetty, Lalor, & Adams, 2018). Thus, each of these cell types plays special roles that together regulate liver function at multiple levels and the structure of the liver in general, which enables the liver to accomplish all regulatory and homeostatic functions.

1.1.2 Functions

The liver is a critical center for many physiological processes in the human organism, e.g. metabolic and hormonal homeostasis, coagulation, detoxification, maintains homeostasis of fats, proteins, and carbohydrates, stores glucose in the form of glycogen as well as fats, proteins, vitamins, and minerals. Liver is responsible for gluconeogenesis, using distinct amino acids, lactate, or glycerol to generate glucose. The glucose then can be stored in form of glycogen, and upon energy demand, the liver use glycogenolysis process to releases glucose into the blood (Trefts et al., 2017). The liver is also responsible for the homeostasis of lipids and cholesterol, thus oxidizes lipids, package excess lipids for secretion and storage in adipose tissue. Moreover, the liver is a major coordinator of the metabolism of proteins and amino acids. Albumin is a major protein produced by the liver that plays an important role in regulating blood osmotic effects and hormone transport. The liver also produces ferritin, which is an iron storage protein particularly in the hepatocytes. In addition, the liver is involved in blood coagulation processes, as it is a producer of coagulation factors. It also produces bile salts, which supports the secretion of non-polar compounds, fatty acid degradation and

detoxification. The liver also acts as a 'gland' as it synthesizes the hormone angiotensinogen as part of a complex system that regulates sodium and potassium levels in the kidneys and in blood pressure control. Further, the liver participate in the production of thrombopoietin (Jelkmann, 2001). The liver also plays a large role in biotransformation of toxic compounds and xenobiotics (Trefts et al., 2017). These extensive physiologic roles make the liver one of the most important organs in the human body.

1.2 Hepatocellular carcinoma (HCC)

Liver cancer is a common and deadly cancer. The most prevalent type of liver cancer is hepatocellular carcinoma (HCC), which derives from transformed hepatocytes (Sia, Villanueva, Friedman, & Llovet, 2017). The term liver cancer comprises also cholangiocarcinoma (CCC), which originate from cholangiocytes, and secondary tumours which spread as metastasis into the liver (Sia, Jiao, et al., 2017). The first two groups are thus classified as primary liver cancer and the metastasis group secondary liver cancer.

Worldwide, liver cancer is the fourth most common cause of death related to cancer and ranks sixth in terms of the number of incidents (International Agency for Research on Cancer, World Health Organization: Cancer today (<https://gco.iarc.fr/today/home>)). Notably, there is a difference in the number of cases in relation to gender. More than 2 times higher incidence and mortality of liver cancer are observed in men than in women patients all over the world. The World Health Organization (WHO) estimates that by 2030, the number of incident liver cancer cases for both males and females will be more than a million of patients. Beyond sex, there are also differences in the number of liver cancer cases regarding geographical zones. Most cases are recorded in South East Asia and North West Africa. In these areas, liver cancer leads also to higher mortality than in the other parts of the world. To better understand the complexity of HCC, in following chapters are presented general information about its etiology, risk factors, as well as diagnosis and treatment.

1.2.1 Etiology, risk factors and pathogenesis

Most cases of HCC occur in Asia (particularly in East Asia, for example in Mongolia, Korea, Japan, and in China) have a very high incidence (more than 20 cases per 100 000 population) (Gomaa, Khan, Toledano, Waked, & Taylor-Robinson, 2008). Another

area of concern is sub-Saharan Africa (the western part of Africa and the Republic of Mozambique) (Gomaa et al., 2008). In contrast, a relatively low incidence (less than 5 cases per 10 000) is found in Canada, the United States and in Scandinavia (Gomaa et al., 2008).

The major risk factors of HCC occur in patients with underlying liver disease, mostly as a result of infection with hepatitis B or C virus (HBV or HCV), addiction to alcohol, aflatoxin B₁, non-alcoholic fatty liver disease (NAFLD) as well as non-alcoholic steatohepatitis (NASH) (Sanyal et al., 2010), (Mittal & El-Serag, 2013), (Refolo, Messa, Guerra, Carr, & D'Alessandro, 2020), (Michelotti, Machado, & Diehl, 2013). Besides, sex, age and smoking are also included as risk (co-)factors for HCC development (Feitelson et al., 2002), (Koh et al., 2011), (Lauby-Secretan et al., 2016). Infection with HBV and HCV virus are the most dominant ground of HCC, whereas the key predisposing factors are chronic inflammation and necrosis resulting from those viral infections. Noteworthy, the main etiology of HCC differs between parts of the Worlds. HBV infection is the major reason of HCC in China. In Western countries and Japan HCV and high alcohol consumption are major etiologies of HCC. In HBV-infected patients, the viral load triggers a massive inflammatory response, which in turn leads to hepatocyte death, influx of immune cells, fibrosis, cirrhosis and HCC development (Pazgan-Simon et al., 2018). HCV-related HCC is often in the company of steatohepatitis, and associated to inflammation. HCV proteins conflict with host lipid metabolism leading to lipid peroxidation and activation of inflammatory cascade of inflammatory cytokines, e.g. tumor necrosis factor α and IL-1, which are closely involved in the development of steatohepatitis, and later HCC (Vescovo, Refolo, Vitagliano, Fimia, & Piacentini, 2016). Furthermore, ethanol metabolites, acetaldehyde and many reactive oxygen species, produced by the activity of alcohol dehydrogenase and cytochrome P450 2E1 induce chronic oxidative damage and further chronic process of inflammation, leading to liver cirrhosis and disease progression (Ghouri, Mian, & Rowe, 2017). Further, aflatoxin B₁ is a mycotoxin that is produced by mold fungus, and after consumption leads to liver inflammation, which as chronic inflammation causes liver fibrosis, then cirrhosis and finally leads to HCC. Aflatoxin B₁ was described as a main etiology of HCC in African countries, where impure nourishment is consumed very often (Feitelson et al., 2002). Another rising cause of severe liver disease is the agglomeration of fat in the liver with structural disorganization called Non-alcoholic fatty liver disease (NAFLD). This accumulation of

the fat is strongly associated with adiposity and the metabolic syndrome. A subset of patients with NAFLD develop NASH, a more dangerous form of liver injury with significant inflammation. Those patients might develop cirrhosis and liver cancer (Michelotti et al., 2013). Noteworthy, it is well documented that most cases of HCC are related to liver cirrhosis irrespective of the etiology (Fattovich, Stroffolini, Zagni, & Donato, 2004), (Stickel, 2015), (M. N. Kim et al., 2015), (Walker et al., 2016). The 5-year cumulative risk of developing HCC for patients with cirrhosis is very high and ranges between 5% and 30% of the cases (Walker et al., 2016). In cirrhotic livers, metabolic and oxidative injury causes a detrimental negative feedback via inflammation, necrosis, repeated balancing regeneration and increased turnover of hepatocytes over a long period of time leads to initiation of genetic mutations (Jhunjhunwala et al., 2014).

The pathogenesis of HCC is a process consisting many steps involving the progressive accumulation of molecular changes. Viral infections and other known risk factors lead to cell damage, which induces an inflammatory response that is chronic. Chronic hepatitis, fibrosis associated with hepatitis and then cirrhosis are the main reasons for malignant cell transformation in the liver (Drucker et al., 2006). In the process of development of liver fibrosis and liver cirrhosis, HSCs play a stimulating task following their activation and transition into myofibroblasts, which are important for control the production and deposition of extracellular matrix (Gressner, Weiskirchen, Breitkopf, & Dooley, 2002). However, it is the interaction of the different cell types by the actions of an excess of growth factors and mediators that work pro-inflammations, including cytokines and reactive oxygen species. The pathophysiology leading to carcinogenesis in the liver is a not balanced and long process of regeneration due to damage (Drucker et al., 2006). It is followed by the growth of a particular tumour microenvironment that can supply sufficient amounts of oxygen and distinct nutrients, e.g. by the initiation of an angiogenic program. Additionally, molecular alterations provide dysplastic cells with invasive, proliferative and survival benefits and terminate the transition of cells to cancer HCC cells.

The sequence of events, changes of the phenotypes of the cells, synthesis as well as genetic programs activated at the stage of pre-cancer, point to their important role in the promoting of HCC (Dooley, Weng, & Mertens, 2009).

1.2.1.1 Molecular pathogenesis/signatures of HCC

There is an increasing interest in molecular mechanisms that are involved in the development of HCC for improvement of novel targeted therapies. The latest achievements in molecular profiling have highlighted the importance of deregulation of gene expression in HCC carcinogenesis (Llovet, Villanueva, Lachenmayer, & Finn, 2015). Multiple signaling pathways were observed to be dysregulated as answer to viral infection in HCC. HCC cells accumulate alterations in DNA (mutations and chromosomal aberrations). HCC is a very heterogenic cancer entity. Thus, no unique and simple pattern of mutations is found, although reports show that the most frequent genetic alterations are in the *TERT* promoter, found in about 60% of cases (Zucman-Rossi, Villanueva, Nault, & Llovet, 2015), (Schulze, Nault, & Villanueva, 2016). Further, several other potential molecular signatures of HCC have been identified, containing mutated genes affecting the cell cycle (tumor protein P53 (*TP53*), in ~ 30% of cases) and WNT signaling (catenin beta 1 (*CTNNB1*), in ~ 30%) (Villanueva, 2019). Several studies suggest that modification in several molecular signaling pathways are essential for carcinogenesis (Dimri & Satyanarayana, 2020). The pathways include receptor tyrosine pathways, phosphatidylinositol 3-kinase (PI3K)/AKT/mammalian target of rapamycin (mTOR), Ras mitogen-activated protein kinase (Ras/Raf/MAPK), Wnt/ β -catenin, and Janus kinase - signal transducer activator of transcription factor (JAK/STAT). Besides these signaling molecules, induction of HCC and progression are notably impacted by several growth factors, including vascular endothelial growth factor (VEGF), hepatocyte growth factor (HGF), epithelial growth factor (EGF) as well as insulin-like growth factor (IGF). The liver as a highly vascularized organ relies on efficient angiogenesis and in HCC, this fact is crucial for growing of the tumour, vascular invasion and tumour metastasis. Thus, upregulation of VEGF and its receptor is observed in HCC (Poon et al., 2004). HGF promotes proliferation of the cancer cells, their migration, invasion and survival as well as grants immunity to therapy (Matsumoto & Nakamura, 1996). Further, mutation in EGF receptor has a meaningful role in the development of blood vessels and proliferation of the tumour. Moreover, the IGF signaling pathway is also frequently upregulated (Lund, Schubert, Niketeghad, & Schirmacher, 2004). In addition, there are studies that identified modifications in expression of several metabolic signatures and in the levels of metabolites, which

provide evidence of altered metabolism in HCC (Pope et al., 2019), (De Matteis et al., 2018), (Ferrarini et al., 2019).

1.2.1.2 Alterations in metabolism

In the 1920s, Otto Warburg and his colleagues reported that cancer cells taking up enormous amounts of glucose compared to what they observed in the surrounding tissue, choosing glycolytic pathway with lactate formation even in the presence of oxygen (Warburg, 1956). This observation was studied several years and finally changes in metabolism became one of the hallmarks of cancer. The cancer cells use mainly the aerobic glycolytic pathway to generate adenosine triphosphate (ATP) instead of using more effective oxidative phosphorylation (Liberti & Locasale, 2016). In cancer cells are many metabolic changes, dysregulation of glycolytic pathway is only one of them (Hanahan & Weinberg, 2011). Although our knowledge of the metabolic changes in HCC is currently at a rather early stage, patterns of deregulated metabolic networks have already been reported. Given that in glycolysis tumour cells produce ATP very fast, but not that productive as by using aerobic process, the cells have to consume high level of glucose to keep needed level of energy (Cairns, Harris, & Mak, 2011). To assess alterations in glucose metabolism in HCC, its uptake in the liver has been investigated. The expression of glucose transporters GLUT1 (Amann et al., 2009), (Sun et al., 2016) and GLUT2 (Paudyal et al., 2008), (Y. H. Kim et al., 2017), is frequently increased. Moreover, high expression levels of GLUT1 correlate with bad prognosis (Sun et al., 2016). In HCC, glucose-6-phosphate levels are increased as well as the responsible enzyme hexokinase 2 (HK2) which mediates the conversion from glucose (Q. Huang et al., 2013), (J. W. Kim, Gao, Liu, Semenza, & Dang, 2007). In the last step of glycolytic pathway, pyruvate is formed which can be converted to lactate by upregulated in HCC lactate dehydrogenase (LDH). Pyruvate can enter the tricarboxylic acid cycle (TCA) for aerobic oxidation. Levels of intermediate metabolites of the TCA cycle, such as fumarate and malate are found to be reduced in HCC (Budhu et al., 2013), (Q. Huang et al., 2013). The conversion of succinate into fumarate is catalysed by succinate dehydrogenase (SDH), a huge enzyme built of four subunits (SDHA, SDHB, SDHC, SDHD). SDH and fumarate hydratase are considered tumour suppressors (King, Selak, & Gottlieb, 2006), (Pollard et al., 2005). In another study it was reported that the expression of *SDHB* was reduced in HCC and associated with

increased proliferation, migration, tumour growth and metastasis as well as a switch from aerobic respiration to glycolysis was monitored (Tseng et al., 2018).

Then, a modulation of the urea cycle also possesses impact on cellular phenotypes and correlate with the repression of invasion and metastasis markers (extracellular matrix protein 2 (*ECM2*) and matrix metalloproteinase 9 (*MMP9*)) (Nwosu et al., 2017), (Chaerkady et al., 2008). Furthermore, liver tumours depend on the amino acid glutamine. Accordingly, the glutamine transporter *SLC1A5* (Sun et al., 2016) and glutamine synthetase (*GLS1*) (Di Tommaso et al., 2007) were found upregulated. Glutamine is important for cell proliferation (involved in synthesis processes, generating alpha-ketoglutarate in the TCA cycle) (Zaidi et al., 2013). One of the features of cancer metabolism is the deregulation of the pathways that control fatty acids biosynthesis (Zaidi et al., 2013). Thus, the tumour cells by proliferation process are able to form lipid membranes and can produce enough energy that they need. It was reported, that upregulation of fatty acid synthase (*FASN*) influenced growing of cancer cells, production of lipids and reduced cell death processes (Calvisi et al., 2011).

In conclusion, HCCs show several alteration in metabolism processes. A detailed understanding of these changes and factors that influence those alterations could lead to improved understanding of events that promote disease progression.

1.2.2 Diagnosis

Liver cancer can often arise and grow for a long time being unnoticeable, because it often develops without giving symptoms. This property leads to late diagnosis, when no curative treatment is possible (Feitelson et al., 2002). However, early diagnosis of HCC is important to increase chances for curative treatment. Cirrhosis is a major risk factor for HCC, but mostly is asymptomatic, thus, people at risk with the presence of clinical symptoms of decompensated cirrhosis (e.g. hepatic encephalopathy) connected with non-specific symptoms of liver diseases (e.g. loss of appetite and weight) (Tsochatzis, Bosch, & Burroughs, 2014) may suggest an underlying HCC. Nevertheless, HCC often gives no symptoms and is therefore diagnosed late, which is accompanied by a high risk of mortality. HCC nodules can be detected computed tomography if they are larger than 1 cm in diameter. For nodules with an inconclusive pattern from imaging the diagnosis relies on biopsy (Villanueva, 2019). Moreover, biomarkers can help in the early detection of HCC although not many have been

established. Current and applied biomarkers include high serum levels of alpha fetoprotein (AFP) and lectin-bound isoform of AFP (AFP-L3) (Villanueva et al., 2011).

1.2.3 Staging systems

Given that cirrhosis is risk factor for the development of HCC, prognosis for the patients depend also on the degree of their liver dysfunction. Thus, staging becomes a key strategy to stratify patients and to determine treatment schedules. In the case of solid tumours in the liver, staging is performed during surgery. The samples are analyzed by pathology experts by using the tumour-node-metastasis (TNM) classification (Marrero et al., 2018). The TNM classification is used to evaluate a three parameters: the extent of the primary tumour (T) as well as if the lymph node are involve (N) and/or the presence of extrahepatic metastasis (M) (Shindoh & Vauthey, 2014). However, the TNM staging system misses two important parameters, namely the degree of liver dysfunction and patient's general condition, which has to be taken to account when planning the treatments.

Moreover, Barcelona clinic liver cancer classification (BCLC) is often used in medical practice. This staging includes five stages, namely 0, A, B, C, D (from very early to advanced HCC) (Kinoshita et al., 2015). Furthermore, they are some optional staging systems that have been suggested, e.g., the Okuda staging system, the Cancer of the Liver Italian Program, the Japan Integrated Staging, the Hong Kong Liver Cancer classification, among others (reviewed in (Kinoshita et al., 2015)).

1.2.4 Treatment

The experts recommend resection of the liver, transplantation and ablation when the patients are diagnosed with early-stage HCC (Roayaie et al., 2015). Resection is correlated with survival rates above 60% at 5 years, but still, ~70% of these patients show tumour recurrence at 5 years (Ishizawa et al., 2008). Meanwhile, patients with diagnosed intermediate stage of HCC are suited for radiofrequency ablation and transarterial chemoembolization, which lead to the local destruction of liver tissue, with focus on the cancerous areas (Bruix & Colombo, 2014). Then, for patients with advanced stage, sorafenib is recommended. Sorafenib is multikinase inhibitor and was the first systemic drug approved by the Food and Drug Administration for the first line therapy of advanced HCC patients (Llovet et al., 2008). However, other compounds are investigated as potential new drugs for HCC and after Sorafenib, other multiple

kinase inhibitors received Food and Drug Administration approval for the cure of HCC - lenvatinib (Kudo et al., 2018) and regorafenib as second-line treatment with sorafenib (Bruix et al., 2017). Moreover, ongoing phase 3 trials are testing immune-based therapies which inspire confidence to be effective in the treatment of HCC (Villanueva, 2019). In end stage HCC is recommended best supportive care to relieve patients suffering (Pons, Varela, & Llovet, 2005).

1.3 TGF- β signaling

The transforming growth factor beta (TGF- β) superfamily is a numerous family of cytokines, which include a transforming growth factor beta family and other families and factors (e.g., bone morphogenetic proteins, activins, inhibins, Müllerian inhibiting substance, left-right determination factor (Lefty), and nodal growth differentiation factor (Javelaud & Mauviel, 2004), (Heldin, Landstrom, & Moustakas, 2009). TGF- β have to be released and activated before it can bind to its related transmembrane receptors (Barton et al., 1988). There are a total of seven type one receptors (ALK1 to ALK7) and five type two receptors (T β RII, ActRII, ActRIIB, BMPRII and AMHRII) for TGF- β family cytokines (Yue & Mulder, 2001). Type I and II receptors are needed upon ligand binding for signal transmission into the cells. Among the TGF- β superfamily cytokines, TGF- β is the most extensively studied (Moses, Roberts, & Derynck, 2016). TGF- β exists as three isoforms, TGF- β 1 to 3 (TGF- β 1 is the most abundant isoform). TGF- β acts through classical canonical signaling as well as by crosstalk with other signaling pathways via non-canonical signaling. Canonical signaling pathway of the TGF- β superfamily depends on SMADs. The SMAD family includes 5 receptors (R)-SMADs, 1 universal signaling partner (SMAD4) and 2 inhibitors (SMAD6-7). (Heldin & Moustakas, 2012). The canonical TGF- β signaling pathway is initiated upon binding of the dimers to the type II receptor, which is then activated by autophosphorylation and incurs the type I receptor ALK-5. As next, phosphorylation activates this receptor and active ligand receptor complexes affect R-SMAD2 and R-SMAD3. R-SMADs are activated through C-terminal phosphorylation and subsequently can form complexes with the signaling partner SMAD4, thereby facilitating transcriptional regulation of target genes in conjunction with other co-transcription factors after having shuttled into the nucleus (Meindl-Beinker, Matsuzaki, & Dooley, 2012). Besides this classical canonical signaling pathway, TGF- β may transiently signal by using the type I receptor ALK-1 in some cell types (inclusive the cells in the liver, hepatic stellate cells and

hepatocytes). This pathway leads to regulation of other TGF- β regulated genes (Meindl-Beinker et al., 2012). Moreover, TGF- β is able to modulate a different pathways without involvement of SMADs. Frequently, TGF- β activates the pathway, which signals influence cell survival (MAPK pathway), or activates signals connected to the stress situation in the cells (c-Jun N-terminal kinase) (Lee et al., 2007). Hartsough and Mulder found activation of ERK through MAPK pathway by TGF- β cytokine in epithelial cells (Hartsough & Mulder, 1995) (Hartsough & Mulder, 1995) and it participates in epithelial-to-mesenchymal transition (EMT) induction (Xie et al., 2004). Phosphatidylinositide 3-kinases (PI3K)/Akt signaling also belong to non-canonical pathway used by TGF- β , which show that TGF- β mediates survival signaling as well as EMT in epithelial cells (Bakin, Tomlinson, Bhowmick, Moses, & Arteaga, 2000) and have impact on proliferation in mesenchymal cells (Wilkes et al., 2005). TGF- β signaling is mostly operated by canonical pathway. Nevertheless, TGF- β influences non-canonical pathways, hence create a more complicated picture and the integration of signaling events is responsible for cell and context dependent TGF- β coordinated cellular phenotypes.

1.3.1 TGF- β in liver disease

TGF- β is upregulated in almost all chronic liver diseases, e.g. in hepatitis, fibrosis of the liver, liver cirrhosis and liver cancer (Dzieran et al., 2013), (Fabregat et al., 2016). In hepatocytes that are under metabolic stress, TGF- β signaling will mediate to their death and accumulation of the lipids, thus, leading to initiation of nonalcoholic steatohepatitis development. (Yang et al., 2014). TGF- β is also identified as a profibrogenic cytokine in view of its role in HSC activation and as it acts as promoter synthesis of extracellular matrix (Dewidar, Meyer, Dooley, & Meindl-Beinker, 2019). Thus, TGF- β influences the progression of most liver diseases.

1.3.2 TGF- β in liver cancer

Depending on cell type and disease stage, TGF- β plays a dual role by acting as either a suppressor or promoter of disease progression (Lebrun, 2012). This duality of function emphasizes the need to understand TGF- β signaling in the details. A functional genomic study suggested that the early TGF- β genes (e.g., BAG3, BTG1, IGFBP3) are connected to suppression of the tumour by TGF- β , this includes arrest of the cell cycle and cell death, while the late TGF- β targets (e.g., VIM, CDH1, SNAI) are essential to advancement of the cancer, being linked with an overall poor prognosis in

HCC patients (Tu, Huang, Huang, Luo, & Yan, 2019). In premalignant epithelial cells, TGF- β suppresses tumorigenesis. Nevertheless, the cancer cells can use TGF- β to promote cell differentiation into an invasive phenotype by losing its tumour-suppressive function. Afterwards, the cells can disseminate from their epithelial layers and form metastasis or expand metastatic colonies (Massague, 2008). Further, TGF- β has been reported to be an activator of SMAD-independent signaling pathways (MAPK signaling pathway, fibroblast growth factor signaling) which induce cell proliferation (Chapnick, Warner, Bernet, Rao, & Liu, 2011). TGF- β has been also linked to the stimulation of relevant in HCC angiogenesis (Ito et al., 1995). TGF- β mainly exerts anti-inflammatory functions (Li, Wan, Sanjabi, Robertson, & Flavell, 2006); therefore, higher TGF- β expression around tumour ultimately support escape of immune surveillance (Niitsu et al., 1988).

1.3.2.1 TGF- β and EMT

Tumour aggressiveness is increasing upon enhanced migration, invasion and metastasizing capacity of cancer cells acquired through molecular changes and TGF- β may be involved in those processes. EMT is a biological process during the cells change their phenotype, namely they lose polarity and change to mesenchymal phenotype (Kalluri & Weinberg, 2009). In EMT process, cells lose adhesion and their cytoskeleton is remodeled. These processes have originally been described in embryonic development and organogenesis. However, this process has very significant role in progression and metastasis of cancer (Du & Shim, 2016). Tumour cells express higher level of mesenchymal protein (N-cadherin, CDH2) and involved in EMT transcription factors, such as SNAI, SLUG, ZEB, and TWIST, while they decrease the expression of epithelial markers (E-cadherin, CDH1). This re-programming thus can induce ability to migration and invasion of the cancer cells (Diepenbruck & Christofori, 2016).

HCC tumours with late-stage gene signatures are distinguished by an upregulation of cell cycle targets, targets engaged in the building of blood vessel which lead to an aggressive phenotype related to a poor prognosis (Mancarella et al., 2019). In the crossing between the stages (early and late), TGF- β does as a strong inducer of EMT process (Giannelli, Koudelkova, Dituri, & Mikulits, 2016). Moreover, TGF- β induced EMT is accompanied with repression of expression of epithelial markers (CDH1, zonula occludens 1 (ZO-1)). In contrast, standard mesenchymal markers, e.g. CDH2,

vimentin (VIM) and collagens are increased (Dooley et al., 2008). *In vitro*, TGF- β treatment induced extensive migration in AML12 hepatocyte cell line or in PLC/PRF/5 human HCC cell lines (Dooley et al., 2008), (Malfettone et al., 2017). Correspondingly, inhibition of TGF- β induce the expression of epithelial marker CDH1 and reduce migratory and invasive properties in highly invasive HCC cell lines (Fransvea, Angelotti, Antonaci, & Giannelli, 2008). These findings underline the capacity of TGF- β to influence EMT processes and possibly enhanced tumourigenicity.

1.4 Paired related homeobox 1 (PRRX1)

Transcription factors are proteins that bind to the promoter or enhancer regions of specific genes to regulate transcriptional processes (Latchman, 1997). In addition, they interact with RNA polymerase II or other transcription factors to control the messenger RNA (mRNA) production of distinct genes (Latchman, 1997). Homeobox transcriptional factors are a family of transcriptional proteins that have a homeobox domain binding to conserved sequences of the DNA (Sugiyama et al., 2015). Homeobox proteins are describes as a kay players in the developmental processes of organisms consisting of many cells, and the accumulated scientific results detected that some homeobox targets have impact on the progression of various kinds of cancers (Shah & Sukumar, 2010).

The paired related homeobox 1 (PRRX1) belong to the paired-type family of homeobox transcription factors. PRRX1 has been shown to be expressed during development mainly in the mesenchyme and has an important role in the development of structures, such as cartilage, bone and tooth structures (ten Berge, Brouwer, Korving, Martin, & Meijlink, 1998), (Mitchell et al., 2006). The mature protein of PRRX1 is located in cell nucleus (www.uniprot.org). The family of paired-related homeobox transcription factors consists of PRRX1 isoforms (PRRX1a, PRRX1b) and PRRX2. The paired related homeobox 1 (PRRX1) is a transcriptional co-activator that is produced in two isoforms by alternative splicing, PRRX1a and PRRX1b (Reichert et al., 2013). PRRX1a is formed by 217 amino acids and weights 24 kDa. Full length isoform b consists of 245 amino acids and weights 27 kDa (www.uniprot.org). The two PRRX1 variants are identical from the N terminus to amino acid 199, while they differ at their C terminus. Within the C-terminus, there is an 14 amino acid motif within the C-terminal region of paired-like homeodomain containing proteins) in isoform b which is not found in isoform a (H. Liu et al., 2012). This implicates that via this strongly conserved domain, isoform specific functions could be mediated (Norris & Kern, 2001). An important paralog of

PRRX1 is PRRX2, formed by 253 amino acids and weighting 27 kDa (www.genecards.org).

1.4.1 General functions of *PRRX1*

Moreover, its role is crucial in embryonic development as its deletion is lethal in mice (Martin & Olson, 2000). Mice that lack both *Prrx1* and *Prrx2* have radical damage in differentiation of mesenchymal cells in the craniofacial region (ten Berge et al., 1998). Further, the PRRX1 protein functions as a transcription co-activator, increasing the DNA-binding activity of serum response factor, a protein needed for the induction of factors involved in cell growth and differentiation. PRRX1 protein regulates muscle creatine kinase, showing a role in the establishment of diverse mesodermal types of muscle (ten Berge et al., 1998), (Mitchell et al., 2006). Moreover, upregulated expression of *PRRX1* may promote activity of TGF- β in adipose tissue and contribute to abnormal function of adipocytes during obesity (Du et al., 2013). Thus, *PRRX1* is an important factor in embryonic development.

1.4.2 *PRRX1* in cancer

To date, contradictory information exists on the role of *PRRX1* in cancer. Transcription factors play a crucial role by controlling key processes in cancer, e.g. cell growth, metabolism, immune evasion, and metastasis (Ell & Kang, 2013), (Bradner, Hnisz, & Young, 2017). *PRRX1* has been found to be overexpressed in breast, pancreas, head and neck squamous cell carcinoma, and colon cancer (Ocana et al., 2012), (Reichert et al., 2013), (Takahashi et al., 2013), (J. Jiang et al., 2019), (Lv et al., 2016). For example, in murine pancreatic cancer and human breast cancer cell lines, the knockdown of isoforms *Prrx1a* or *Prrx1b* reduced migration and invasion indicating functional similarities (Reichert et al., 2013), (Lv et al., 2016), (Takano et al., 2016). Furthermore, Ocana et al. reported that *PRRX1* overexpression causes the induction of EMT related transcription factors *VIM*, *SNAI2*, *TWIST1* (but not *SNAI1*) and reduction of the epithelial marker *CDH1* in breast cancer (Ocana et al., 2012). Next to that, Reichert et al. showed induction of cell migration in pancreatic cancer after overexpression of *PRRX1a*, while *PRRX1b* was more involved in cell cycle regulation (Reichert et al., 2013), thus supporting a divergent molecular function between the isoforms. Further, the knockdown of *PRRX1b* inhibited proliferation as well as migratory and invasive capabilities of triple negative breast cancer cell lines (Lv et al., 2016). In another study, knockdown of *PRRX1* reduced tumour volume of MDA-MB-

231 mice xenografts, and its overexpression in colon cancer cell lines increased colony formation and anchorage independent growth (Takahashi et al., 2013). These data indicate a tumour-promoting role of *PRRX1* in some cancer settings. On the contrary, *PRRX1* has also been shown to exert tumour suppressor functions. For example, low expression of *PRRX1* enabled metastatic colonization of lung by breast cancer cells (Ocana et al., 2012). In clinical contexts, *PRRX1* has been associated with contradictory prognostic outcomes. For example, high expression of *PRRX1* predicted improved overall survival in colorectal cancer (Takahashi et al., 2013), but was associated with metastasis and poor survival outcome in breast cancer (Ocana et al., 2012). Although the precise roles of *PRRX1* and its isoforms, *PRRX1a* and *PRRX1b*, are unclear in human cancer, *PRRX1* was often associated with cancer stemness and epithelial-mesenchymal transition (EMT) (Ocana et al., 2012), (Reichert et al., 2013), (Takano et al., 2016). In human colon cancer cell lines, overexpression of *PRRX1* induced EPH receptor B2 – an intestinal stem cell marker (Takahashi et al., 2013). In contrast, stemness features were increased upon knockdown of *PRRX1* in breast cancer (Ocana et al., 2012). Regarding EMT, a crucial process in cancer metastatic dissemination (J. Wan et al., 2013), overexpression of *PRRX1* caused the upregulation of the EMT gene *TWIST1* (Ocana et al., 2012). In addition, its knockdown reversed invasiveness (Takano et al., 2016). Taken together, *PRRX1* plays a role in cancer, but the effects can be contradictory. There are also few studies that investigated *PRRX1* in liver cancer.

1.4.3 *PRRX1* in liver cancer

To date, only little is known on the role of *PRRX1* in liver cancer. Few studies have investigated *PRRX1* expression in HCC (Hirata et al., 2015), (Fan et al., 2017), (Yi et al., 2016), (Tang et al., 2019), and its functions are largely unknown. Hirata et al. performed *in silico* analyses from HCC gene expression data sets and showed that reduced expression of *PRRX1* is correlated with poorer overall survival of HCC patients (Hirata et al., 2015), indicating that in liver cancer, *PRRX1* expression is beneficial. Yi and colleagues proved that loss of E-cadherin had prognostic value to predict recurrence of HCC, but *PRRX1* was not correlated with EMT nor prognosis nor recurrence, as determined by immunohistochemical analyses of HCC tissue. They concluded that further studies with a larger series of HCC samples are required to elucidate the significance of *PRRX1* in HCC (Yi et al., 2016). Further, Fan et al. reported that *PRRX1* regulates p53 by inhibiting apoptosis in HCC cells and the

reduction of *PRRX1* expression induces cell invasion and metastasis, therewith contributing to poor clinical outcome (Fan et al., 2017). In addition, Tang and colleagues suggested that loss of *PRRX1* expression is associated with regulation of the STAT3 pathway and synergistically influences HCC metastasis (Tang et al., 2019). These few available studies indicate that *PRRX1* has a role in HCC, but that further experimental work is needed for a detailed clarification of its functions.

2 AIMS OF THE STUDY

Liver cancer is the fourth most common cause of cancer-related death and ranks sixth in terms of incident cases (International Agency for Research on Cancer, World Health Organization: Cancer today (<https://gco.iarc.fr/today/home>)). HCC accounts for the majority of primary liver cancers. Chemoresistance, tumour relapse and molecular heterogeneity are characteristics of HCC, which, in conjunction with late diagnosis, lead to limited curative treatment options.

PRRX1 is a transcription factor and has been linked to epithelial to mesenchymal transition (EMT) processes. A role in diverse cancer entities has been described, but information in liver cancer is scarce. EMT is a hallmark of cancer progression leading to spread of tumour cells into surrounding liver tissue and other organs. Here, the TGF- β cytokine exerts a crucial role as it is a known/well acknowledged EMT inducer and plays an important role in HCC. Based on current knowledge the aim of this study was to clarify the regulation of *PRRX1* expression and its functions in HCC. The specific questions to be addressed in this study are as follows:

2.1 Regulation of *PRRX1*

- How *PRRX1* and its isoforms are expressed in HCC?
- Whether TGF- β affect *PRRX1* expression?

2.2 Functions of *PRRX1*

- Does *PRRX1* have clinical impact on patients with HCC?
- Which cell functions are modulated by *PRRX1* in HCC (e.g. proliferation, apoptosis, clonogenicity)?
- Does *PRRX1* change metabolic activities in HCC?

3 MATERIALS AND METHODS

3.1 Materials

3.1.1 Equipment and consumables

Material	Source
- 80°C freezer	Panasonic Healthcare Co. Ltd, Japan Ultra-low Temperature Freezer MDF-DU500VH #15030041
Autoclave	Systec GmbH, Wetttenberg, Germany
Cell culture flasks	Greiner Bio-One, GmbH, Germany 550 ml (175 cm ²), Ref. 660175 250 ml (75 cm ²), Ref. 658175 50 ml (25 cm ²), Ref. 690175
Cell culture hood	Kendro Laboratory Products GmbH, Germany Hera Safe Type KS9 (S/N 40347630)
Centrifuges	Eppendorf AG, Hamburg, Germany Model 5418 #0006937 Kendro Laboratory Products, Hanau, Germany Biofuge Fresco Heraeus Order #75005521/01 Biofuge Promo R Heraeus #75005440
Culture plates	Grainer Bio-One GmbH, Germany 6 well, Ref. 657160; 12 well, Ref. 665180; 24 well, Ref. 662160; 48 well, Ref. 677180; 96 well, Ref. 655180
Electrophoresis Power Supply	PeqLab, Belgium S/N 85895
GC/MS-QP2010 Plus	Shimadzu, Germany
Imaging System Fusion SI4	PeqLab Erlangen, Germany #13200703
Incubator	Thermo Scientific, Germany Hera Cell 240i CO ₂ incubator

Material	Source
Inverted Microscope (Bright Field/ Phase Contrast/ Fluorescent)	Leica Microsystems W, GmbH, Germany Type 090-143.010.000
Magnetic Stirrer Hotplate	Heidolph Instruments GmbH & Co. KG, Schwabach, Germany (MR3001K, S/N 110479466)
Microflex Powder-Free Nitrite Exam Gloves	Ansell Healthcare Europe NV, Belgium Lot #1700113100565
Microplate Reader (Infinite M200)	TECAN Austria GmbH S/N 9040000933
Neubauer Chamber	Sondheim, Germany
Nanoquant Plate	TECAN Austria GmbH #30035094
Nitrocellulose Blotting Membrane	GE Healthcare Life Sciences, Freiburg
Amersham Protran 0.2µM NC	Cat# 10600001
Petri dish 145x20mm	Carl Roth, Mannheim, Germany XH90.1
Peqstar Thermocycler	VWR International GmbH, Germany
pH Meter (Inolab Ph7110)	WTW Weilheim, Germany #1518038
Pipettes	Greiner Bio-One GmbH, Germany 5 ml, Ref. 606107; 10 ml, Ref. 607180
Pipette Tips	Eppendorf AG, Hamburg, Germany 10 µl, Ref. 1984124; 20 µl, Ref. 1969534; 100 µl, Ref. 3839209; 200 µl, Ref. 3900193; 1000 µl, Ref. 2897987
StepOnePlus Real-Time PCR System (Applied Biosystems)	Life Technologies Holdings Pte Ltd, Singapore S/N 272008110, Cat # 4376592
ThermoStat Plus (Heating block)	Eppendorf AG, Hamburg, Germany #5352 01869
Tubes	Greiner Bio-One GmbH, Germany 15 ml, Ref. 188271; 50 ml, Ref. 210261 Cryo.S Freezing Tubes, Ref. 126280

Material	Source
Ultrasonic bath	Bandelin Electronic, Berlin, Germany Sonorex RK100 (Instr. #301201066)
Vortex	Heidolph Instruments GmbH & Co. KG, Schwabach, Germany REAX Top, S/N 070108806
Water bath	Mettler GmbH + Co. KG, Schwabach, Germany Type WNB 14, F Nr.L413.1238
Weight balance	Sartorius AG, Göttingen, Germany

3.1.2 Reagents

Item	Catalogue number	Company
5x HOT FIREPol EvaGreen qPCR Mix Plus (ROX)	08-24-00020	Sigma-Aldrich, Munich, Germany
Acrylamide/bis-acrylamide, 30% solution	10688.02	Serva, Heidelberg Germany
Agar	5210.1	Carl Roth, Mannheim, Germany
Ammonium persulfate (APS)	A3678-25G	Sigma-Aldrich, Munich, Germany
ATP determination kit	A22066	Life Technologies, Oregon, USA
Bovine serum albumin (BSA) powder	11930	Serva, Heidelberg Germany
Caspase-3 Assay	30401	Biomol, Hamburg, Germany
Chloroform	Y015.1	Carl Roth, Mannheim, Germany
Crystal violet	Q21A018	ThermoFisher, Kandel, Germany
Dulbecco's modified eagle medium (DMEM)	BE12-709F/12-M	Lonza, Basel, Switzerland
Dimethyl sulfoxide (DMSO)	41639-500ml	Sigma-Aldrich, Munich, Germany
DNA/RNA free water	W4502	Sigma-Aldrich, Munich, Germany
Deoxynucleoside triphosphates mix (dNTP Mix), 10 mm each, 0.2 ml	R0191	Thermo Fischer Scientific, Massachusetts, USA
Dulbecco's Phosphate Buffered Saline (DPBS)	9124.1	Carl Roth, Mannheim, Germany
Ethanol 99%	T171.4	Carl Roth, Mannheim, Germany

Item	Catalogue number	Company
Fetal bovine serum (FBS)	10270	Thermo Fischer Scientific, Massachusetts, USA
Glycerol	G5516-500ml	Sigma-Aldrich, Munich, Germany
Hank's Balanced Salt Solution (HBSS)	BE10-547F	Lonza, Basel, Switzerland
Heptadecanoic acid	H3500	Sigma-Aldrich, Munich, Germany
Hydrogen peroxide (30%)	K43258310210	Merck KGaA, Darmstadt, Germany
InviTrap Spin Universal RNA Mini Kit	MJ160021	Stratec Molecular, Berlin, Germany
L-glutamine	G7513	Sigma-Aldrich, Munich, Germany
Lipofectamine RNAiMAX	13778-075	Invitrogen, USA
Luminol	09253-25G	Sigma-Aldrich, Munich, Germany
Ly2157299	S2230	Selleckchem, Munich, Germany
Methanol	4627.2	Carl Roth, Mannheim, Germany
Methoxyamine hydrochloride	226904	Sigma-Aldrich, Munich, Germany
N,N,N',N'-tetramethylethylenediamine (TEMED)	T9281-25ML	Sigma-Aldrich, Munich, Germany
Opti-MEM I (1x)	31985-070	Gibco Life Technologies, Paisley, UK
PageRuler Plus Prestained Protein Ladder	26620	Thermo Fischer Scientific (UE), Lithuania
<i>p</i> -Coumaric acid	C9008-5G	Sigma-Aldrich, Munich, Germany

Item	Catalogue number	Company
Penicillin-streptomycin 100x (P/S)	P0781	Sigma-Aldrich, Munich, Germany
Phosphatase inhibitors cocktail	P5726	Sigma-Aldrich, Munich, Germany
Ponceau S	P7170-1L	Sigma-Aldrich, Munich, Germany
Powder milk	T145.3	Carl Roth, Karlsruhe, Germany
Protease Inhibitor Coctail Tablets	4693116001	Sigma-Aldrich, Munich, Germany
Random Hexamer Primer	SO142	Thermo Fischer Scientific, Massachusetts, USA
Pyridine	270970	Sigma-Aldrich, Munich, Germany
Revertaid H Minus Reverse Transcriptase	EP0451	Thermo Fischer Scientific, Massachusetts, USA
Ribitol	A5502	Sigma-Aldrich, Munich, Germany
Sodium dodecyl sulfatate (SDS)	2326.2	Carl Roth, Mannheim, Germany
TGF- β 1/2/3	100-21/100-35/100-36E	PeproTech, Hamburg, Germany
Tris	5429.5	Carl Roth, Mannheim, Germany
Thiazolyl Blue Tetrazolium Bromide (MTT)	M5655-1g	Sigma-Aldrich, Munich, Germany
Trypsin-EDTA solution 10x	T4174-100M	Sigma-Aldrich, Munich, Germany
Tween 20	1247ML500	neoLab, Heidelberg, Germany
β -mercaptoethanol	A4338,0250	AppliChem, Darmstadt, Germany

3.1.3 Buffers

Name	Recipe
10% SDS	10 g SDS in 100 ml ddH ₂ O
10x TBS	12.1 g Tris, 87.66 g NaCl, fill up to 1 L with H ₂ O
Crystal violet working solution	0.5% Crystal violet in water, mixed 50% with absolute methanol prior use
ECL Blot signal detection buffer	Solution 1 (5 ml of 0.1 M Tris buffer, 50 µl of 250 mM Luminol, 22 µl of 90 mM <i>p</i> -cumaric acid); Solution 2 (5 ml of 0.1 M Tris buffer, 3ul of 30% Hydrogen peroxide H ₂ O ₂). Solution 1 and 2 were mixed together
Laemmli Protein Loading buffer (5x)	2.5 ml β-mercaptoethanol, 2 g SDS, 10 mg bromophenol blue, 6 ml of 1 M Tris, pH 6.8, 200 µl of 0.5 M EDTA, 10 ml glycerin, 1.3 ml ddH ₂ O
MTT Reagent	5 mg/ml in PBS
Protin lysis buffer (RIPA)	25 mM Tris (pH 7.4), 150 mM NaCl, 0.1% SDS, 0.5% sodium deoxycholate, Nonident P40, Protease Inhibitor Coctail Tablet, Phosphatase Inhibitor (used 1:100)
Solubilization reagent	4 parts DMSO, 4 parts 10% SDS, 2 parts PBS, acetic acid (0.012% of total reagent volume). Mixed 5 minutes before use (prepared freshly prior use)
TBST	0.1% Tween 20 per 1000 ml TBS
WB Blocking solution	5 % milk or BSA in TBST
WB Electrophoresis gel (12%)	1.6 ml ddH ₂ O, 3.2 ml 30% Acrylamide Solution, 3.04 ml 1.5 M Tris (pH 8.8), 80 µ 10% SDS, 80 µl APS, 3.2 µl TEMED
WB Running buffer	10x Laemmli – 144 g glycine 30.34 g Tris, 100 ml 10% SDS, adjust to pH 8.3, fill to 1L with ddH ₂ O Diluted to 1x laemmli as working solution
WB Transfer buffer	100 ml 10x TRIS, 200 ml methanol, 700 ml ddH ₂ O

3.1.4 Antibodies

Primary antibodies	Catalogue number	Company
PRRX1 (rabbit)	GTX17237	GeneTex, California, USA
PRRX1 (rabbit)	GTX56163	GeneTex, California, USA
PRRX1 (rabbit)	ab208919	Abcam, Cambridge, United Kingdom
pSMAD3 (rabbit)	ab52903	Abcam, Cambridge, United Kingdom
GAPDH (mouse)	SC-32233	Santa Cruz Biotechnology, Heidelberg, Germany

Secondary antibodies	Catalogue number	Company
Goat anti-mouse IgG- HRP	sc-2060	Santa Cruz Biotechnology, Heidelberg, Germany
Goat anti-rabbit IgG-HRP	sc-2301	Santa Cruz Biotechnology, Heidelberg Germany

3.1.5 Gene primer sequences used for qPCR

Gene	Forward sequence	Reverse sequence
<i>ACACA</i>	ATGTCTGGCTTGCACCTAGTA	CCCCAAAGCGAGTAACAAATTCT
<i>ACACB</i>	CCCCAGACAAGTATCCCAAAG	GGGTA CTCTGGGTCTTAAAC
<i>ACOX2</i>	GAACATGCTGAGTCGCTTTG	GGGAAGGTAGTTGCTCTGTG
<i>ACSL5</i>	GTGCCTCGACTCCTTAACAG	TGTCCCAGAACTATCATGCC
<i>CDH1</i>	CGAGAGCTACACGTTACCG	GGGTGTCGAGGGAAAAATAGG
<i>CDH2</i>	CATCCAGACCGACCCAAACA	ACAGACACGGTTGCAGTTGA
<i>CPT2</i>	TTGAGTGCTCCAAGTACCATG	GCAAACAAGTGTCTGGTCAAAG
<i>FASN</i>	ACAGCGGAATGGGTAC	GACTGGTACAACGAGCGGAT
<i>FH</i>	CGTTTTGGCCTCCGAACG	CATGCGTTCTGTACACCTC
<i>GOT1</i>	CAACTGGGATTGACCCAACT	GGAACAGAAACCGGTGCTT
<i>GOT2</i>	TAACTTCTGCCTAGCGTCC	ACTTCGCTGTTCTCACCCAG
<i>GLS1</i>	GCAACAGCGAGGGCAAAGAG	CTGGGATCAGACGTTCCGCAAT
<i>GPT1</i>	GGTCTTGGCCCTCTGTGTTA	TCCGCCCTTTTCTTGGCATC
<i>GPT2</i>	GACCCCGACAACATCTACCTG	TCATCACACCTGTCCGTGACT
<i>HK1</i>	CCAACATTTCGTAAGGTCCATTCC	CCTCGGACTCCATGTGAACATT
<i>HK2</i>	CCAGATGGGACAGAACACGG	TGGAGCCCATTGTCCGTTAC
<i>IDH3A</i>	ATCGGAGGTCTCGGTGTG	AGGAGGGCTGTGGGATTC
<i>IDH3B</i>	TCTCAGCGGATTGCAAAGTTTG	CTTGTGGACAGCTGTGACCTT
<i>LDHA</i>	GCAGCCTTTTCCTTAGAACAC	AGATGTTACAGTTACGCTGG
<i>LDHB</i>	CTTGCTCTTGTGGATGTTTTGG	TCTTAGAATTGGCGGTCACAG
<i>MDH1</i>	CATTCTTGTGGGCTCCATGC	AGGCAGTTGGTATTGGCTGG
<i>OGDH</i>	GAGGCTGTCATGTACGTGTGCA	TACATGAGCGGCTGCGTGAACA
<i>PCK1</i>	GCAAGACGGTTATCGTCACCC	GGCATTGAACGCTTTCTCAAAT
<i>PDHX</i>	TTGGGAGGTTCCGAC	CAACCACTCGACTGTCACTTG
<i>PPARγ</i>	GTGGCCGCAGAAATGACC	CCACGGAGCTGATCCCAA
<i>PRRX1</i>	GAAGAGAAAGCAGCGAAGGA	ACTTGGCTCTTCGGTTCTGA
<i>PRRX1a</i>	CGAGAGTGCAGGTGTGGTTT	AATCCGTTATGAAGCCCCTCG
<i>PRRX1b</i>	GTCTCCGTACAGCGCCAT	GGCCTTCAGTCTCAGGTTGG
<i>SNAI1</i>	AATCGGAAGCCTAACTACAGCG	GTCCCAGATGAGCATTGGCA
<i>SNAI2</i>	GCTGGCCAAACATAAGCAGC	AGGGTCTGGAAAACGCCTTG
<i>SDHA</i>	TGATGGGAACAAGAGGGCATC	ACCTGGTAGGAAACAGCTTGG
<i>SDHB</i>	CACCCGAAGGATTGACACCA	GTTGCTCAAATCGGGAACAAGA
<i>SDHC</i>	TCCTCTGTCTCCCACATTACT	CCAGACACAGGGACTTCACAA
<i>SDHD</i>	GCAGCACATACTTGTACC	CTGACAACCCTCTCGCTAGTC
<i>SLC1A5</i>	TTTGCGGGTGAAGAGGAAGT	AGCATTCCGAAACAGGTAAC TTT
<i>SNAIL2</i>	GCTGGCCAAACATAAGCAGC	AGGGTCTGGAAAACGCCTTG
<i>SUCLG1</i>	ATTATGCCGGGTACATCCA	AAAAGGATCCCCACCAATTC
<i>SUCLG2</i>	TTTGCTATGGACGACAAATCAGA	CTGGCTTCCCACCATTAAGG
<i>TWIST</i>	TGCATGCATTCTCAAGAGGT	CTATGGTTTTGCAGGCCAGT
<i>TWIST2</i>	CTACAGCAAGAAGTCGAGCGA	AGCGTGGGGATGATCTTGC

VIM
ZEB1
ZEB2
PPIA

CACGTCTTGACCTTGAACGC
CAGCTTGATACCTGTGAATGGG
GGAGACGAGTCCAGCTAGTGT
AGGGTTCCTGCTTTCACAGA

CTCCTGGATTCCTCTTCGTGG
TATCTGTGGTCGTGTGGGACT
CCACTCCACCCTCCCTTATTTC
CAGGACCCGTATGCTTTAGG

3.1.6 Bioinformatics platforms and analytical tools

Name	Outcome	Link	References
cBioPortal	Visualization, analysis, download of cancer genomic data	http://www.cbioportal.org/	(Gao et al., 2013)
DAVID	Gene functional annotation	https://david.ncifcrf.gov/	(W. Huang, 2017)
GCMS solution software	Metabolomics data		
Gene Expression Omnibus (GEO)	Functional genomics data repository	http://www.ncbi.nlm.nih.gov/geo/	(Barrett et al., 2013)
Genecards	Description of genes and their function	http://www.genecards.org/	(Safran et al., 2010)
GEO2R	Comparison of samples	https://www.ncbi.nlm.nih.gov/geo/geo2r/	
GraphPad Prism v. 6	Graphs, statistic		
ImageJ	Image analysis	https://imagej.nih.gov/ij	
NCBI – Primer Blast	Gene primer design	https://www.ncbi.nlm.nih.gov/tools/primer-blast/index.cgi?LINK_LOC=BlastHome	
Oncomine	Transcriptomics data	https://www.oncomine.org/	(Rhodes et al., 2007)
Venny	Plotting Venn diagram	http://bioinfogp.cnb.csic.es/tools/venny/	

3.2 Methods

3.2.1 Bioinformatics

3.2.1.1 Collection of liver cancer microarray datasets

Eight liver cancer microarray datasets were obtained from the National Center for Biotechnology Information Gene Expression Omnibus (NCBI GEO) and the expression values for *PRRX1* and other genes of interest were accessed by using the NCBI GEO2R tool. Additionally, the Cancer Genome Atlas (TCGA) liver cancer data was assessed via cBioPortal platform. The expression values for *PRRX1* probes were compiled for each dataset, and its differential expression in HCC compared to normal or adjacent non-tumour tissues was determined using Student *T-test* in GraphPad Prism version 6. Furthermore, OncoPrint platform was used to analyze *PRRX1* expression in HCC samples in five further datasets. In total, 1,421 human HCC gene expression profiles were compared to control tissues, which included 755 adjacent non-tumour and 259 healthy liver samples (**Table 1**). Statistical significance was considered with a $P < 0.05$.

3.2.1.2 Correlation of deregulated genes in HCC with *PRRX1*

Genes positively or negatively correlating with *PRRX1* in liver cancer data were downloaded from cBioPortal platform and overlapped with genes that have previously been associated with cancer recurrence (Zucman-Rossi et al., 2015). Furthermore, genes were overlapped with deregulated metabolic genes in HCC as defined in (Nwosu et al., 2017) and EMT related genes (*MMP9*, *MMP2*, *VIM*, *CDH1*, *ZEB1*, *ZEB2*, *SNAIL*, *TWIST*). Overlapping genes were used for Pearson correlation analyses in the TCGA and GSE14520 datasets using GraphPad Prism. For extensive analysis, *PRRX1* was correlated with TGF- β family genes. Expression values were accessed from datasets mentioned in the **Table 1**. Statistical significance was considered with a $P < 0.05$.

3.2.1.3 Clinicopathological parameters

To assess the role of *PRRX1* for clinical outcome of HCC patients, their clinical data were used for additional analyses. The dataset GSE14520 is available online with

published clinical data and was used for survival analysis as well as for correlation analysis of other clinicopathological parameters. *PRRX1* expression was analyzed with focus on tumour size, BCLC and TNM staging, alanine transaminase (ALT) and AFP levels in HCC patients. For Kaplan-Meier overall survival analyses of *PRRX1* in conjunction with other genes, it was considered whether these genes were directly or inversely correlating with *PRRX1*, i.e. for genes directly correlating with *PRRX1*, the tumours with high expression of the gene and *PRRX1* were compared with tumours with low expression of both. In contrast, for genes inversely correlating with *PRRX1*, tumours with high *PRRX1* and low expression of the selected gene were selected and compared with tumours showing low *PRRX1* and high level of the gene. The number of patients for each group is indicated in the respective figure.

3.2.1.4 Pathway analyses and gene ontology

The Database for Annotation, Visualization and Integrated Discovery (DAVID) (W. Huang, 2017) was used to perform functional annotation and gene ontology analysis of the differentially expressed genes in TCGA dataset (HCC samples n=371). For this analysis, the gene list was first ranked by logFC. Thereafter, as threshold, the 5% of top upregulated (n=1022) and top downregulated (n=1022) genes with *PRRX1* being significantly upregulated were used for functional annotation with reference to the pathway database of the Kyoto Encyclopedia of Genes and Genome (KEGG). Subsequently, these gene lists (upregulated or downregulated genes) were used for gene ontology analysis under terms: biological processes and cellular components. The results were prepared as graphs in Excel (2016).

3.2.2 Cell Biology

3.2.2.1 Cell culture

Commercially available HCC cell lines were used in this work. The Hep3B, HLF and HUH7 cell lines were provided by Prof. Kern (Pathology, Heidelberg). SNU398 cells were obtained from Dr. Francois Helle (University of Picardie Jules Verne, France). The HUH7 cell line was established in 1982 from a well-differentiated hepatocellular carcinoma that was originally taken from a liver tumor in a 57 years old Japanese male (Nakabayashi, Taketa, Miyano, Yamane, & Sato, 1982). Those cells show an epithelial phenotype. The Hep3B cell line was isolated from a well-differentiated early stage HCC

from an 8 year old black American male. These cells have epithelial features and contain an integrated HBV genome (Knowles, Howe, & Aden, 1980). The SNU398 line was established in 1990 from a hepatocellular carcinoma that was resected from a 42-year old Korean male (Park et al., 1995). The SNU398 cells contain HBV DNA and have epithelial morphology. Nevertheless, this cell line is reported as poorly-differentiated HCC cell line, because of the lack of expression of hepatocyte lineage and epithelial cell markers. Additionally, SNU398 cell line shared many features with mesenchymal cells, such as the expression of mesenchymal markers, high motility and invasiveness (Yuzugullu et al., 2009). The HLF cell line was established from hepatocellular carcinoma cells of a 68 years old patient (Dor, Namba, & Sato, 1975). The cells are poorly-differentiated and own more mesenchymal (Dor et al., 1975). The cells were cultured at 37°C in a humidified atmosphere of 5% CO₂. The cell culture media was Dulbecco Modified Eagle's medium (DMEM, High glucose, Lonza, BE12-709) supplemented with 2 mM glutamine (Gln), 10% fetal bovine serum (FBS), penicillin (100 U/l), and streptomycin (100 mg/ml). All used cell lines were authenticated by short tandem repeat profiling (STR). PCR Mycoplasma Test (PromoCell, Huissen, Netherlands) was performed frequently to prove that cells were free of mycoplasma.

3.2.2.2 Knockdown of *PRRX1*

The sequence of siPRRX1 (UUCUGAGUUCAGCUGGUCAUUGUCC), not distinguishing the *PRRX1* isoforms, was obtained from a published paper (Ocana et al., 2012), and oligos were purchased from Eurofins Genomics (Ebersberg, Germany). Transfection of siRNAs or non-targeting control (siControl) (Qiagen, Hilden, Germany) was performed with Lipofectamine RNAiMAX according to manufacturer's instructions (Invitrogen, Darmstadt, Germany). Prior transfection, cells were seeded into 12 well plates at ~ 70 % density (Greiner Bio-One, Frickenhausen, Germany) and allowed to attach overnight (o/n). Next day, the transfection mix was prepared as follows: tube A) 50 µl Opti-MEM and siRNA with final concentration 25 nM were gently mixed by pipetting up and down; tube B) 50 µl Opti-MEM and 2 µl RNAiMAX were gently mixed. Tube A and B were subsequently mixed together und incubated 15 minutes in room temperature. 100 µl of transfection mix were added to the well with cells containing 1 ml of fresh medium with subsequent incubation as indicated. Thereafter, cells were cultured in fresh complete media for the indicated duration of the experiments.

3.2.2.3 Western blot

To assess protein abundance and signaling activity in HCC cells, western blot was performed. Following cell culture, culture media was aspirated off, the cells were washed once with 1x HBSS, placed on ice, and cell protein lysates were prepared using RIPA buffer supplemented with protease inhibitor cocktail and phosphatase inhibitor. Protein concentration was determined with Bio-Rad Protein Assay Kit according to manufacturer's instruction. For electrophoresis, 50-70 µg of protein samples were loaded on 12% SDS-PAGE gels and separated by applying 120V for 80 min. Proteins were subsequently transferred onto nitrocellulose membranes (EG Healthcare Life Sciences) with a current of 300 mA for 90 minutes. Thereafter, membranes were briefly stained with Ponceau S solution to visualize protein bands and verify successful blotting. The blots were then washed 3x in TBST to remove stains. The membranes were then blocked for 1 h with 5% milk dissolved in TBST (pSMAD3 antibody in 5% BSA dissolved in TBST), washed briefly in TBST and later incubated o/n at 4°C with the primary antibody of interest diluted 1:1000 in TBST (except pSMAD3 in BSA). The membranes were then washed 3x in TBST for 10 minutes each. For detecting the target protein, the corresponding mouse or rabbit secondary antibodies were first diluted 1:10000 in TBST and incubated for 1 h at room temperature, followed by washing 3x for 10 minutes each. Subsequently, membranes were briefly incubated in enhanced chemiluminescence (ECL) detection buffer, prepared as described in 3.1.3. Afterwards, immunoreactive bands were detected and visualized in the Fusion SL Imaging system (PeqLab). The primary and secondary antibodies used in this study are described in section 3.1.4. *PRRX1* was not detectable at protein level in any HCC cell line. In this study 3 different primary antibody for *PRRX1* were tested (listed in section 3.1.4), but *PRRX1* was not detected under any condition, whereas the overexpression of the protein could be detected.

3.2.2.4 Migration scratch assay

The wound healing assay, also termed migration scratch assay because it is conducted by making a scratch on a cell monolayer, is a standard *in vitro* technique for examination of ability of the cells to migrate. Thus, to investigate migration capacity of the cancer cells upon *PRRX1* modulation, 50.000 cells were seeded in 24 well plates, incubated o/n and thereafter siRNA transfection was performed using siRNA oligos as

described in 3.2.2.2 (scaled down for 24 wells plate) to knock down *PRRX1*. Next day, the cell monolayers were scratched using 200 µl pipette tips (1 scratch perwell) and the middle point of the well was marked with a needle. Then media was changed and 2 images (left and right side of the middle point) per well were taken (as time point 0, t_0) from each well. After 24h, images were taken again (t_{24}). Using ImageJ, 25 equidistant measurements of the gap (the scratch) were taken and distances were calculated from each image (t_0 and t_{24}). Percentage of migration was calculated as:

$$100 \times (\text{measured gap distance at } t_0 - t_{24}) / \text{gap distance at } t_0$$

75 measurements per condition were analyzed and significance of the difference in migration between control and *PRRX1* knock down samples was determined by Student t-test.

3.2.2.5 Proliferation assay

Cell growth is associated with the activity of proliferation associated proteins, such as proliferating cell nuclear antigen or MKI-67. Thus, these markers can be used as proliferation markers (Kelman, 1997), (Sahin et al., 1994). Nevertheless, proliferation measurements were also performed with the thiazolyl blue tetrazolium bromide (MTT) assay. For this assay, 7.000 cells per well were seeded in quadruplicate in 48-well plates. After attachment o/n, cells were transfected with siRNA to knock down *PRRX1* as described in 3.2.2.2 (scaled down for 48 wells plate) and treated for the indicated time(s). At the end of the experiments, 25 µl of MTT reagent was added to each well and incubated for 3 – 4 h at 37°C to enable formation of formazan crystals. Then, media was aspirated, 250 µl of solubilization reagent (prepared as described in 3.1.3) added to the wells and the plate was then incubated o/n at 37°C to dissolve the formazan crystals. Absorbance was read next day at 560 nm with background correction at 670 nm using an Infinite 200 Spectrophotometer (Tecan GmbH, Austria). Data were normalized to control (transfection with siControl).

3.2.2.6 Clonogenic assay

The clonogenic assay is an *in vitro* cell survival assay used to study cancer cell behaviour, i.e. to proof the ability of a single cell (cells seeded in very low density) to grow into colonies. Thus, 50.000 cell per well were seeded in 12 well plates and allowed to attach o/n. The next day, transfection was performed with siRNA oligos as

described in 3.2.2.2 to knock down *PRRX1*. 24 h later the cells were trypsinized and 1.500 cell per well were transferred to 6 well plates. After 8 days, cells in each well were fixed with methanol for 5 minutes, followed by a staining with 0.5% crystal violet solution diluted 50% v/v with methanol for 20 min. Then, the solution was removed and the wells were washed with water. Thereafter, the plates were allowed to dry at room temperature and overview images of the plates were taken by camera and representative pictures were shown in results part of this work. Afterwards, the crystal violet stain on the cells was further quantified. For this, 10% acetic acid was added to each well to solubilize the stain, followed by absorbance measurement at 595 nm.

3.2.2.7 Apoptosis assay

To assay apoptotic processes, caspase-3 activity was measured in HCC cell lines. 5×10^4 cells (HUH7 and HLF) per well were seeded in triplicate in 24 well plates and allowed to attach o/n. Next, transfection was performed with siRNA oligos as described in 3.2.2.2 (scaled down for 24 well plates) to knock down *PRRX1*. Next day, the cells were treated with 5 ng/ml of TGF- β as apoptosis trigger for 48 h. Thereafter, the cells were lysed in 40 μ l of lysis buffer. Lysates were transferred to reaction tubes and then centrifuged at 13.000 rpm for 10 min at 4°C in a table top centrifuge and supernatant was collected. Thereafter, 30 μ l of each protein lysate was incubated for 90 min at 37°C in 60 μ l of reaction buffer and 10 μ l AC-DEVD-AFC caspase 3 fluorometric substrate to allow cleavage of the substrate. Subsequently, activity of the cleaved fluorescence substrate as an indicator of caspase-3 activity was detected by fluorometric measurement using Tecan Infinite M200 (excitation 400 nm; emission 505 nm). Caspase-3 activity signal was normalized to protein content in collected cell lysates.

3.2.2.8 Glucose consumption and lactate output

To assess metabolic activity, first glycolytic activity was measured by determining glucose and lactate levels in cells upon modulated *PRRX1* expression. For glucose and lactate measurements, 150.000 cells/well were cultured o/n in triplicates on 12 well plates. Then, transfection with siRNA was performed as described in 3.2.2.2 to knock down *PRRX1*. After 48 h, 1 ml cell culture medium was collected from each well and centrifuged in reaction tubes in a tabletop centrifuge for 10 min at 13.000 rpm at

room temperature. Measurements of the supernatant were performed using the Roche Cobas C311 Chemistry Analyzer according to the manufacturer's instruction for the quantification of the two metabolites. Staff at the Zentrum für Medizinische Forschung (ZMF, Universitätsklinikum Mannheim) performed the measurements. Raw data was provided and processed by normalization to protein content in collected cell lysates.

3.2.2.9 Analysis of metabolites in cells

1 million of HUH7 and HLF cells per dish were seeded in triplicate in 14.5 cm petri dishes and allowed to attach o/n. The next day, transfection with siRNA was performed as described in 3.2.2.2, but scaled up for 1 million cells. Thus, transfection mix for 1 plate was prepared as follows: tube A) 1.5 ml Opti-MEM and siRNA with final concentration 25 nM was gently mixed by pipetting up and down; tube B) 1.5 ml Opti-MEM and 30 µl RNAiMAX were gently mixed by pipetting up and down. Tube A and B were then mixed together und incubated for 15 minutes at room temperature. 3 ml of the transfection mix were added to the plate with cells containing 15 ml of fresh medium. The next day, medium was changed and cells maintained for 48 h. Thereafter, medium was removed and cells were washed with pre-warmed deionized autoclaved pure water. Then, plates were placed on dry ice and cells were quick frozen by adding liquid nitrogen. Plates were stored in -80°C before further processing. The samples were then delivered to Metabolomics Core Technology Platform at the University of Heidelberg on dry ice, where the next steps were performed. There, extraction of the samples was performed as follows: frozen HUH7 and HLF cells on 14.5 cm petri dishes were extracted directly on culture dishes by adding pre-cooled 1 ml 50% methanol and 10 µl Ribitol (0.2 mg/ml; internal standard for polar phase, which is a stable isotopically labelled compound that can be easily distinguished from endogenous metabolites by mass spectrometry). Cells were then scraped off the plate and all liquid containing the cell debris was transferred to a 2 ml reaction tube on ice. To each tube, 0.5 ml 100% chloroform containing 0.1 mg/ml heptadecanoic acid (internal standard for organic phase) were added and samples were vortexed for 10 seconds. In the next steps, a protocol was used as described in the work by Abu El Maaty and colleagues (protocol adapted from their work) (Abu El Maaty, Alborzina, Khan, Buttner, & Wolf, 2017). Firstly, to separate polar and organic phases samples were centrifuged for 10 minutes at 11.000x g. For derivatization, 0.9 ml of the polar (upper) phase were transferred to a fresh tube and dried in a speed-vac (vacuum concentrator) without heating and

derivatization was performed. Pellets of the aqueous phase after extraction were dissolved in 20 μ l methoximation reagent containing 20 mg/ml methoxyamine hydrochloride in pyridine and incubated for 2 h at 37°C with vigorous shaking. For silylation, 35 μ l N-methyl-N-(trimethylsilyl)trifluoroacetamide were added to each sample. After incubation for 45 min at 50°C, samples were transferred to glass vials for Gas Chromatography/Mass Spectrometry (GC/MS) analysis.

Next to this, to analyze total fatty acids, 150 μ l of the lower organic (chloroform) phase after extraction were transferred to a fresh 1.5 ml reaction tube and dried in a speed-vac without heating. For transmethylation reactions, pellets were dissolved in 40 μ l tert-butyl methyl ether and 20 μ l trimethylsulfoniumhydroxide, incubated for 45 min at 50°C and transferred to glass vials for GC/MS analysis of the fatty acid methyl esters. Afterwards, GC/MS analysis was performed. A GC/MS-QP2010 Plus (Shimadzu, Germany) fitted with a Zebron ZB 5MS column (Phenomenex; 30 m x 0.25 mm x 0.25 μ m) was used for GC/MS analysis. The GC was operating with an injection temperature of 250°C and 1 μ l sample was injected with split mode (diluted 1:5). The GC temperature program for polar compounds started with 1 min hold at 40°C followed by a 6°C/min ramp to 210°C, a 20°C/min ramp to 330°C and a bake-out for 5 min at 330°C. The GC temperature program for FAMEs started with a 2 min hold at 100°C followed by a 10°C/min ramp to 300°C, a 60°C/min ramp to 330°C and a bake-out for 1 min at 330°C. Helium was used as carrier gas with consistent linear velocity. The MS was operated with ion source and interface temperatures at 250°C, a solvent cut time of 5 min and a scan range (m/z) of 40-700 with an event time of 0.1 sec. Raw data were processed using the „GCMS solution software“ (Shimadzu) and normalized to cell number.

3.2.2.10 ATP determination assay

To determine intracellular energy levels, ATP levels were to be measured. For this purpose, the ATP Determination kit (Invitrogen, USA) was used. This kit contains a bioluminescence assay for quantitative determination of ATP with recombinant firefly luciferase and its substrate D-luciferin. The assay is based on luciferase's absolute requirement for ATP in producing light (emission maximum ~560 nm at pH 7.8). Thus, for ATP determination, 7.000 cells per well were seeded in 48 well plates and allowed

to attach o/n. The next day, siRNA transfection was performed as described in 3.2.2.2 (scaled down for 48 wells plates) to knock down *PRRX1*. After 48 h, ATP measurement was performed. For this, culture media was aspirated from the wells and the cells were washed once with 1x DPBS prior lysis with RIPA buffer supplemented by phosphatase inhibitors cocktail (40 µl/well). The luminescence was measured for ATP determination according to manufacturer's protocol. Values were normalized to total protein concentration of the cell lysates.

3.2.3 Molecular Biology

3.2.3.1 RNA isolation and cDNA synthesis

Total RNA was isolated using InviTrap Spin Universal RNA Mini Kit according to the manufacturer's protocol (Stratec Biomedical AG, Germany). RNA concentration was quantified using Infinite 200 NanoQuant Plate (Tecan GmbH, Austria). Next, RNA (0.5 or 1 µg, depending on RNA concentration) was reverse transcribed to cDNA. cDNA synthesis was carried out as follows: 0.5 µl 100 µM random hexamer primers were mixed with RNA. Nuclease-free water was added to a final volume of 6.25 µl. This mix was incubated in a thermocycler at 65°C for 5 minutes. To this solution, the reverse transcriptase mix was added (2 µl of 5x reaction buffer, 1 µl of 10 mM dNTP and 0.25 ul RevertAid H Minus M-MuLV reverse transcriptase) to a total volume of 10 µl. The cDNA synthesis mix was then incubated at 42°C for 60 minutes, followed by 5 minutes reverse transcriptase denaturation step at 70°C. Thereafter, the cDNA samples were stored at -20°C for later use. A cDNA dilution of 1:10 was used for quantitative polymerase chain reaction (qPCR).

3.2.3.2 Quantitative polymerase chain reaction

cDNA was used for qPCR reactions to measure changes in gene expression levels. qPCR analysis was performed in a 10 µl reaction volume using EvaGreen PCR Master Mix on the StepOnePlus device. The qPCR reaction mix was as follows: 2 µl EvaGreen, 25 ng cDNA volume, 1 µl of gene primer mix, and then filled up to 10 µl with nuclease-free water. The samples were pipetted for each target in triplicates into a 96 well plate, plate was briefly centrifuged. The reaction parameters were set: initial denaturation at 95 °C for 15 minutes, followed by 40 reaction cycles of: denaturation at 95 °C for 15 s, annealing at 60 °C, for 20 s, and elongation at 70 °C for 20 s. The

experiments were performed in triplicate using peptidylprolyl isomerase A (PPIA) as an internal reference (house-keeping gene). The threshold of fluorescence above the background of fluorescence was defined as cycle threshold value which was then used for calculation. The results were displayed as the cycle threshold values at which the fluorescence of a sample crossed the threshold. mRNA relative expression level of targeted genes was calculated based on $2^{-\Delta\Delta C_t}$ method, where C_t means cycle threshold value. Gene primer sequences are listed in 3.1.5.

3.2.4 Statistical analyses

Results were presented as mean \pm SD. Data analyses were performed using GraphPad Prism v6 (La Jolla, USA) as well as Microsoft Excel. Where applicable, ANOVA or Student t-test were used for data comparison and significance testing. Kaplan-Meier overall survival analyses were performed with log-rank (Mantel-Cox) test in GraphPad Prism. Statistical significance was accepted for P values less than 0.05. Statistical significance is indicated as follows: * $P < 0.05$, ** $P < 0.01$, *** $P < 0.001$, and **** $P < 0.0001$.

4 RESULTS

4.1 *PRRX1* expression in HCC

4.1.1 *PRRX1* is frequently upregulated in HCC

Firstly, an *in silico* approach was conducted to assess expression of *PRRX1* in human HCC tissues compared to non-tumour control tissues using previously published cohorts. Thus, *PRRX1* expression was analyzed in nine online available human HCC gene expression datasets and five datasets in OncoPrint platform (**Table 1**). In total, 1,421 HCC tissue samples were compared to control tissues, which included 755 adjacent non-tumour and 259 healthy liver samples. Analysis of the logFC of *PRRX1* expression in nine datasets showed that its level was upregulated in seven (in 865 HCC samples; $P < 0.05$) and not significantly changed in two datasets (in 264 HCC samples) (**Figure 1A**). In addition to this analysis, the expression level of *PRRX1* was compared across the liver cancer cohorts in OncoPrint using five HCC datasets containing 292 tumours and 210 non-tumour samples. In the OncoPrint platform analysis, *PRRX1* was upregulated in two datasets, but not significantly changed in the three other datasets (**Figure 1B**). Overall, this cross-platform analysis revealed that *PRRX1* was upregulated in 990 HCC samples and was not significantly changed in 431 tumour samples. No dataset showed the downregulation of *PRRX1*. Thus, the comprehensive *in silico* analyses showed that ~ 70 % of analyzed tumour samples present with an upregulated expression of *PRRX1* compared to control tissue.

Note: A part of the results of my work will be published in a research article (Piorońska et al., Dysregulated *Paired related homeobox 1* impacts on hepatocellular carcinoma phenotypes). The manuscript was written by myself, edited by co-authors (Dr. Nwosu, Dr. Meyer and Prof. Dooley) and was partially used in this thesis.

Table 1. Human liver cancer expression datasets

	Main etiology	No. of human tissues	
		NL/NT	HCC
TCGA	HBV, HCV & others	^a 47	371
GSE25097	NA	^a 243	268
GSE64041	NA	^a 60	60
GSE55092	HBV	^a 81	39
GSE36376	HBV	^a 32	38
GSE39791	HBV	^a 72	72
GSE62232	HBV, HM	^{NL} 10	17
GSE57957	HBV	^a 39	39
GSE14520	HBV	^{NL} 220	225
		804	1129
Oncomine platform:			
Chen Liver	HBV, HCV	^a 69	94
Guichard Liver	HBV	^a 86	99
Guichard Liver 2	HBV	^a 26	26
Mas Liver	HCV	^{NL} 19	38
Wumbach Liver	HCV	^{NL} 10	35
		210	292
	Total:	1.014	1.421

^a - adjacent non-tumorous

NL - normal liver

NA - etiology is not available

HBV - hepatitis B virus

HCV - hepatitis C virus

HM - hemochromatosis

HCC - hepatocellular carcinoma

4.1.2 Expression patterns of *PRRX1* in HCC cell lines

Next to analyzing expression of *PRRX1* in human cancer gene expression cohorts, the aim was to determine its expression in human HCC cell lines, which are models for the functional study of the role of *PRRX1* in HCC. A key question was whether *PRRX1* relates to the differentiation status of HCC cell lines. Well differentiated HCC cells are usually slow-growing, have more intact metabolism and less migratory. In contrast, the

poorly differentiated HCC cells proliferate faster, have more impaired metabolic state and are often highly migratory (Nwosu et al., 2018). These features, i.e. high proliferation, metabolic alteration and migration are typical hallmarks of cancer (Hanahan & Weinberg, 2011). For expression analysis, four cell lines were used, namely HUH7, Hep3B, SNU398 and HLF. The HUH7 and Hep3B cell lines are defined as well-differentiated cells, while SNU398 and HLF are poorly-differentiated HCC cell lines – prior studies in our group has extensively characterized these cell lines (Dzieran et al., 2013; Meyer et al., 2013; Nwosu et al., 2018; Nwosu et al., 2020). Cell lines were cultured for 48 h in full growth medium to a confluence of ~90% and RNA was collected subsequently for measurement of total *PRRX1* expression. Expression values were normalized to expression of *PRRX1* in HLF cells. In the investigated cell lines, total *PRRX1* expression, not considering isoforms, was variable. Highest expression was found in SNU398 cells with almost 60-fold higher expression levels than in HLF cells. Expression in Hep3B cells was almost identical with HLF (1.8-fold higher), and HUH7 showed almost a 6-fold higher expression than HLF cells (**Figure 1C**). These expression differences are currently hard to confirm at the protein level after testing 3 antibodies from different companies (GeneTex and Abcam, described in 3.1.4) and indeed basal endogenous *PRRX1* could not be detected by Western blot in any of the four HCC cell lines. However, based on RNA profiles, expression level of *PRRX1* does not correlate with differentiation status.

Further, for a more detailed understanding of *PRRX1* expression in HCC, in the same four cell lines, expression of *PRRX1* isoforms a and b was analyzed. With the exception of SNU398, all tested HCC cell lines expressed less of the truncated isoform *PRRX1a* compared to the longer isoform *PRRX1b* (**Figure 1D**). The highest ratio of isoform a to b was in SNU398 (2.69:1) and lowest in HLF cells (0.37:1, **Figure 1E**). In well-differentiated cells (HUH7 and Hep3B), the ratio was 0.38:1 and 0.66:1, respectively.

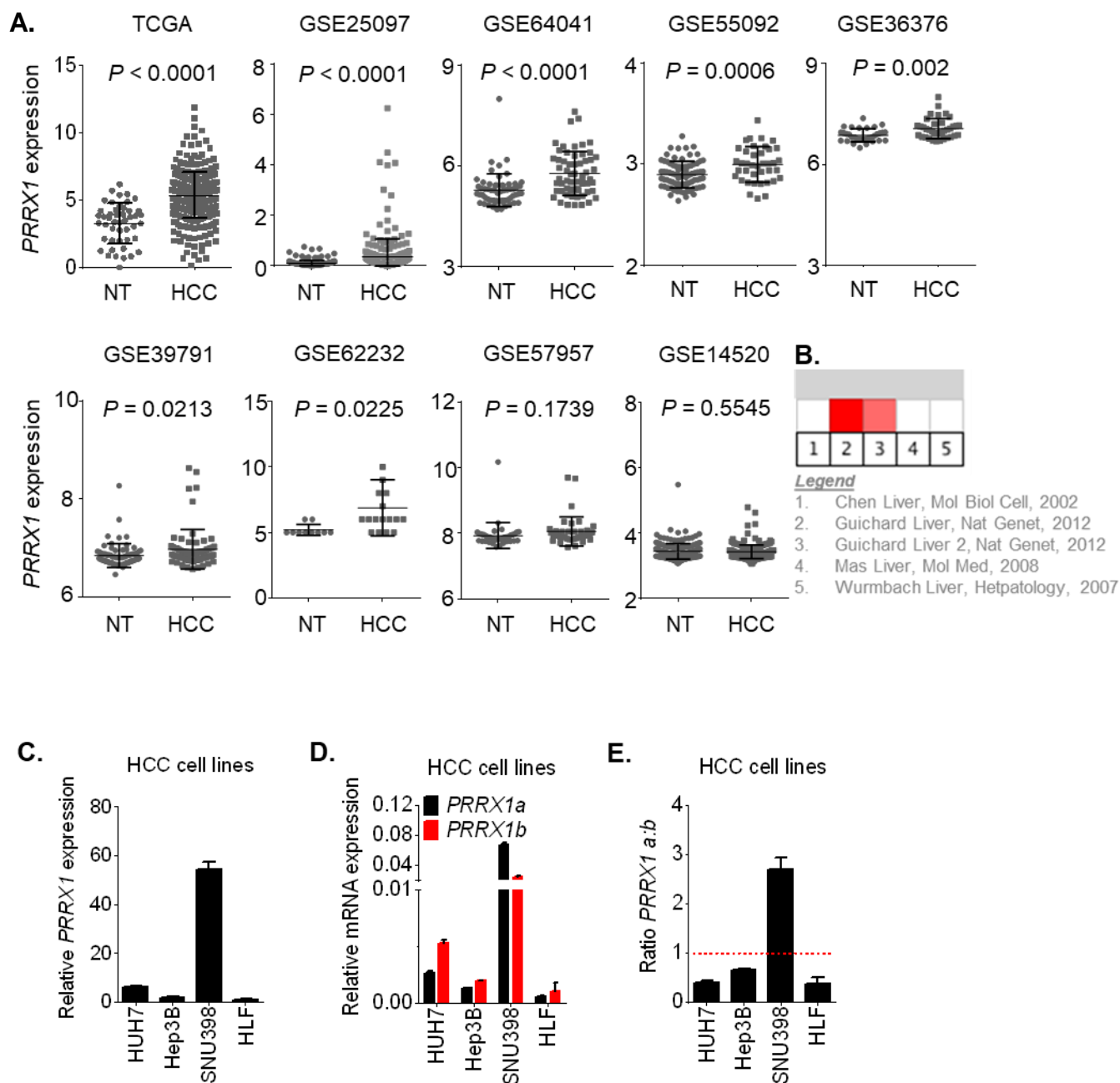


Figure 1. *PRRX1* is upregulated in human HCC and shows a variable pattern *in vitro*. (A) *PRRX1* expression in human HCC cohorts. NT - non-tumour, HCC - hepatocellular carcinoma. Data was analysed with Student's t-test. Information about sample size per cohort is provided in Table 1. (B) *PRRX1* expression in 5 HCC datasets available on Oncomine platform. The number of control/HCC samples in each cohort is provided in Table 1 Red - upregulation, white – not significantly altered. Three datasets show *PRRX1* overexpression. (C) *PRRX1* expression in human HCC cell lines after 48 h culture. Normalized to the basal expression in HLF (lowest *PRRX1* level). (D) *PRRX1a* and *PRRX1b* expression in human HCC cell lines after 48 h culture. (E) Ratio of *PRRX1a* to *PRRX1b* isoform expression in HCC cell lines after 48 h culture. Bars indicate mean \pm SD, n=3 per group. In C, D, E bars indicate mean \pm SD, n=3 per group.

4.1.3 Correlation of *PRRX1* with *TGF-β* isoforms and receptors

Transforming growth factor beta is the most and best studied member of the TGF- β superfamily (Weiss & Attisano, 2013) and is noted to play diverse roles in several cellular contexts, including regulation of cell growth and being the main inducer of EMT transcription factors in epithelial cells (Massague, 2012), (Thiery, Acloque, Huang, & Nieto, 2009). It has been examined and described that TGF- β take part in all stages of liver disease development, including early stages like inflammation, steatosis, and fibrosis as well as advanced stages, namely cirrhosis and cancer (Dooley & ten Dijke, 2012). As a next step, the aim was to investigate whether there is a correlation between *PRRX1* expression and abundance of *TGF-β* isoforms or receptors in clinical HCC tumour samples. The mRNA expression data for TGF- β genes (*PRRX1*, *TGFB1*, *TGFB2*, *TGFB3*, *TGFBR1*, *TGFBR2*, *TGFBR3*) were assessed in four cohorts (GSE25097, GSE64041, GSE57957, GSE14520; numbers of HCC samples shown in **Table 1**) by using the NCBI GEO2R tool and applying the Pearson correlation. Up- or downregulation of indicated targets were shown based on logFC values as heatmap (**Figure 2A**). In two cohorts, *PRRX1* was significantly higher expressed (e.g., by 2.05 fold in GSE25097, 1.50 fold in GSE64041; $P < 0.0001$). In the other two datasets not significantly changed compared to non-tumour samples. Thus, two groups of patients were defined, one with altered and one with unaltered *PRRX1* expression in HCC, in which TGF- β signatures were investigated. *TGFB1* and *TGFB3* were significantly lower expressed in two cohorts: in GSE25097 (with upregulated *PRRX1*) by 37 % and by 129 %, while in GSE14520 with unchanged *PRRX1* by 16 % and 12 %, respectively. Interestingly, *TGFB2* was highly expressed in one from two cohorts with upregulated *PRRX1* (in GSE64041 1.42 fold higher than in control) and significantly downregulated in the other cohort with unaltered *PRRX1* expression (i.e., GSE14520). Further, expression of TGF- β receptors was investigated. *TGFBR1* was significantly higher in patient samples with upregulated *PRRX1* (in GSE25097 1.47 fold, in GSE64041 1.20 fold). In contrast, in a cohort with unaltered *PRRX1*, *TGFBR1* showed a tendency to downregulation (in GSE14520) that was not statistically significant. Patients with elevated *PRRX1* either showed downregulation of *TGFBR2* (by 39 %) or no change, while patients with unchanged *PRRX1* expression, showed a significant upregulation of *TGFBR2* (in GSE57957 1.45 fold, in GSE14520 1.49). *TGFBR3* was significantly downregulated throughout the cohorts, with strongest downregulation when *PRRX1* was strongly upregulated (GSE25097).

In addition, a Pearson correlation analysis was performed for each of the TGF- β related genes and *PRRX1* based on gene expression values from the GSE25097 and the GSE14520 cohort (**Figure 2B**). *TGFB1*, *TGFB2*, *TGFB3* as well as *TGFBR1* showed a significant positive correlation with *PRRX1* in both cohorts, regardless of *PRRX1* expression. Among the receptors, *TGFBR3* did not show a significant correlation with *PRRX1*, whereas *TGFBR2* showed a positive correlation with *PRRX1* in GSE25097 ($r = 0.2685$, $P < 0.0001$) with significantly upregulated *PRRX1*, but a negative correlation in GSE14520 ($r = -0.1774$, $P < 0.0001$) with unaltered *PRRX1*. Taken together, patients with high *PRRX1* showed elevated *TGFBR1*, while patients with unchanged *PRRX1* showed increased *TGFBR2* levels. Moreover, *TGFB1-3* and *TGFBR1* as well as *TGFBR2* showed a positive correlation with *PRRX1* in cohorts with significantly higher *PRRX1* expression (GSE25097, GSE64041).

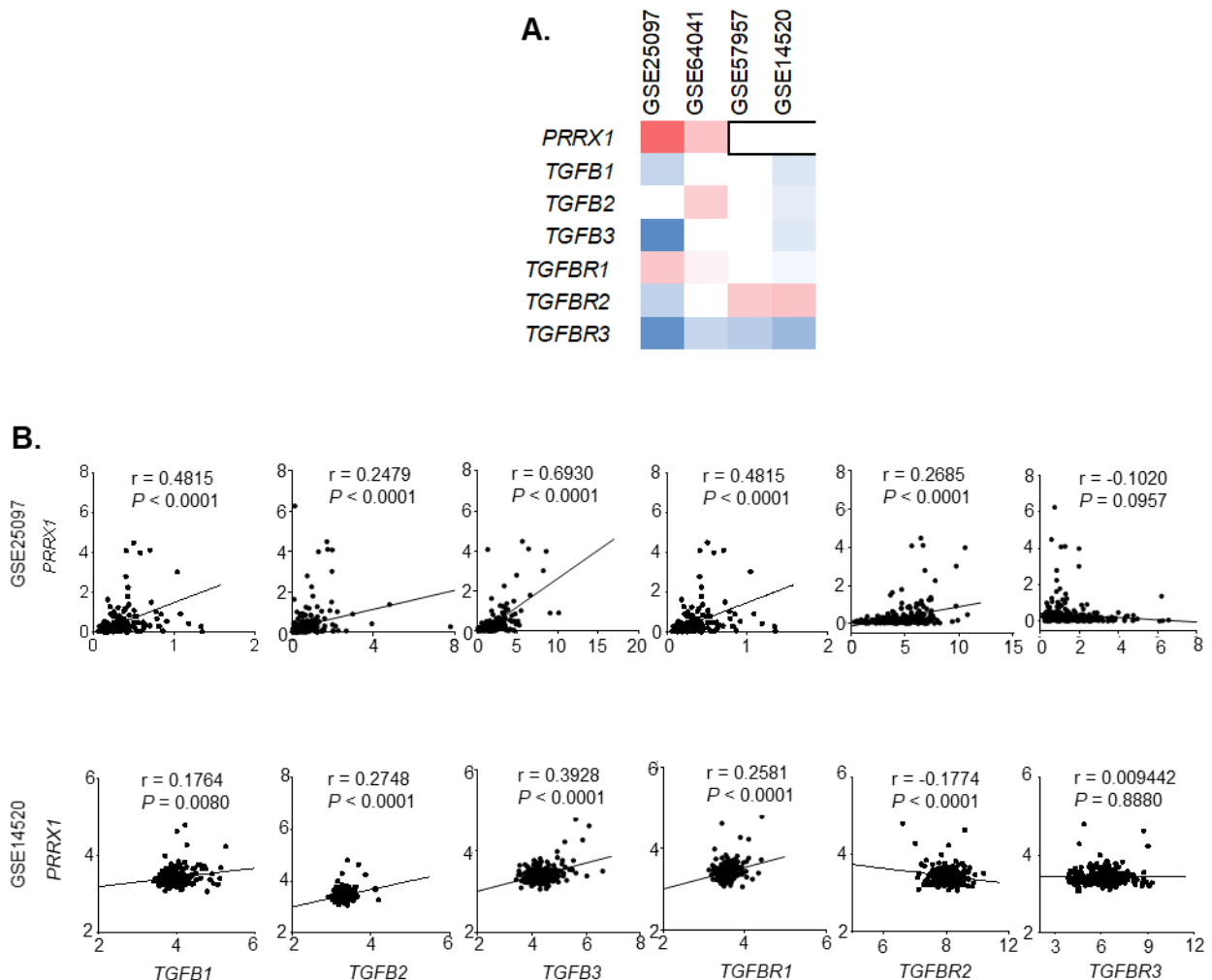


Figure 2. *PRRX1* and *TGF* β s. (A) Heatmap showing expression of genes in HCC cohorts. Red = upregulation, blue = downregulation, blank = not significant changed with $P > 0.05$. **(B)** Pearson correlation of *PRRX1* and TGF- β isoforms and their receptors in human HCC cohorts.

4.1.4 TGF- β regulates *PRRX1* expression

Based on the diverse functions of TGF- β , its role in liver diseases and the result from the dataset analysis, the aim was to investigate the relationship between TGF- β and *PRRX1* in HCC. Interestingly, prior evidence indicated that TGF- β induced *PRRX1* expression in the kidney MDCK cell line (Ocana et al., 2012). Thus, initially the ability of TGF- β isoforms to induce *PRRX1* expression was studied. HUH7 and HLF cells were treated with 5 ng/ml of TGF- β 1, TGF- β 2, TGF- β 3 for 24 h. TGF- β signaling activation was confirmed at the protein level by measuring the pSMAD3 status (**Figure 3A**). Indeed, quantitative PCR showed that the expression of total *PRRX1* was significantly increased after treatment with TGF- β 1 (6.15 fold, $P < 0.0001$), TGF- β 2 (2.83 fold, $P < 0.01$) and TGF- β 3 3.47 fold, $P < 0.001$) in the well-differentiated HCC cell line HUH7 (**Figure 3B**). In HLF cell lines, which are poorly differentiated, TGF- β 1 also induced total *PRRX1* expression (1.64 fold, $P < 0.01$), but TGF- β 2 showed only a tendency for a reduction of its expression and TGF- β 3 did not significantly affect *PRRX1* expression (**Figure 3B**). Further, whether TGF- β isoforms influence the ratio of *PRRX1* isoforms expression was examined. In untreated control settings, the *PRRX1a:b* ratio in HUH7 cells was 0.38:1 while in HLF 0.37:1. The experiment showed that TGF- β 1 significantly influenced expression of *PRRX1* isoforms, inducing expression of *PRRX1a* in HUH7 (0.84:1, $P < 0.001$) and HLF (0.89:1, $P < 0.05$) cells (**Figure 3C**). In both cell lines, the ratio of *PRRX1* was not significantly affected by TGF- β 2 (0.39:1 and a slightly increased to 0.62:1 in HUH7 and HLF, respectively). Interestingly, TGF- β 3 led to a significant change in ratio between *PRRX1a* and *PRRX1b* inducing expression of isoform *a* and repressing *b* in HLF (1.46:1, $P < 0.01$), but did not affect HUH7 cells ratio.

Complementing the analyses, the effects on *PRRX1* expression upon the inhibition of intrinsic TGF- β signaling was investigated by using Galunisertib. HUH7 and HLF cells were treated with 5 nM of LY2157299 for 24 h. LY2157299 reduced *PRRX1* expression by 70 % ($P < 0.01$) in HUH7 cells, indicating that intrinsic TGF- β signaling plays a role in the relative high expression of *PRRX1*, while it did not affect expression of *PRRX1* in HLF cells (**Figure 3D**). Taken together, there is a crosstalk between TGF- β and *PRRX1* in HCC. The results prove that TGF- β isoforms impact *PRRX1* expression and significantly influence the ratio of *PRRX1a:b* isoforms in HUH7 and HLF cells. Furthermore, intrinsic TGF- β signaling seems to be relevant in regulation of *PRRX1* expression in distinct cell-settings, because a TGF- β receptor I inhibitor decreased

PRRX1 expression in epithelial HUH7 cells, but did not affect its expression in mesenchymal HLF cells.

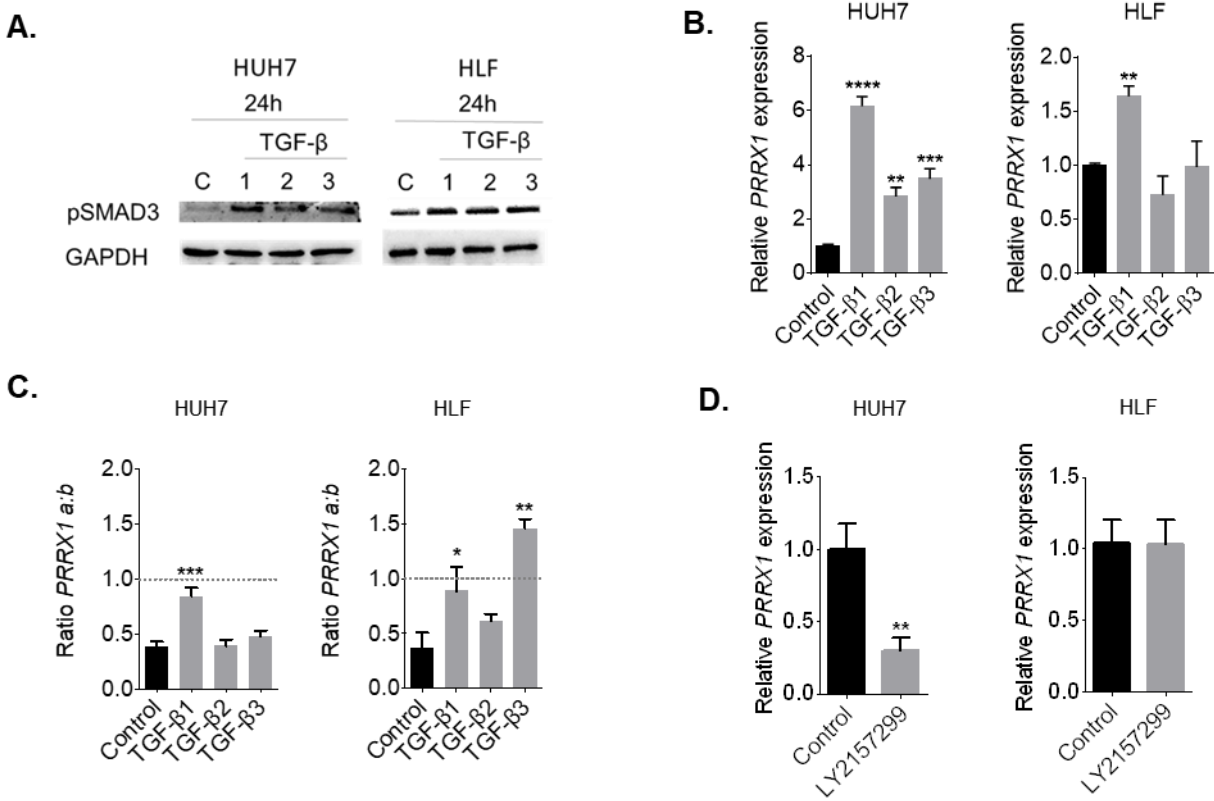


Figure 3. *PRRX1* expression regulated by TGF-β. (A) pSMAD3 protein expression 24 h after TGF-β treatments (5 ng/ml) in HUH7 and HLF cell; C = control; 1, 2, 3 = TGF-β isoforms (B) *PRRX1* expression 24h after TGF-β treatments (5 ng/ml) in HUH7 and HLF cell lines. (C) Ratio of *PRRX1*a:b 24h after TGF-β treatment (5 ng/ml) in HUH7 and HLF cell lines. (D) Relative *PRRX1* expression 24h after treatment with Galunisertib (LY2157299, 5 ng/ml) in human HCC cell lines. Bars indicate mean ± SD, n=3 per group.

4.2 *PRRX1* functions in HCC

4.2.1 *In silico* analysis of *PRRX1* related genes

To predict functions and pathways associated with the expression of *PRRX1*, *in silico* analyses were performed by using bioinformatics tools. Firstly, *PRRX1* co-expressed genes were identified in TCGA HCC data from the cBioPortal platform. This cohort has the highest number of HCC samples (N=371, **see also Table 1**) and showed the upregulation of *PRRX1* in the tumours (**Figure 1A**). The top twenty genes positively and negatively co-expressed with *PRRX1* were identified (**Figure 4A**). The correlating top ranked genes include *TGFB3* (mentioned in chapter 4.1.3) as well as several well-known HCC related genes, e.g. *IL10*, *PTN*, *MRC2*, *PLXDC1* (upregulated), or *HNF1A*, *HNF4A*, and *FOXA2* *DHCR24*, (downregulated) (Zucman-Rossi et al., 2015), (Bai, Xia, Sun, & Kong, 2017), (Cheng et al., 2014), (Taniguchi et al., 2018), (J. Liu et al., 2018), (Chan & Chan, 2015). Thereafter, the web platform DAVID was used to perform KEGG (Kyoto Encyclopedia of Genes and Genomes) pathway functional annotation analyses using the top positively correlating genes (n=1022 genes). Results show an overrepresentation of extracellular matrix (ECM) genes, signal transduction or regulation of actin cytoskeleton as well as gap junctions, which are consistent with cell-cell interaction (**Figure 4B**). Specific alterations include ECM-receptor interaction (n=15 genes, e.g. *COL6A1/A2/A3*, *ITGA8/10*, *LAMA2/4*), focal adhesion (n=29 genes, e.g. *CAV1*, *PDGFRA*, *PDGFRB*, *TNC*, *COL1A1*), and PI3K-AKT signaling (n= 35 genes, e.g. *PDGFRA/RB*, *FGF1/9*, *FGFR1*, *LPAR1/4/5/6*, *GNG2*, *PIK3R3/R5*). Crosstalk in stroma, reorganization of the cytoskeleton, or changes in adhesion are all processes connected to cancer. Consistently, gene ontology (GO) analyses for biological processes supported a positive correlation with stroma remodeling by changes in ECM organization and collagen catabolic processes as well as involvement in cell adhesion and signal transduction (**Figure 4C**). Moreover, involvement in neuronal processes could be confirmed as upon KEGG analysis.

The GO classification “cellular components” supported the finding of KEGG analysis and showed the importance of co-expressed genes for extracellular matrix and plasma membrane. 293 genes were clustered to plasma membrane, and those included *MMP2*, *CAV1*, *FGFR1*, *PLPPR4*, *TGFB3*, *MSR1*, and transporters such as *SLC1A5*, *SLC6A6*, *SCN3A* and *SLC7A3* (**Figure 4D**). Similarly, >300 genes were assigned as integral membrane components, altogether implicating *PRRX1* in membrane

dynamics, plasticity and molecule transport. Furthermore, a gene set enrichment analysis (GSEA) of *PRRX1* co-expressed genes was performed to better understand the underlying biological processes. This analysis identified association of *PRRX1* with interactions of cytokines with cytokines receptors. Next to this, EMT was identified as a process in which genes positively correlated with *PRRX1* (**Figure 4E**). In cancer, EMT is associated with tumor invasion and metastasis. Further analysis of *PRRX1* and EMT were conducted and shown in chapter 4.2.3 and 4.2.4. Taken together, the genes positively correlating with *PRRX1* are involved in stroma remodeling, contribute to signal transduction and are participating in focal adhesion as well as in EMT, crucial cancer hallmarks.

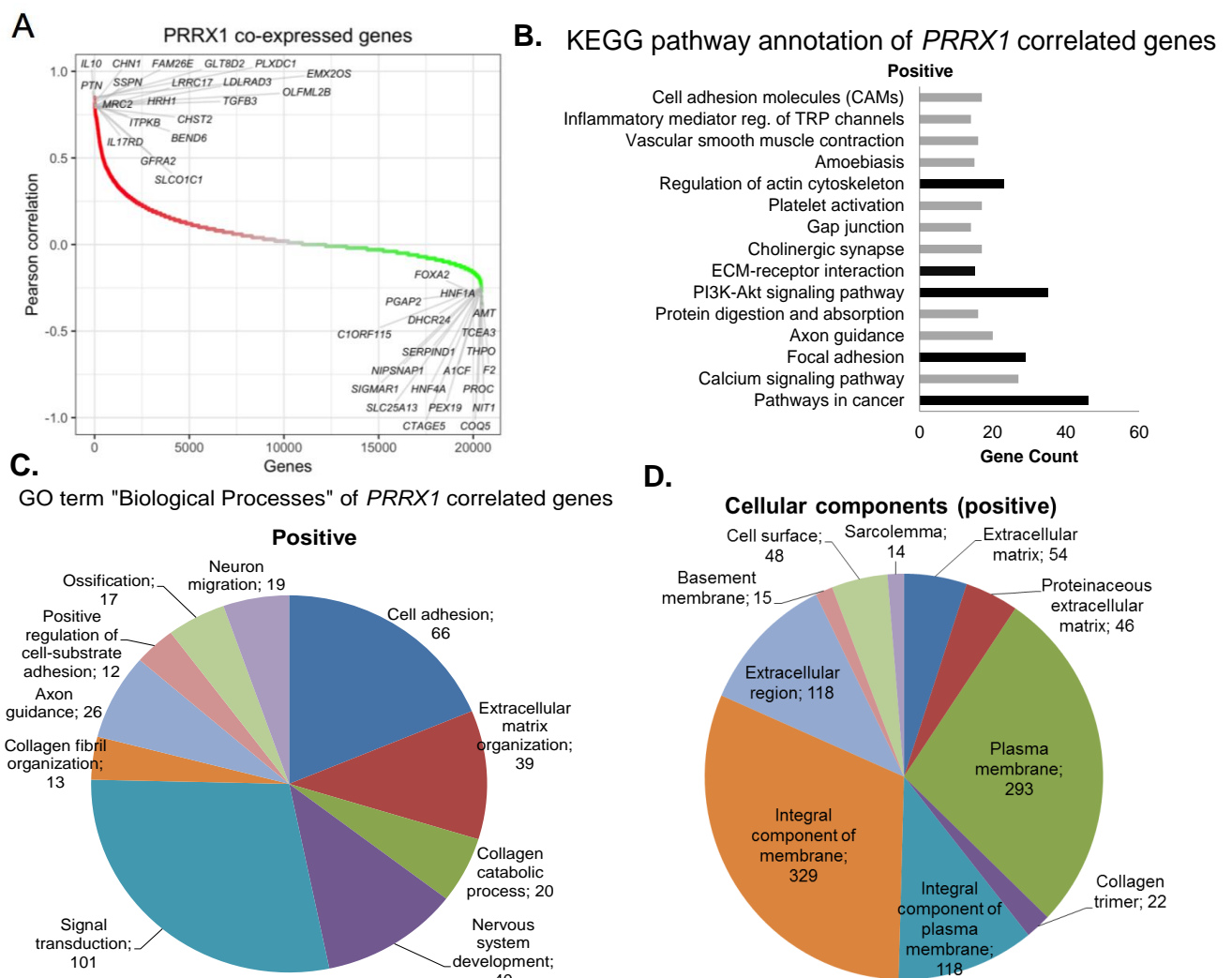


Figure 4 (A-D). Functional enrichment analyses of *PRRX1* co-expressed genes. (A) Genes positively or negatively correlated with *PRRX1* in TCGA liver cancer data. *PRRX1* correlated genes were obtained from cBioPortal platform (<http://www.cbioportal.org/>). **(B)** KEGG pathway annotation of genes positively correlated with *PRRX1*. **(C)** Gene ontology 'biological process' of *PRRX1* positively correlated genes. **(D)** GSEA plot showing enrichment of cytokine-cytokine receptor interaction and epithelial–mesenchymal transition in the genes positively correlated with *PRRX1*.

E.

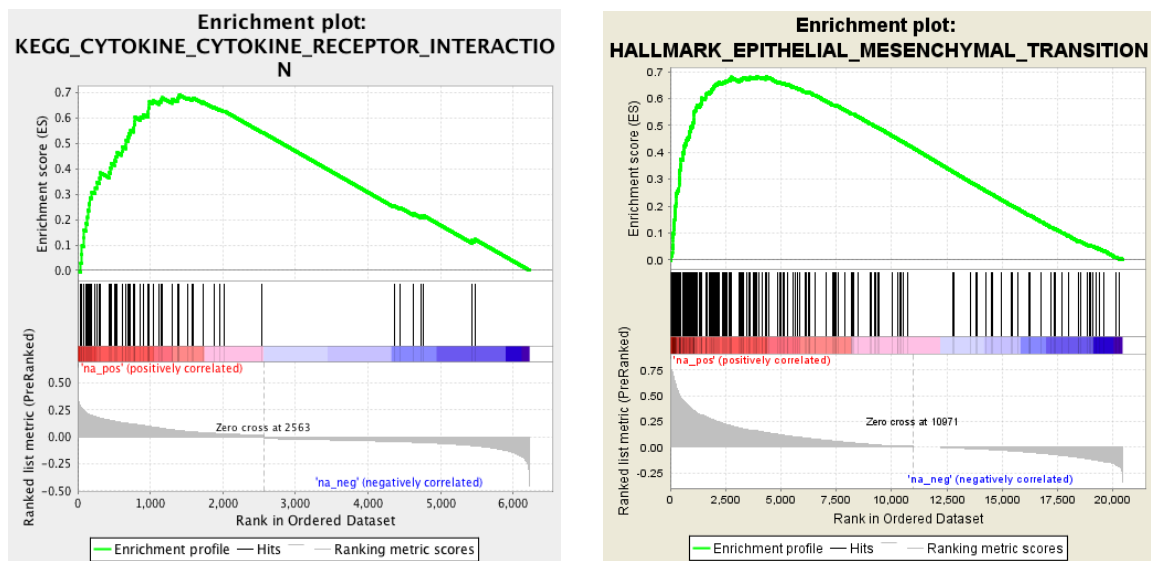


Figure 4E. Functional enrichment analyses of *PRRX1* co-expressed genes. (E) Gene ontology 'cellular components' of *PRRX1* positively correlated genes. Numbers in C, E = gene count.

4.2.2 Correlation with clinicopathological variables

To gain insight on the association of *PRRX1* with clinicopathological variables, clinical data from the GSE14520 cohort (GPL3921, n = 225 HCC samples) were analyzed. This cohort contained data for various clinical variables, including overall survival, tumour size, Barcelona clinic liver cancer and tumour-node-metastasis classification as well as ALT and AFP levels. Kaplan-Meier overall survival (OS) analysis showed a tendency towards improved outcome for patients with high *PRRX1*-expressing tumours compared to patients with low *PRRX1*-expressing tumours (**Figure 5A**). Considering tumour size, there was a strong tendency with larger tumour sizes (diameter > 5 cm) when *PRRX1* was highly expressed (**Figure 5B**). *PRRX1* was not associated with other clinical variables analyzed, e.g. stage (defined by BCLC or TNM staging), ALT, and AFP level (**Figure 5B**).

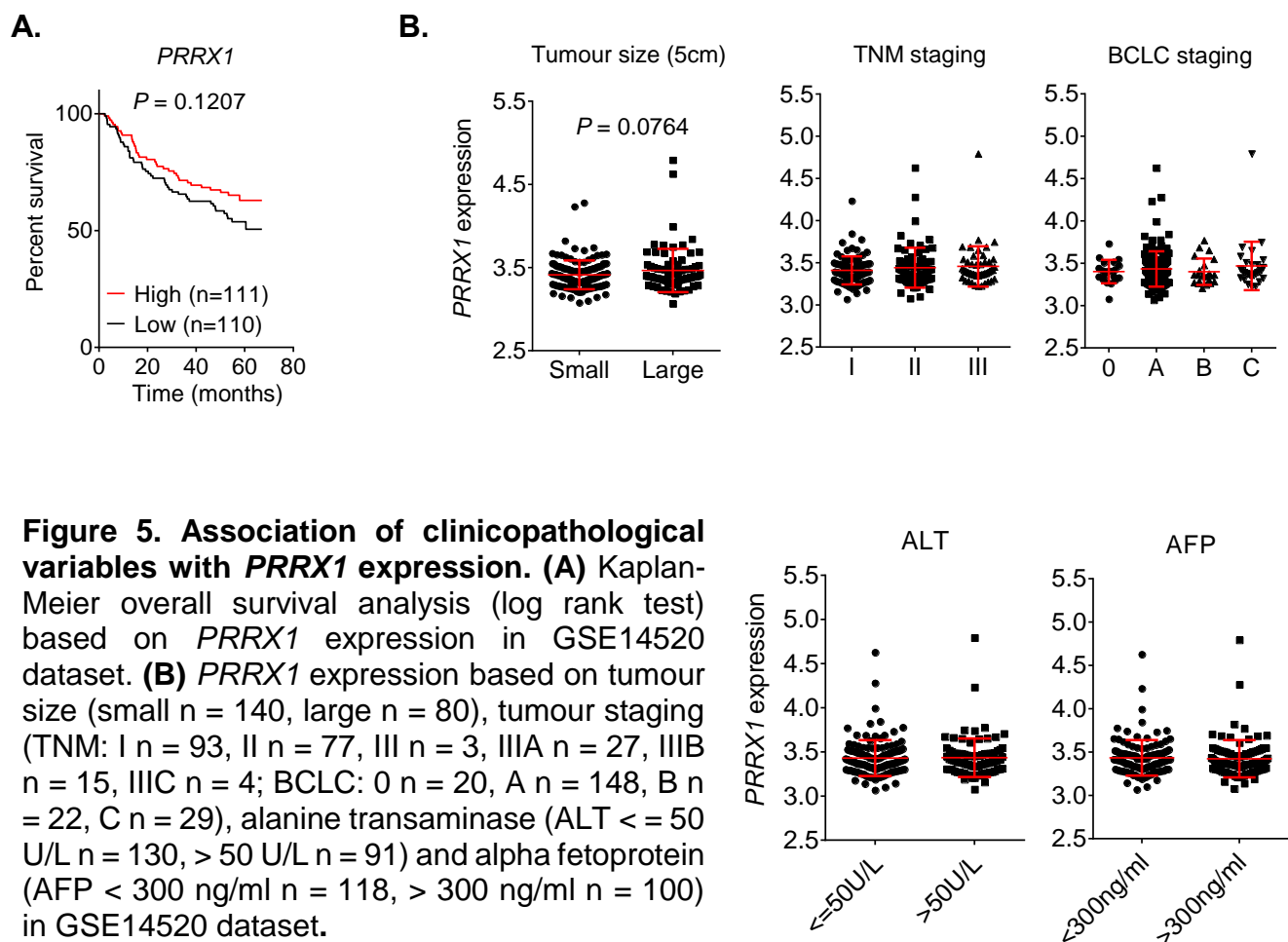


Figure 5. Association of clinicopathological variables with *PRRX1* expression. (A) Kaplan-Meier overall survival analysis (log rank test) based on *PRRX1* expression in GSE14520 dataset. (B) *PRRX1* expression based on tumour size (small n = 140, large n = 80), tumour staging (TNM: I n = 93, II n = 77, III n = 3, IIIA n = 27, IIIB n = 15, IIIC n = 4; BCLC: 0 n = 20, A n = 148, B n = 22, C n = 29), alanine transaminase (ALT ≤ 50 U/L n = 130, > 50 U/L n = 91) and alpha fetoprotein (AFP < 300 ng/ml n = 118, > 300 ng/ml n = 100) in GSE14520 dataset.

4.2.3 *ZEB1* and *ZEB2* as novel transcription factors related to *PRRX1*

Besides correlating *PRRX1* expression with TGF- β family members, the gene expression datasets were used for further analysis. Specifically, TCGA dataset was stratified into *PRRX1*-high and *PRRX1*-low *PRRX1* tumour samples (N = 122, N = 123). This analysis revealed that *PRRX1*-high tumours express several genes that were associated with the EMT (e.g., *MMP2*, *MMP9*, *ZEB2*, *VIM*) (Figure 6A). Based on this clear link to EMT, a list of EMT targets (*CDH1*, *MMP2*, *MMP9*, *SNAIL*, *TWIST*, *VIM*, *ZEB1*, *ZEB2*) was compiled and used to identify the candidates most correlated with *PRRX1* in the two largest HCC cohorts used in this study (i.e., TCGA and GSE14520). Among those genes, the EMT transcription factors *ZEB1* and *ZEB2* were significantly correlating with *PRRX1* in both datasets (Figure 6B). To validate these findings, correlation analyses of *ZEB1/2* and *PRRX1* were performed in seven additional cohorts. *ZEB2* expression correlated directly with *PRRX1* in 6 out of 9, namely in the TCGA ($r = 0.5939$, $P < 0.0001$), GSE14520 ($r = 0.1710$, $P = 0.01$), GSE25097 ($r = 0.7781$, $P < 0.0001$), GSE64041 ($r = 0.4355$, $P = 0.0005$), GSE55092

($r = 0.3293$, $P = 0.04$) and GSE39791 ($r = 0.6395$, $P < 0.0001$) cohorts, but negatively in GSE36376 ($r = -0.3403$, $P = 0.04$). *ZEB1* showed a direct correlation with *PRRX1* in 3 out of 9, i.e. TCGA ($r = 0.2512$, $P < 0.0001$), GSE25097 ($r = 0.2880$, $P < 0.0001$), and GSE55092 ($r = 0.3384$, $P = 0.04$) datasets. In contrast, in GSE14520 (with *PRRX1* not being significantly regulated), the correlation was significantly negative ($r = -0.2033$, $P = 0.002$), while in five datasets no significant associations were observed (Figure 6B).

Overall, *ZEB1/2* correlates with *PRRX1* in multiple HCC datasets.

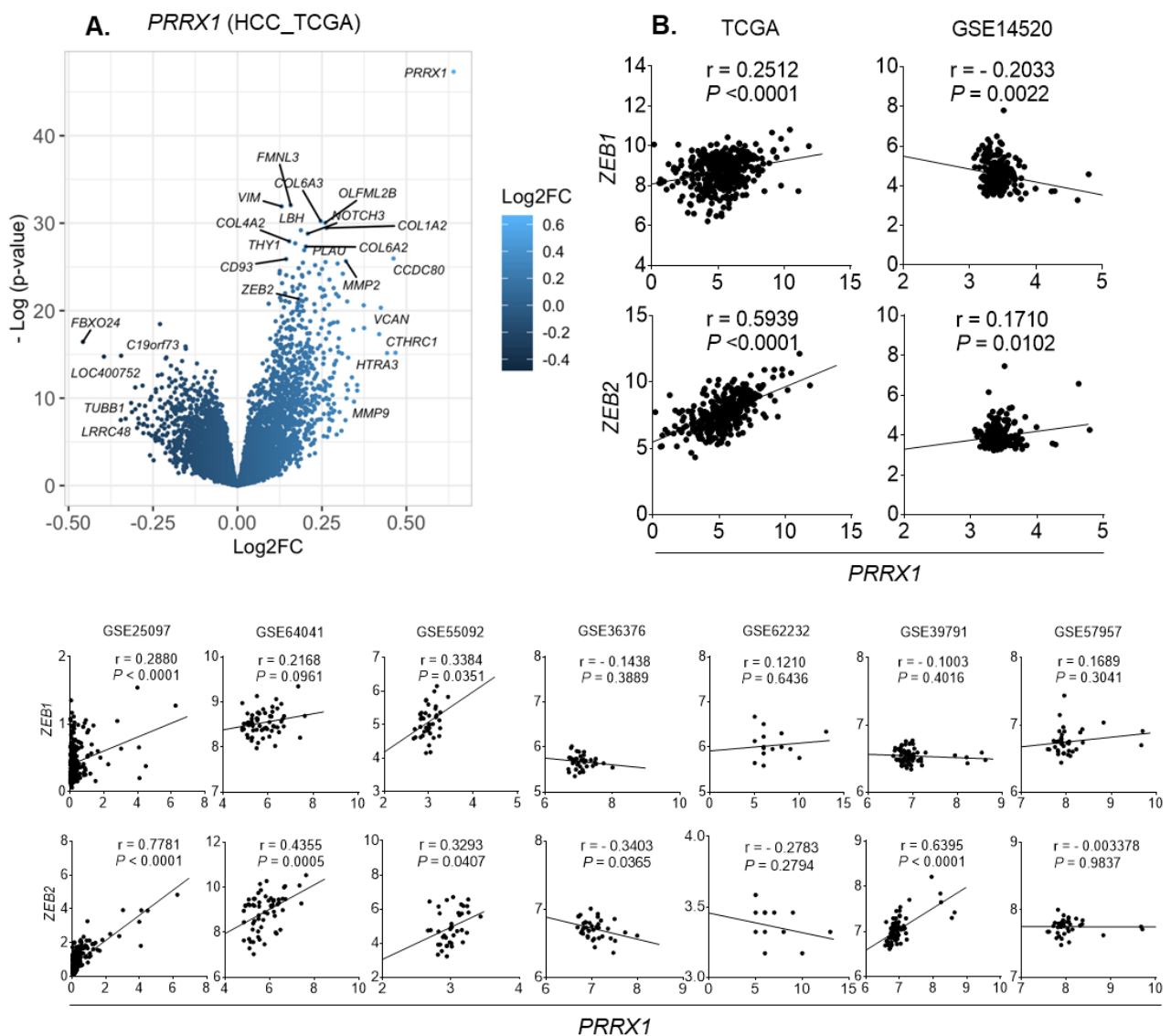


Figure 6 (A-B). *PRRX1* correlation with *ZEB1* and *ZEB2* in HCC. (A) Volcano plot showing genes differentially expressed in *PRRX1*-high tumours from TCGA dataset. **(B)** Pearson correlation of *PRRX1* and *ZEB1* or *ZEB2* in indicated HCC collectives.

The clinical data from the GSE14520 dataset were further analysed in the context of co-expression with *ZEB1/2* and *PRRX1*. Firstly, similar to *PRRX1* (**Figure 5A**), neither *ZEB1* ($P = 0.08$) nor *ZEB2* ($P = 0.15$) predicted overall survival when analyzed alone (**Figure 6C**). Overall survival analyses were then performed for *ZEB1* and *ZEB2* in combination with *PRRX1*. Liver tumours with high *PRRX1* and low *ZEB1* ($P = 0.04$) or high *ZEB2* ($P = 0.03$) predicted improved overall survival outcome (**Figure 6C**). However, besides overall survival, *ZEB1* or *ZEB2* when combined with *PRRX1* showed no significant association with other clinicopathological variables such as ALT level, tumour size, presence of cirrhosis, TNM and BCLC staging, and AFP level (**Tables 2 and 3**).

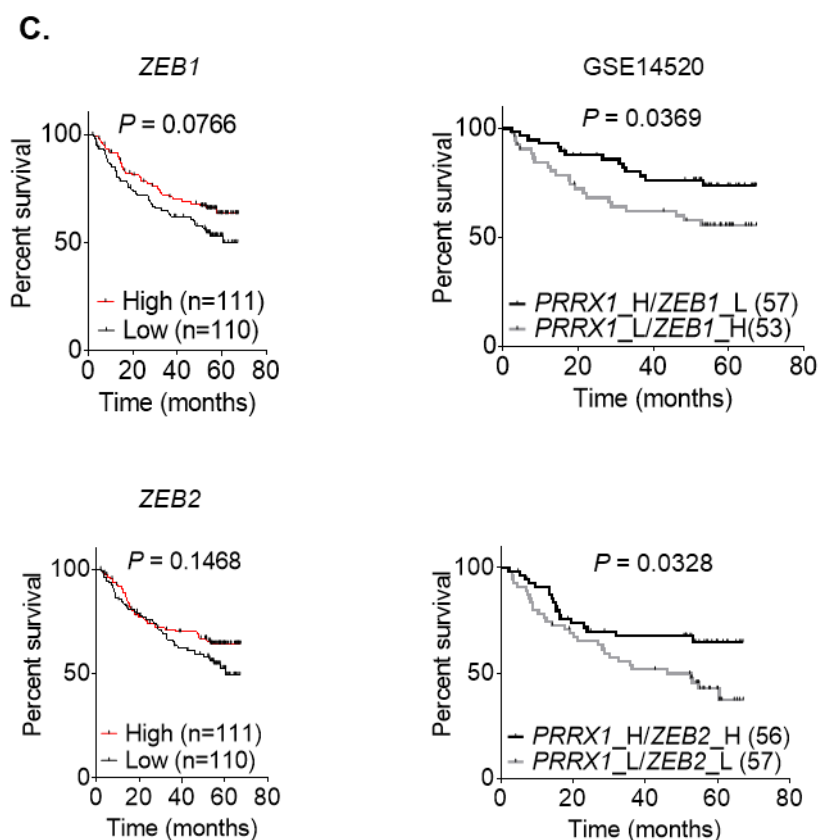


Figure 6C. Overall survival analysis in context *ZEB1/2* and *PRRX1*. Kaplan Meier OS analysis (log rank test) of high *PRRX1* combined with low *ZEB1* or high *ZEB2* in GSE14520 dataset, based on its negative correlation with *ZEB1* and positive correlation with *ZEB2* in this dataset. H = high, L = low.

Previous studies have reported the overexpression of *ZEB1* and *ZEB2* in HCC (Yamada et al., 2014), (T. Wan, Zhang, Si, & Zhou, 2017). In HCC cell lines, basal mRNA levels of *ZEB1/2* relative to *PRRX1* was heterogeneous. Specifically, the poorly

differentiated cell line HLF, which express low level of *PRRX1* (**Figure 1C**), showed comparatively higher levels of both *ZEB1/2*: 14.25 and 27.37 fold higher than *PRRX1*, respectively (**Figure 6D**). SNU398 cells, which express high *PRRX1*, showed also a high level of *ZEB2* (6.83 fold higher) but low *ZEB1* (87 % lower), reflecting the positive correlation between *PRRX1/ZEB2* in human HCC datasets. HUH7 cells expressed 2.02 fold higher *ZEB1* and lower *ZEB2* compared to *PRRX1* expression (**Figure 6D**). To causally link *PRRX1* with *ZEB* expression, *PRRX1* was knocked down in HCC cell lines (**Figure 6E**) followed by assessment of *ZEB1/2* mRNA expression (**Figure 6E**). The knockdown of *PRRX1* led to the downregulation of both *ZEB1/2* except *ZEB2* in HUH7 cells (**Figure 6F**). Expression of *ZEB1* was decreased by about 53 % in HUH7 and 56 % SNU398 cells, and 26 % in HLF cells ($P < 0.0001$). *ZEB2* was decreased by ~ 16 % in SNU398 ($P < 0.05$) and HLF ($P < 0.01$) cells. Taken together, these data identify *ZEB1* and *ZEB2* as *PRRX1*-regulated genes, likely acting in concert with *PRRX1* to influence survival of HCC patients.

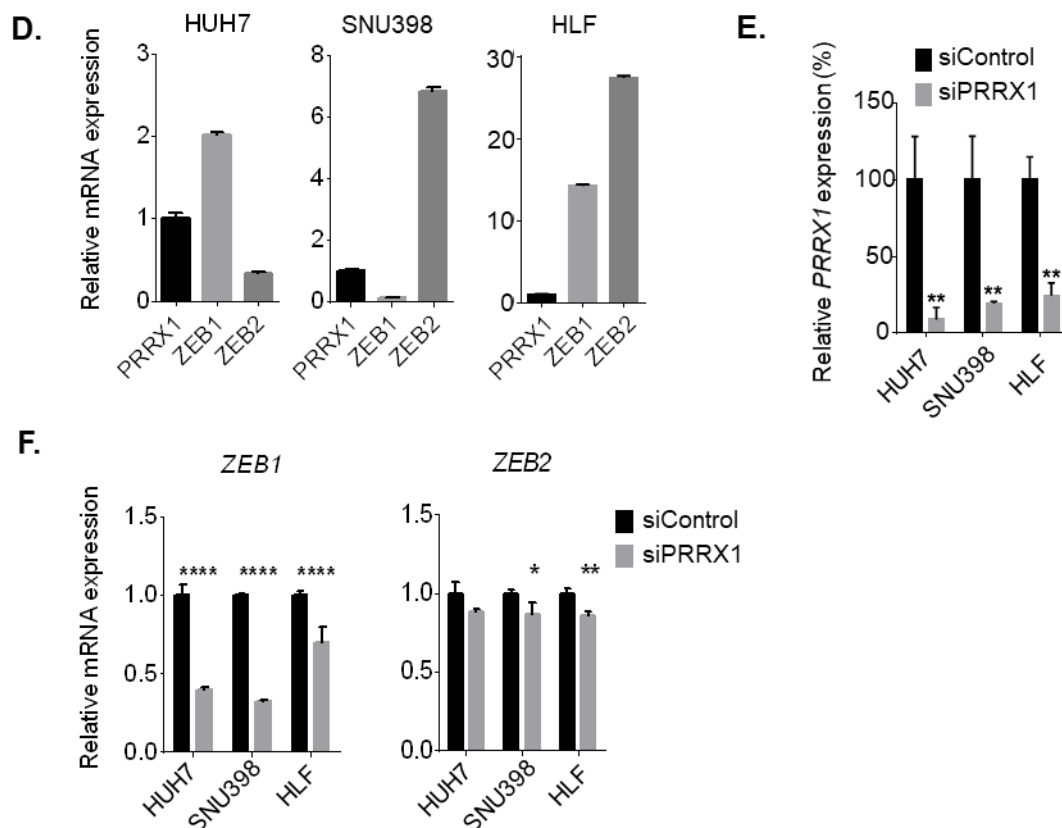


Figure 6 (D-F). (D) Differential expression of *ZEB1* and *ZEB2* compared to *PRRX1* in HCC cell lines. Cells were cultured for 48 h prior to analysis, bars indicate mean \pm SD, $n=3$ per group. (E) *PRRX1* knockdown in HUH7, SNU398, HLF HCC cell lines as determined by qPCR analysis. The knockdown was induced by transfection of 25 nM siPRRX1. Bars indicate mean \pm SD, each in triplicate. (F) *ZEB1* and *ZEB2* expression as determined by qPCR 48 h after siPRRX1 knockdown. Bars indicate mean \pm SD and representative of 3 experiments each in triplicates.

Table 2. *ZEB1* expression in combination with *PRRX1* with respect to the clinicopathological variables (n = number of patients)

Characteristics	PRRX1 ↑ ZEB1↓ n	PRRX1 ↓ ZEB1↑ n	<i>P</i> -value
ALT			
Low	36	36	ns
High	21	21	
Tumor size			
Small	35	35	ns
Large	22	22	
Cirrhosis			
Yes	52	55	ns
No	5	2	
TNM staging			
I	27	23	ns
II	18	20	
III	11	14	
BCLC			
0	9	6	ns
A	40	35	
B	4	8	
C	3	8	
AFP			
Low	29	27	ns
High	26	30	

Table 3. *ZEB2* expression in combination with *PRRX1* with respect to the clinicopathological variables (n= number of patients)

Characteristics	PRRX1 ↑ ZEB2↓	PRRX1 ↓ ZEB2↓	P-value
	n	n	
ALT			
Low	32	28	ns
High	24	27	
Tumor size			
Small	37	36	ns
Large	19	19	
Cirrhosis			
Yes	52	53	ns
No	4	2	
TNM staging			
I	23	23	ns
II	18	20	
III	14	12	
BCLC			
0	6	3	ns
A	37	37	
B	2	8	
C	10	7	
AFP			
Low	31	30	ns
High	25	25	

4.2.4 Influence of *PRRX1* on migration and the expression of EMT markers in HCC

One of the properties of distinct cancer cells is their ability to migrate and form metastases. Analysis of correlated genes revealed a link between *PRRX1* and cell migration, cell adherence and the regulation of actin cytoskeleton. Gene set enrichment analysis (GSEA) indicated that *PRRX1* participates in EMT processes. Further, studies have reported that *PRRX1* influences the expression of EMT related transcription factors in breast cancer (Ocana et al., 2012) and promotes cell migration in pancreatic cancer (Reichert et al., 2013). Thus, the aim was to investigate the impact of *PRRX1* on cell migration and expression of EMT markers in HCC cell lines. Accordingly, in the control conditions, HLF cells migrated about 20% faster in a scratch assay than HUH7 cells after 48 h, as expected due to differentiation status of the two cell lines. Upon the knockdown of *PRRX1*, migration was increased in HUH7 by 6.01% ($P < 0.001$), but was decreased in the mesenchymal cell HLF by 5.21% ($P < 0.01$; **Figure 7A**). At the mRNA level, the expression of EMT markers (*CDH1/2*, *VIM*, *TWIST*, *SNAI1/2*) was assessed after 48 h of *PRRX1* knocked down (**Figure 7B**). Firstly, efficiency of the *PRRX1* knock down was confirmed in both cell lines to be ~ 80% (**Figure 6E**). In addition, the EMT marker *CDH1* expression was increased by 2.20 fold ($P < 0.0001$) in HUH7 and not changed in HLF cells upon *PRRX1* knockdown. Further, *CDH2* was decreased by ~ 30% in both HUH7 and HLF cells ($P < 0.0001$). *VIM*, another EMT gene, was slightly decreased in HUH7 ($P < 0.05$), but not significantly changed in HLF. EMT transcription factors *TWIST1* and *SNAI2* were downregulated in both cell lines, but more strongly in HUH7 cells. In contrast, *SNAI1* was upregulated (1.58 fold, $P < 0.05$ and 1.56 fold, $P < 0.01$) in both cell lines. Taken together, the cell line HUH7 showed an increased migration after the loss of *PRRX1*, but the epithelial phenotype was unaffected, as indicated by alterations in EMT markers, except of *SNAI1* (**Figure 7B**). In contrast, the mesenchymal HLF cells showed a reduced migration, but did not change expression of epithelial marker *CDH1* upon *PRRX1* knockdown. Nevertheless, in this cell line, a tendency was found towards a decrease of mesenchymal markers (except *SNAI1*). Thus, these data reveal that *PRRX1* influences HCC cell migration and is able to modulate expression of EMT markers in HCC in a cell type dependent-manner.

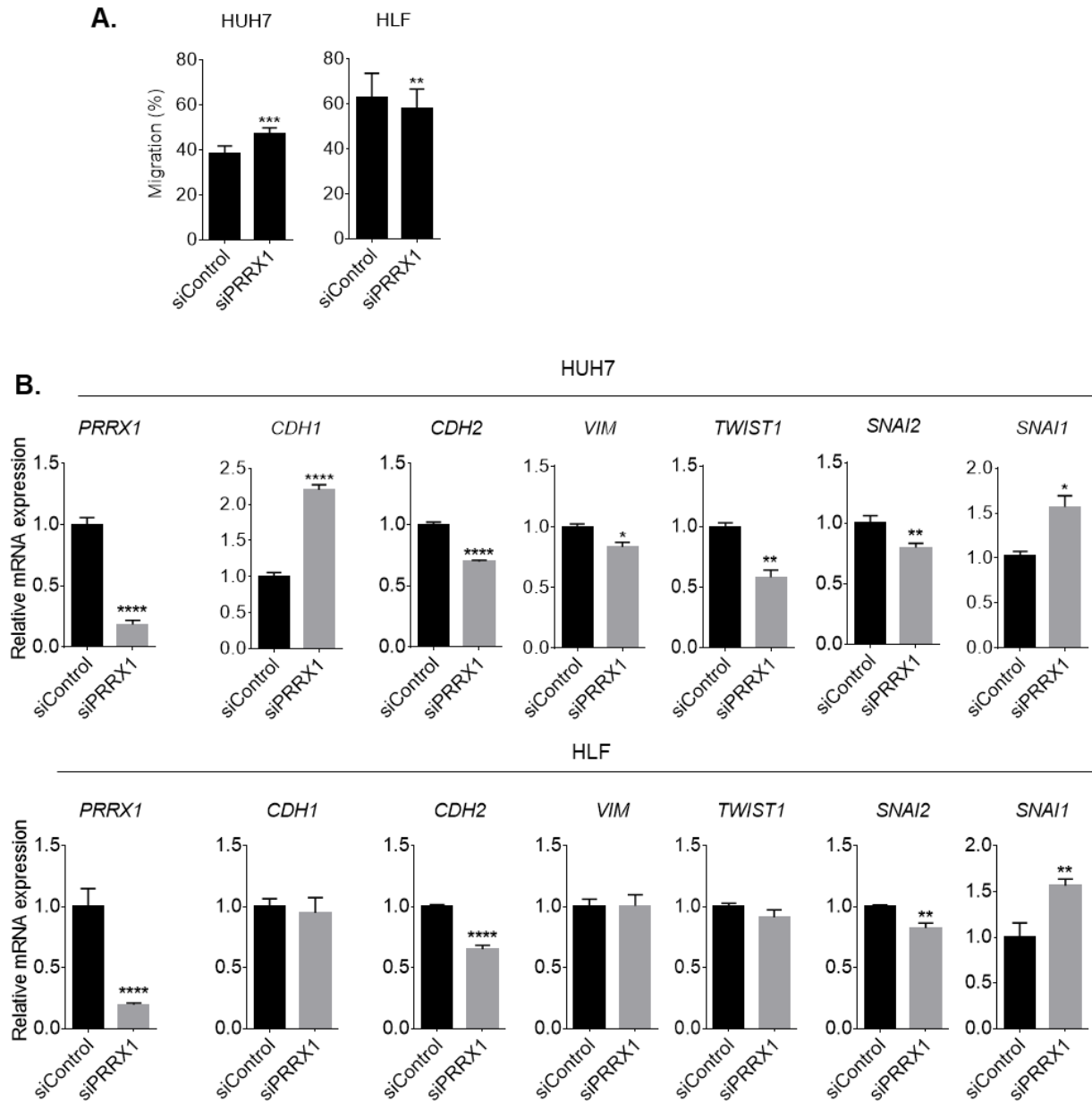


Figure 7. Cell migration and EMT markers upon *PRRX1* modulation (A) Cell migration scratch assay 24 h after siPRRX1 transfection. Bars indicate mean \pm SD of gap distance (n=18 equidistant measurements) after scratching the monolayer with 200 μ l pipette tip. **(B)** Expression of indicated targets in HUH7 and HLF cells 48 h after PRRX1 knockdown. Normalized to expression in cells transfected with non-targeted siControl.

4.2.5 Cell proliferation

Cell proliferation must be tightly regulated as uncontrolled proliferation is an important hallmark of cancer development and progression. It was previously reported that the loss of *PRRX1* reduced proliferation of breast cancer cells (Lv et al., 2016). To

investigate whether *PRRX1* played a role in the proliferation of HCC cells, three HCC cell lines were used for these studies: HUH7, SNU398 and HLF. *PRRX1* was knocked down in these cells (**Figure 6E**) and 48 hours later, proliferation was measured by MTT assay. In SNU398, proliferation rate was unaltered by *PRRX1* knockdown. In contrast, HUH7 and HLF cell lines showed a significant increase in cell proliferation after 48 h by 43% and 51% ($P < 0.001$), respectively (**Figure 8A**). The change in HUH7 cell proliferation was supported by significantly increased RNA expression of *Ki67* (1.48 fold, $P < 0.0001$) and a tendency of increased *PCNA* expression. The changes in proliferation of HLF cells could not be connected to RNA expression profiles of *PCNA* and *Ki67*, as the markers were significantly downregulated when *PRRX1* was knocked down (**Figure 8B**).

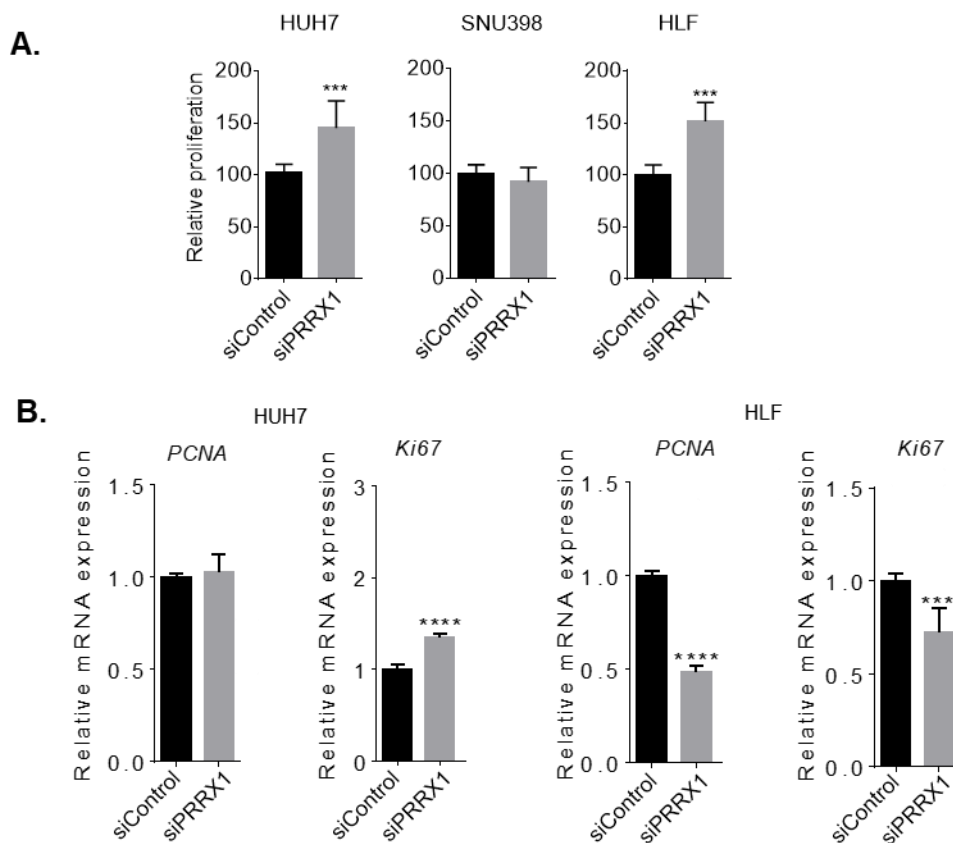


Figure 8. *PRRX1* and cell proliferation. (A) MTT proliferation assay as measured 48 h after knockdown of *PRRX1*. Experiment was repeated at least 3 times. Bars indicate mean \pm SD, $n=12$ per group (4 from each experiment). **(B)** Expression of *PCNA* and *Ki67* in HUH7 and HLF cells 48 h after *PRRX1* knockdown. Normalized to expression in cells transfected with non-targeted siControl. Bars indicate mean \pm SD, $n=3$ per group.

4.2.6 Cell clonogenicity

Next, the role of *PRRX1* was investigated in context of HCC cells' ability to form colonies. The clonogenic assay bases on the ability of cells to grow into colonies and this is a crucial aspect for recurrence of tumors from single remaining tumor cells after surgery or other systemic treatments. Therefore, the importance of *PRRX1* on clonogenic growth was tested. For this purpose, HUH7, SNU398 and HLF cells were seeded in very low density (~ 10% confluence) in 6 well plate after *PRRX1* was knocked down. 8 days later, the effects of *PRRX1* on colony formation was visualized by crystal violet staining. Under control conditions, poorly-differentiated HLF cells showed strongest ability to form colonies (30% more than HUH7 and 100% more than SNU398). In general, HCC cells had a higher capacity to form colonies when *PRRX1* level were reduced (**Figure 9**). In SNU398 cells, with a different a:b *PRRX1* ratio compared to HUH7 and HLF cells, strongest effects on colony formation occurred. SNU398 cells formed ~ 4 times more colonies when *PRRX1* was knocked down ($P < 0.0001$). An increase of colonies by 7.45% and 37.55% ($P < 0.01$) was found in HUH7 and HLF cells upon *PRRX1* knock down compared to control groups, respectively. Taken together, *PRRX1* impacts the ability of HCC cells to form colonies.

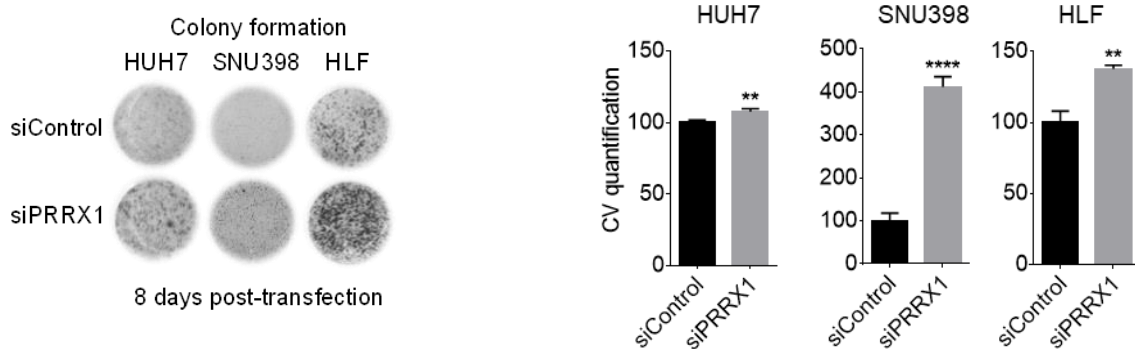


Figure 9. *PRRX1* and colony formation. Colony formation assay 8 days after *PRRX1* knockdown. Experiment was repeated at least 3 times and a representative picture is shown. CV = crystal violet. Bars show CV quantification mean values \pm SD.

4.2.7 *PRRX1* and cell death

Knowing that *PRRX1* affects proliferation, further investigations focused on apoptosis, a process tightly connected to cell growth. A hallmark of cancer is the ability of malignant cells to avoid apoptosis. The mechanisms of apoptosis execution are

complex and involve diverse pathways. Escape mechanisms can develop at any step within these pathways, supporting malignant growth of tumor cells. A crucial step during apoptosis execution is the activation of caspase 3, thus, its abundance and function can be measured as an indicator of the degree of apoptosis. *PRRX1* functions on apoptosis of HCC cells was determined by measurement of caspase 3 activity. Loss of *PRRX1* did not affect cell apoptosis in HUH7, but increased caspase 3 activity by ~25% in HLF ($P < 0.001$; **Figure 10**). Considering the stimulating impact of *PRRX1* knockdown towards HLF proliferation (**Figure 9**), an increase in cell death is not surprising for fast growing cancer cells.

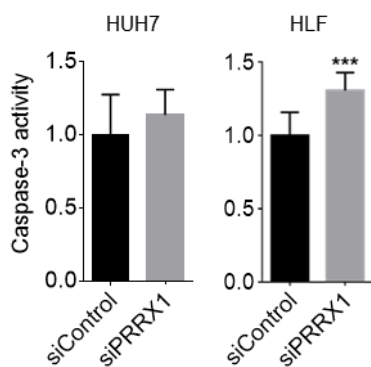


Figure 10. *PRRX1* and cell apoptosis. Caspase 3 activity measured 48 h after *PRRX1* knockdown. Bars indicate mean \pm SD, $n = 9$ per group.

4.3 *PRRX1* and liver cancer cell metabolism

4.3.1 Inverse correlation with metabolic pathways

For further predictions of functions or pathways associated with the expression of *PRRX1*, *in silico* analyses was expanded. As described in chapter 4.2.1, *PRRX1* co-expressed genes were identified in TCGA HCC data from cBioPortal. KEGG pathway analysis of the top 1022 genes negatively correlated with *PRRX1* (based on Pearson score) identified genes involved in metabolism – a link that had not yet been shown for *PRRX1* in HCC (**Figure 11A**). Among the affected metabolic processes were amino acid metabolism, e.g. glycine, serine and threonine metabolism ($n = 16$ genes, e.g. *SHMT1*, *CHDH*, *GATM*), tryptophan metabolism ($n = 13$ genes, e.g. *ALDH2*), histidine metabolism ($n = 9$ genes, e.g. *MAOA*, *MAOB*), valine, leucine and isoleucine degradation ($n = 16$ genes, e.g. *ACADSB*, *EHHADH*, *ECHS1*). Also processes such as fatty acid degradation ($n = 16$ genes, e.g. *ECI1*, *ECI2*, *ACOX1*), steroid biosynthesis ($n = 9$, e.g. *CYP51A1*, *NSDHL*), bile secretion ($n = 15$ genes, e.g. *ABCB4*, *ABCC2*, *SLC51A*, *SLC27A5*) and peroxisome activity ($n = 42$ genes, e.g. *ACOX1/2*, *HACL1*,

PEX1, 5, 6, 7, 16, and 19) (**Figure 11A**) were regulated. Metabolism also dominated the GO term 'biological processes' of the *PRRX1* negatively correlated genes, e.g. fatty acid biosynthetic process, fatty acid beta-oxidation, cholesterol biosynthesis and homeostasis, peroxisome organization and processes of oxidation-reduction reactions (**Figure 11B**). Further, the GO term 'cellular component' implicated peroxisomes and mitochondria (**Figure 11C**) – two organelles involved in important metabolic processes, antioxidant defense and cellular respiration, respectively. These results provide a clear link to metabolism. Furthermore, the GSEA of *PRRX1* negatively correlating genes was performed to deepen our understanding on the underlying biological processes. This analysis identified bile acid metabolism and glycine, serine and threonine metabolism as processes closely related to *PRRX1* (**Figure 11D**). This again underlines the correlation of *PRRX1* with amino acid and bile acid metabolic processes. Additionally, the 1022 *PRRX1* inversely correlated genes were aligned with the gene list recently published as consistently altered metabolic genes (Nwosu et al., 2017). Indeed, overlap of the inversely *PRRX1* correlated genes with genes described as downregulated (n = 350) or upregulated (n = 284) metabolic genes in human HCC revealed 135 overlapping targets (124 downregulated and 11 upregulated genes) (**Figure 11E, Table 4**). Of these, 124 metabolic genes that are negatively correlating with *PRRX1* and were described as downregulated in HCC, several belonged to amino acid and fatty acid metabolism, and also to small molecule transport (**Figure 11F**). To summarize these analyses, *PRRX1* expression correlated with the downregulation of metabolic pathways, and thus contributes to a suppressed metabolic gene pattern.

Table 4. Metabolic targets in the *PRRX1* inversely expressed gene list altered in HCC

In HCC	Gene Symbol
Up (n=11)	<i>ALG3, FLAD1, COX11, FDPS, NAT9, ALG6, PPOX, GNPAT, SLC35B1, ALG8, MPC2</i>
Down (n=124)	<i>A1CF, ABAT, ABCA6, ABCC6, ABCD3, ABHD6, ACAA1, ACADSB, ACBD4, ACOX1, ACOX2, ACSL5, ACSM5, ADH6, ADI1, AGXT, AKR7A3, ALAS1, ALDH1L1, ALDH2, ALDH7A1, ALDH9A1, AQP9, BDH1, BHMT2, CAT, CBS, CDO1, CES1, CES3, CRAT, CRYL1, CYB5A, CYP2C9, CYP2J2, CYP4A11, CYP4F12, CYP4F2, CYP4F3, DAO, DCXR, DDAH1, DDT, DERA, DHRS1, DHRS12, DHTKD1, DPYS, ECHDC2, ECHDC3, ECHS1, EHHADH, EPHX2, FAAH, FAH, FDX1, FMO3, FMO4, FTCD, GAMT, GATM, GLYAT, GNE, GPHN, GRHPR, GSTA1, HAAO, HAGH, HAO1, HIBCH, HMGCL, HNMT, HSD17B6, HYAL1, IVD, KHK, LIPC, MAOB, MAT1A, MGST2, MMACHC, MTHFS, MTPP, NIT2, OTC, PAH, PAOX, PCCB, PCK2, PECCR, PEMT, PFKFB1, PGM1, PHYH, PIGV, PIPOX, PON1, PON3, PRODH2, QPRT, RBKS, RETSAT, SARDH, SCP2, SFXN1, SHMT1, SLC10A1, SLC17A2, SLC25A20, SLC27A5, SLC2A2, SLC37A4, SLC47A1, SLC6A12, SOD1, SORD, ST3GAL6, ST6GAL1, SULT2A1, SUOX, TF, THNSL1, UAP1, UPB1</i>

KEGG pathway annotation of *PRRX1* correlated genes

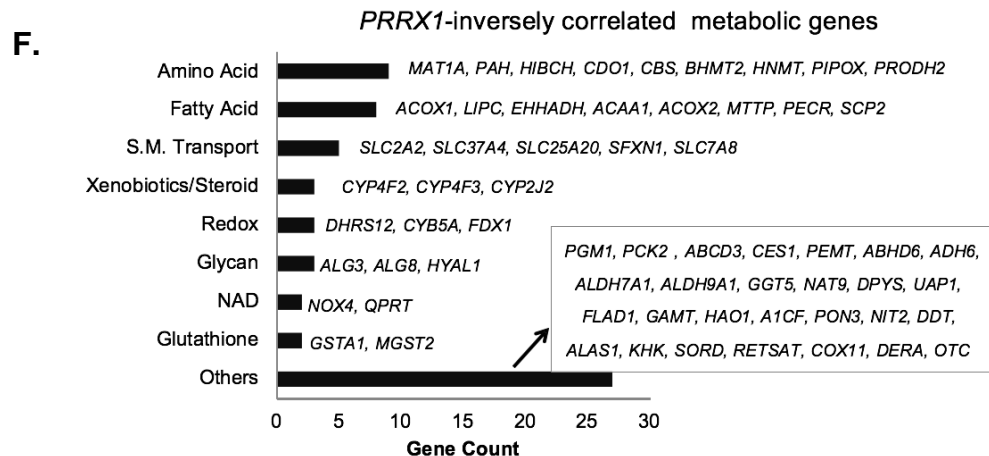
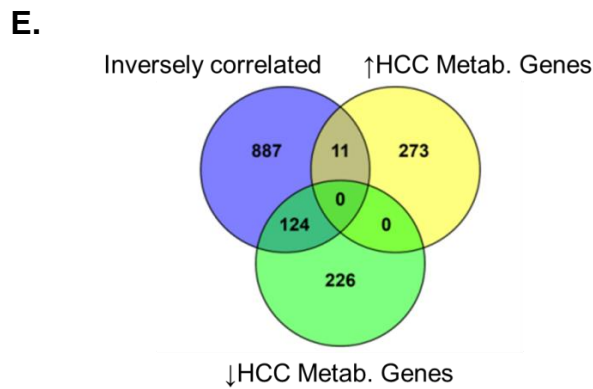
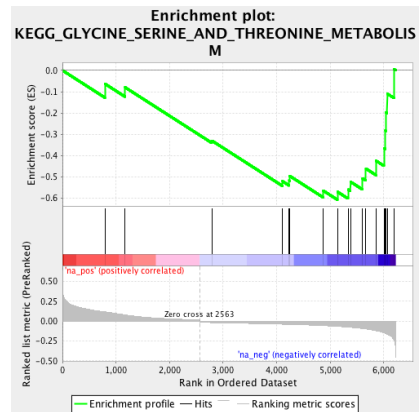
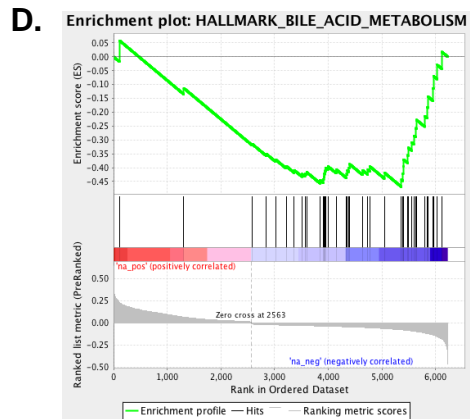
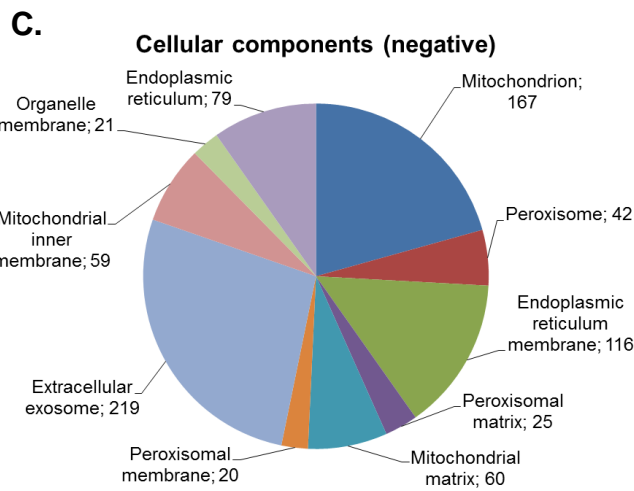
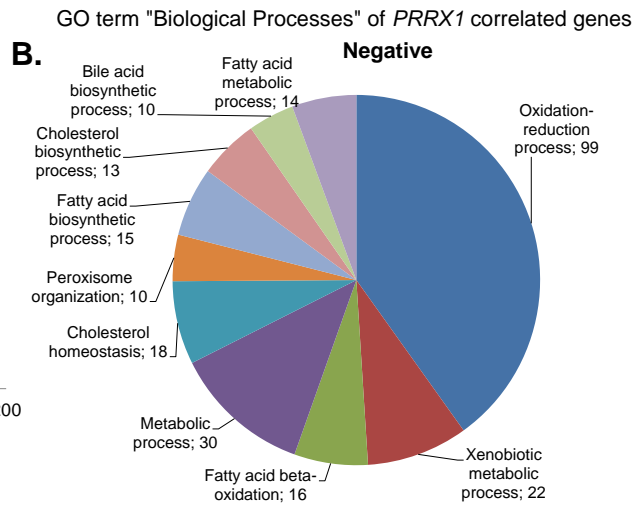
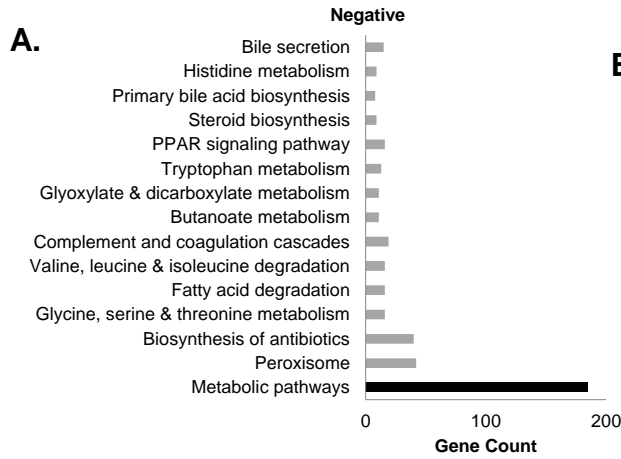


Figure 11. Functional enrichment analyses of *PRRX1* negatively correlated genes. (A) KEGG pathway annotation of genes negatively correlated with *PRRX1*. (B) Gene ontology 'biological process' of *PRRX1* negatively correlated genes. (C) Gene ontology 'cellular components' of *PRRX1* positively correlated genes. Numbers in B, C = gene count. (D) GSEA plot showing enrichment of bile acid metabolism and glycine, serine and threonine metabolism in the genes negatively correlated with *PRRX1*. (E) Venny diagram for number of genes inversely correlated with *PRRX1* in TCGA liver cancer data overlapped with genes consistently up or downregulated in HCC (Nwosu et al., 2017). (F) Metabolic processes reflected by genes inversely correlated with *PRRX1* in TCGA and altered in HCC. S.M. – small molecule, NAD – nicotinamide adenine dinucleotide.

4.3.2 *PRRX1*, glycolysis and the TCA cycle

4.3.2.1 Gene expression level

Altered metabolism is a known cancer hallmark. Given that patients tumor gene analysis linked *PRRX1* to metabolic processes, further *in vitro* experiments was focused on metabolic rearrangements in the context of *PRRX1*. Firstly, targets involved in glycolysis, glutaminolysis and TCA cycle were investigated. Therefore, *PRRX1* was knocked down in HUH7 and HLF cells and 48 h later, RNA was isolated to determine the expression levels of genes involved in metabolic processes. The results are presented in the following and are shown in **Figures 12A** and **12B**.

Glycolysis

One of the key characteristics of cancer cells is their increased glycolytic activity. The first step of glycolysis is catalyzed by hexokinase enzymes, HK1 and HK2. *HK1* is widely expressed in most normal adult tissue, whereas *HK2* expression in normal tissue is limited, it is overexpressed in cancer. Reduction of *PRRX1* in HUH7 cells significantly increased expression of genes regulated glycolysis pathway by induction of *HK1* (1.60 fold, $P < 0.01$) and *HK2* (1.95 fold, $P < 0.0001$) in HUH7 cells, while in HLF it caused a slight reduction of *HK1* and did not affect *HK2*. The transmembrane sodium-dependent transporter of amino acids *SLC1A5*, delivering pyruvate to glycolysis, was also increased by 1.42 fold ($P < 0.001$) in HUH7 cells, but unchanged in HLF. Further, the pyruvate dehydrogenase complex, *PDHX*, catalyzes the converting of pyruvate to acetyl coenzyme A, which links glycolysis to TCA cycle. *PDHX* was increased by 1.62 fold ($P < 0.0001$) upon reduction of *PRRX1* in HUH7 and reduced by 37% ($P < 0.0001$) in HLF cells. Then, pyruvate Kinase M 2 (*PKM2*) was

also affected by loss of *PRRX1*. Its expression was downregulated by 20% ($P < 0.01$) and 30% ($P < 0.01$) in HUH7 and HLF, respectively. This might change the transfer of a phosphoryl group from phosphoenolpyruvate to ADP for generating energy as ATP molecules and pyruvate during glycolysis. Furthermore, lactate dehydrogenase A and B (*LDHA*, *LDHB*) catalyze the conversion of pyruvate to lactate under anaerobic conditions and are key in glycolytic metabolism. The expression of *LDHA* was also increased by 1.96 fold ($P < 0.001$), while *LDHB* was reduced by 73% ($P < 0.05$) in HUH7. In HLF, both *LDHA* and *LDHB* were increased by 1.48 and 1.61 fold ($P < 0.001$, $P < 0.05$).

These results showed that *PRRX1* regulates prominent targets involved in glycolysis, and lactate synthesis.

Glutaminolysis

During glutaminolysis, glutamine is converted into glutamate and this process is highly activated in cancer cells. Thus, the genes encoding key enzymes in glutaminolysis (notably glutaminase, glutamate pyruvate transaminases and glutamic-oxaloacetic transaminases) were investigated after the knockdown of *PRRX1*. Glutaminase 1 (*GLS1*), an aminohydrolase enzyme, catalyzes the hydrolysis of glutamine to glutamate. Reduction of *PRRX1* increased *GLS1* by 1.67 fold in HUH7 cells and 1.13 fold in HLF cells ($P < 0.01$). Then, glutamate-pyruvate transaminases 1/2 (*GPT1* and its paralog *GPT2*) are enzymes that catalyze the reversible transamination between alanine and 2-oxoglutarate to generate pyruvate and glutamate, and therefore are important in the intermediary metabolism of glucose and amino acids. *GPT1* expression was significantly decreased (by 88%) in HUH7 and (by 61%) in HLF cells ($P < 0.01$), while *GPT2* was significantly increased (1.70 fold, $P < 0.01$) in HUH7 and decreased (by 13%, $P < 0.05$) in HLF upon reduction of *PRRX1*. Furthermore, glutamic-oxaloacetic transaminases 1/2 (*GOT1* and its paralog *GOT2*) are important regulators of glutamate and participate in the biosynthesis of L-glutamate from L-aspartate or L-cysteine. The level of *GOT1* after *PRRX1* knockdown was significantly increased by 1.13 fold ($P < 0.01$) in HUH7 cells, while decreased by 23% ($P < 0.0001$) in HLF cells. Expression of *GOT2* was significantly increased by 1.35 fold ($P < 0.01$) in HUH7 cells, while decreased by 35% ($P < 0.001$) in HLF cells upon reduction of *PRRX1* expression. Taken together, varying regulations were observed for targets involved in glutaminolysis in HUH7 and HLF cell lines. Reduced *PRRX1* influenced expression of

genes involved in glutaminolysis positively (except reduced *GPT1*) in epithelial HUH7 cells and negatively (except induced *GLS1*) in mesenchymal HLF cells.

The tricarboxylic acid cycle

TCA cycle is the main source of ATP for healthy cells and an important part of aerobic respiration. However, this cycle is often altered in cancer cells. Therefore, the influence of *PRRX1* on genes of the TCA cycle was investigated. Indeed, many genes involved in the TCA cycle were altered by *PRRX1* knockdown in HUH7 and HLF cells. For example, isocitrate dehydrogenases 3A/B (*IDH3A* and *IDH3B*) participate in catalysing of the oxidative decarboxylation of isocitrate to 2-oxoglutarate. Reduction of *PRRX1* significantly increased *IDH3A* and *IDH3B* by 1.27 fold ($P < 0.001$) and 1.17 fold ($P < 0.05$) in HUH7, respectively. In HLF cells, *IDH3A* was increased by 1.73 fold ($P < 0.05$), while *IDH3B* was reduced by 34% ($P < 0.01$) upon reduced *PRRX1*. Next, oxoglutarate dehydrogenase (*OGDH*) was increased upon *PRRX1* knockdown in HUH7 (1.68 fold, $P < 0.001$) and in HLF (1.52 fold, $P < 0.05$) cells, which might have consequences on the overall converting of 2-oxoglutarate (α -ketoglutarate) to succinyl-CoA. Then, expression of both succinate-CoA ligase GDP/ADP-forming subunit 1/2 (*SUCLG1/SUCLG2*) was reduced in HLF by 52% ($P < 0.01$) and 28% ($P < 0.05$), respectively, whereas in HUH7 cells, the knockdown of *PRRX1* did not significantly affect *SUCLG1*, but increased *SUCLG2* (1.86 fold, $P < 0.0001$), which might affect the converting of succinyl-CoA and ADP or GDP to succinate and ATP or GTP. Further, succinate dehydrogenase complex flavoprotein subunits A/ B/ C/ D (*SDHA/ SDHB/ SDHC/ SDHD*), under conditions of reduced *PRRX1* level, were induced by 2.46 fold ($P < 0.0001$), 1.27 fold ($P < 0.001$), 1.35 fold ($P < 0.001$) and 1.42 ($P < 0.0001$) fold in HUH7 cells, respectively. Similarly, induction of *SDHA* (1.75 fold, $P < 0.0001$), *SDHB* (1.15 fold, $P < 0.05$), *SDHC* (1.20 fold, $P < 0.01$) was observed in HLF cells, whereas only isoform D was reduced (by 35%, $P < 0.0001$). Thus, the electron transfer from succinate to ubiquinone might be affected. Then, fumarate hydratase (*FH*) was increased by 2.36 fold in HUH7 cells and by 1.63 fold in HLF cells in the *PRRX1* knockdown group ($P < 0.0001$), which might imply that the catalysis of L-malate from fumarate is altered. Furthermore, the expression of malate dehydrogenase 1 (*MDH1*) is significantly upregulated (1.25 fold, $P < 0.05$) upon reduction of *PRRX1* in HUH7, but was not changed in HLF cells. *MDH1* catalyzes the NAD/NADH-dependent, reversible oxidation of malate to oxaloacetate, which reacts with acetyl-CoA to form

citrate. Phosphoenolpyruvate carboxykinase 1 (PCK1) showed decreased expression upon *PRRX1* knockdown in HUH7 (by 36%, $P < 0.01$) and HLF (by 57%, $P < 0.001$) which is responsible for the regulation of gluconeogenesis.

To conclude, the reduction of *PRRX1* causes severe alterations in glycolysis, glutaminolysis and the TCA cycle (**Figure 13A & 13B**). The pattern of changes in HUH7 and HLF cells was not entirely overlapping. A strong upregulation of genes involved in glycolysis and the TCA cycle were observed in HUH7 cells, while in HLF the pattern was not the same for all targets. As changes in gene expression were observed, the next step was to investigate metabolite levels.

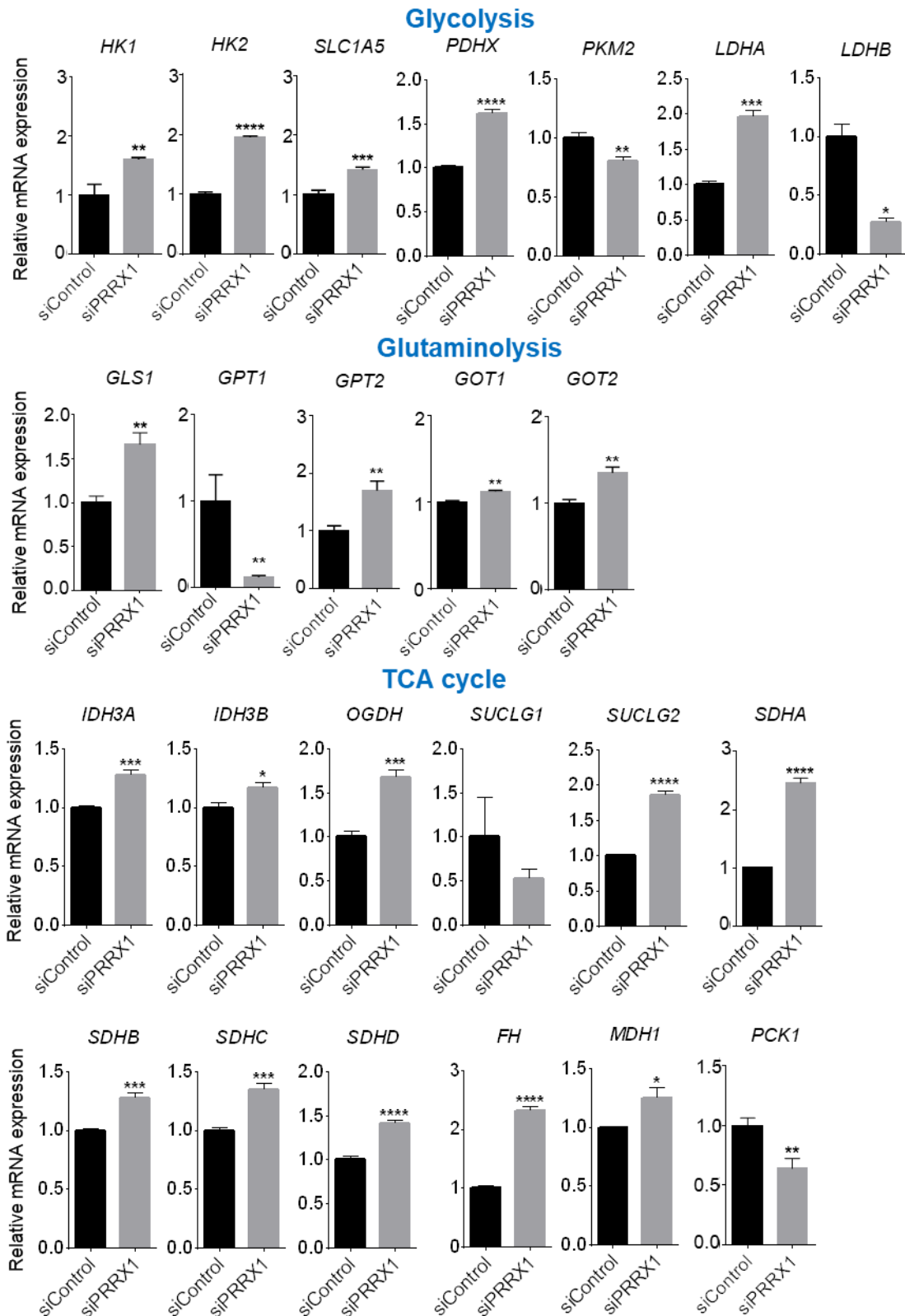


Figure 12A. Metabolic genes after knockdown of *PRRX1* in HUH7 cell line. Expression of indicated targets in glycolysis, glutaminolysis, the TCA cycle in HUH7 cells 48 h after *PRRX1* knockdown. Normalized to expression in cells transfected with non-targeted siControl.

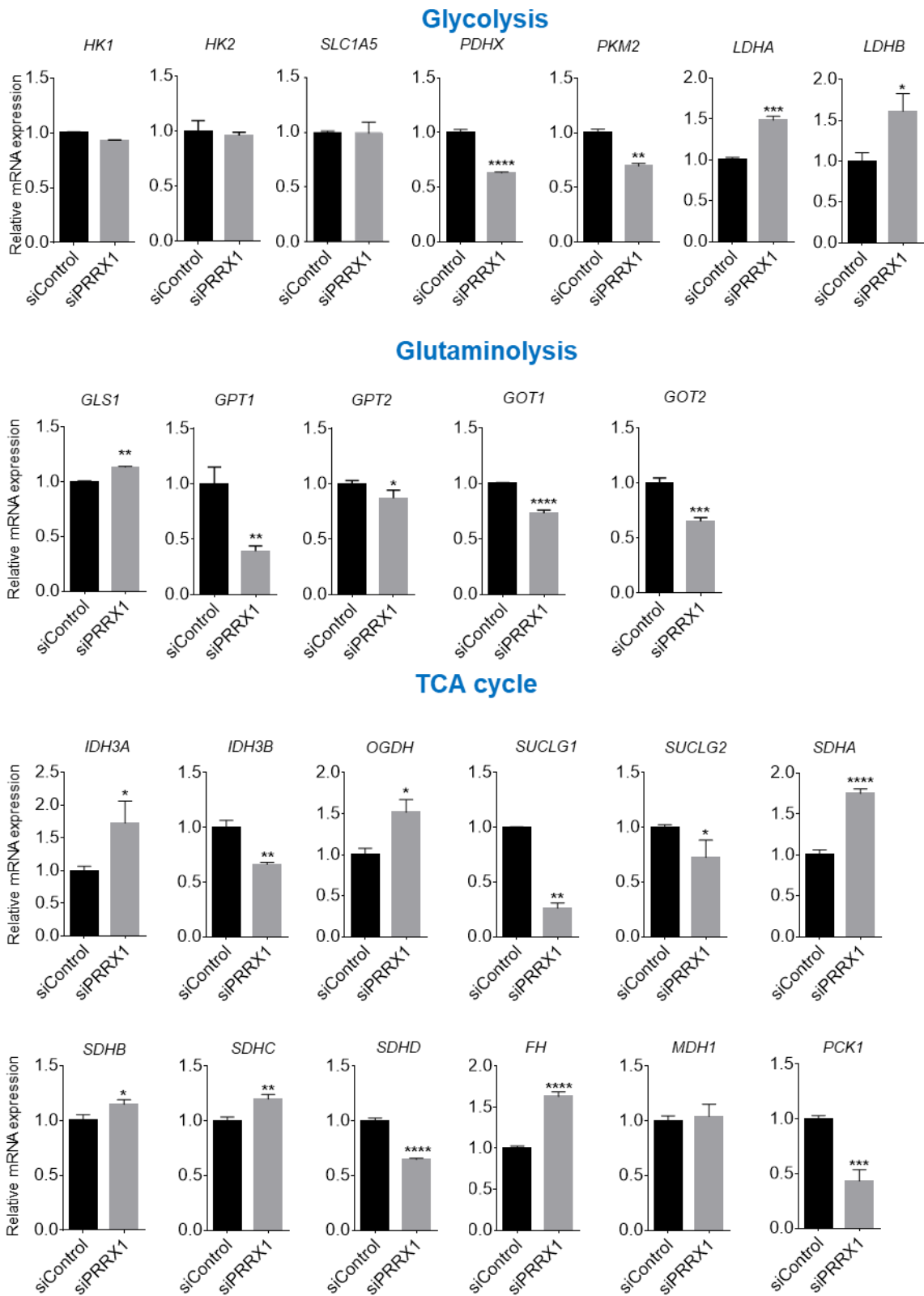


Figure 12B. Metabolic genes after knockdown of *PRRX1* in HLF cell line. Expression of indicated targets in glycolysis, glutaminolysis, the TCA cycle in HLF cells 48 h after *PRRX1* knockdown. Normalized to expression in cells transfected with non-targeted siControl.

4.3.2.2 Role in glucose consumption and lactate output

Following alterations in expression of metabolic genes after modulation of *PRRX1*, the aim was to establish a functional link with glycolysis, namely if the observed gene expression changes did also manifest on the metabolite level. Therefore, HUH7, SNU398 and HLF cells were used and glucose consumption and lactate output were measured from cell culture medium after modulation of *PRRX1* after 48 h. The knockdown of *PRRX1* led to an increase in glucose consumption in HUH7 (by 27.96%, $P < 0.01$) and HLF (by 16.1%, $P < 0.0001$) cells, while in SNU398 a non-significant increase by ~ 14% was determined (**Figure 13**). Furthermore, lactate output was significantly increased (by 13.34%, $P < 0.01$) in HUH7 and (by 17.77%, $P < 0.05$) SNU398 cell lines, while HLF cells showed only a slight tendency (~ 6%, $P = 0.40$) in the same direction (**Figure 13**). These data support the findings that *PRRX1* increases glycolytic activity, i.e. in terms of glucose consumption and lactate secretion, irrespective of the differentiation state of the cell.

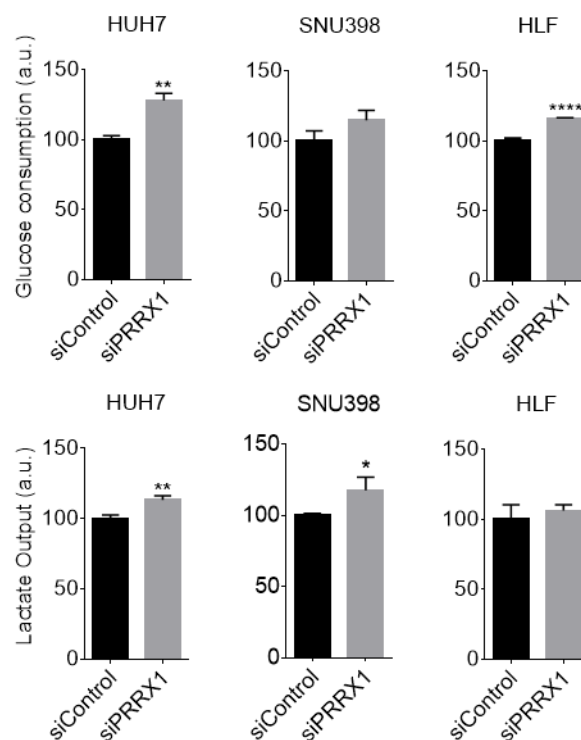


Figure 13. Biochemical parameters of glycolysis. Glucose consumption and lactate output as measured 48 h after siPRRX1 transfection. Bars indicate mean \pm SD and a representative figure of 2 experiments is shown, each in triplicates.

4.3.2.3 Alteration of metabolites in sugar metabolism and the TCA cycle

Next to the alterations in glucose consumption and lactate output, the aim was to determine whether *PRRX1* affects metabolites involved in sugar metabolism in general and TCA cycle. Therefore, metabolomics profiling was carried out following the knockdown of *PRRX1* in HUH7 and HLF cells using gas chromatography-mass spectrometry. Results on different metabolic pathways are presented in the following and are shown in **Figure 14**.

Sugar metabolism/Glycolysis

Glycolysis converts glucose to pyruvate via a series of intermediate metabolites and as shown in chapters 4.3.2.1 and 4.3.2.2, factors and metabolites were changed by *PRRX1* knockdown. In addition, metabolomics revealed that *PRRX1* influences levels of some other key metabolites. Reduction of *PRRX1* significantly increased glucose 6-phosphate (Glc-6-P, 2.24 fold, $P = 0.006$), fructose-6-phosphate (Frc-6-P, 3.37 fold, $P = 0.03$) and glycerol (1.74 fold, $P = 0.02$). Hexose ($P = 0.67$, $P = 0.30$), gluconic acid phosphatate ($P = 0.61$, $P = 0.80$), glycerol-3-P ($P = 0.23$, $P = 0.24$), sorbitol ($P = 0.45$, $P = 0.64$), phosphoenolpyruvic acid (PEP) ($P = 0.32$, $P = 0.32$), and pyruvic acid ($P = 0.30$, $P = 0.65$) showed no significant changes in HUH7 and HLF, respectively.

The tricarboxylic acid cycle

Due to observed changes in expression of genes involved in TCA cycle upon *PRRX1* modulation, the level of key metabolites were investigated for a broader understanding of the function of *PRRX1* regarding TCA cycle. Pyruvate created by glycolysis is converted into acetyl-CoA, fuelling the TCA cycle. The condensation of acetyl-CoA with oxaloacetate then leads to formation of citrate. Reduction of *PRRX1* abundance led to a significant upregulation of citric acid (2.87 fold, $P = 0.006$) and α -ketoglutarate (2.81 fold, $P = 0.001$), key intermediates of isocitrate metabolism, in HUH7 cells. In contrast, effects in HLF cells were less pronounced. Citrate was downregulated (reduced by 43 %, $P = 0.02$), while α -ketoglutarate was not altered. Then, the entire cycle can be divided into two phases: a) decarboxylating stage including conversion of citrate to succinyl-CoA and b) the reductive stage involving successive oxidation of succinate to fumarate, fumarate to malate and malate to oxaloacetate. Here, the reduction of *PRRX1* led to a significant upregulation of succinic acid (1.53 fold, $P = 0.03$) and malic acid (1.16 fold, $P = 0.01$), but did only affect fumaric acid ($P = 0.06$) in HUH7 cells by

tendency. In contrast, in HLF cells, a reduction of *PRRX1* caused significant downregulation of fumaric (reduced by 24%, $P = 0.03$) and malic acid (reduced by 33%, $P = 0.002$), but did not affect succinic acid ($P = 0.12$).

Further, α -ketoglutarate is used to synthesize glutamic acid. Glutamic acid may be also formed by glutamine and the reaction delivers pyroglutamic acid, which is an intermediate in glutathione metabolism. Reduction of *PRRX1* led to upregulation of glutamic acid (1.73 fold, $P = 0.002$) in HUH7 and to a downregulation (reduced by 29%, $P = 0.02$) in HLF.

Amino acid metabolism

There is a close connection of the TCA cycle with amino acid metabolism, and thus, *PRRX1* downregulation also affected amino acid abundance. Amino acids as substrates for protein synthesis can be divided into distinct groups: non-polar, polar, positively and negatively charged amino acids. Reduction of *PRRX1* significantly increased non-polar amino acid alanine in both, HUH and HLF (1.53 fold, $P = 0.01$; 1.18 fold $P = 0.0007$, respectively) cell lines. Glycine (1.32 fold, $P = 0.005$), phenylalanine (1.37 fold, $P = 0.05$) and methionine (2.28 fold, $P = 0.03$) were increased in HUH7, while not changed in HLF. In contrast to increased proline levels (2.35 fold, $P = 0.001$) in HUH7 cells, it was decreased (reduced by 16 %, $P = 0.07$) in HLF upon knockdown. Moreover, reduction of *PRRX1* led to upregulation of polar threonine (2.18 fold, $P = 0.01$) in HUH7, but did not change its level ($P = 0.31$) in HLF. *PRRX1* did not affect other amino acids, such as valine, tryptophan, isoleucine, leucine, cysteine, polar asparagine or positively charged lysine in both cell lines.

Taken together, complementing data on gene expression changes, *PRRX1* influenced intermediate metabolites of glycolysis and TCA cycle as well as affected levels of amino acids. Similar to the *in silico* analysis data, HUH7 cells showed a negative correlation of *PRRX1* with levels of many cell metabolites. A significant induction of several metabolites of glycolysis was observed in those cells after reduction of *PRRX1*. Furthermore, reduction of *PRRX1* led to a strong induction of several intermediate metabolites of the TCA cycle, followed by the induction of amino acids connected to TCA cycle (except serine, which was contrary to other changed metabolites reduced after knockdown of *PRRX1* in HUH7 cells). In stark contrast, alterations in HLF cells showed that lower number of metabolites were affected by the reduction of *PRRX1* compared to HUH7 cells and those changes showed positive correlation with *PRRX1*

expression. Regarding glycolysis of HLF cells, *PRRX1* reduced expression caused tendency to decreased level of intermediates metabolites. Moreover, several metabolites from TCA cycle were reduced after reduction of *PRRX1* expression. Further, reduction of *PRRX1* did not have impact on amino acids (except significantly induced alanine and reduced proline). The overview of metabolic changes in HUH7 and HLF cells under loss of *PRRX1* are presented in **Figures 15A and 15B**.

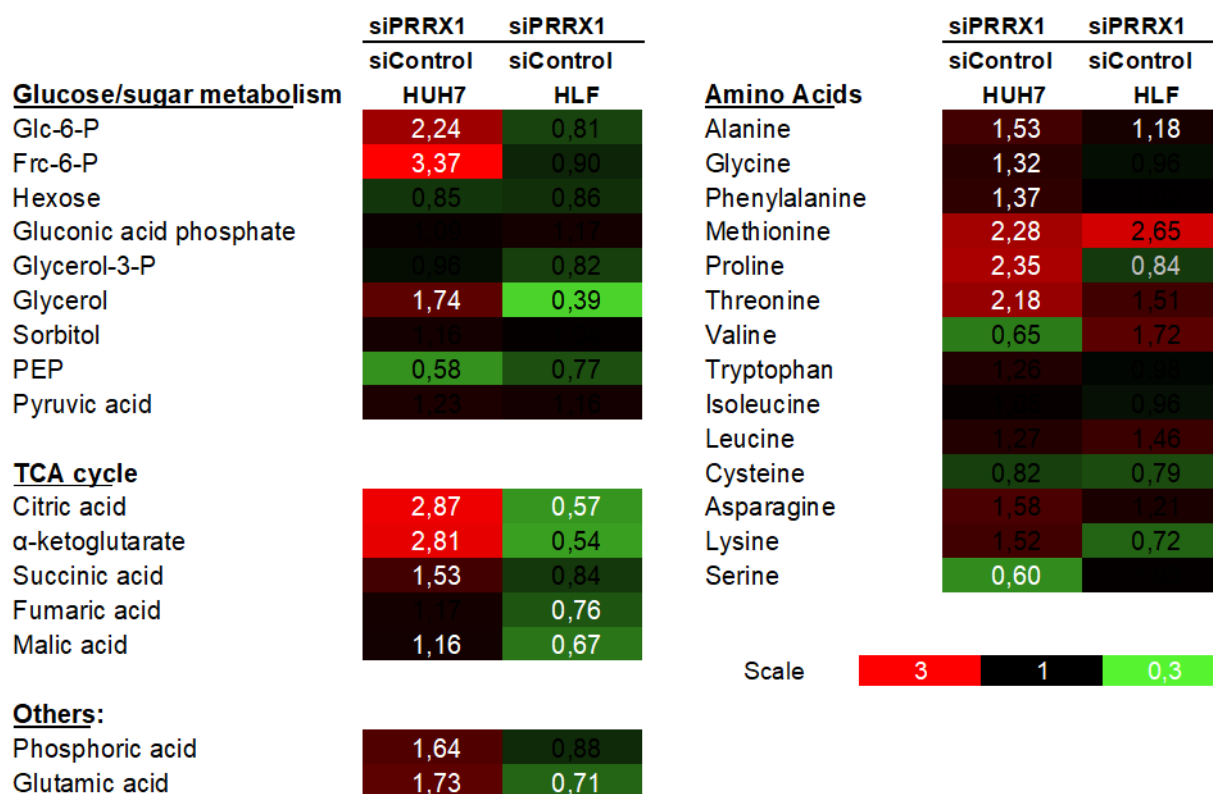


Figure 14. Alteration in metabolites. Heatmap of changes in metabolite levels of sugar metabolism, TCA cycle and amino acids in HUH7 and HLF cells 48 h after *PRRX1* knock down. White numbers for $P < 0.05$; black not significant. Experiment was performed in triplicates.

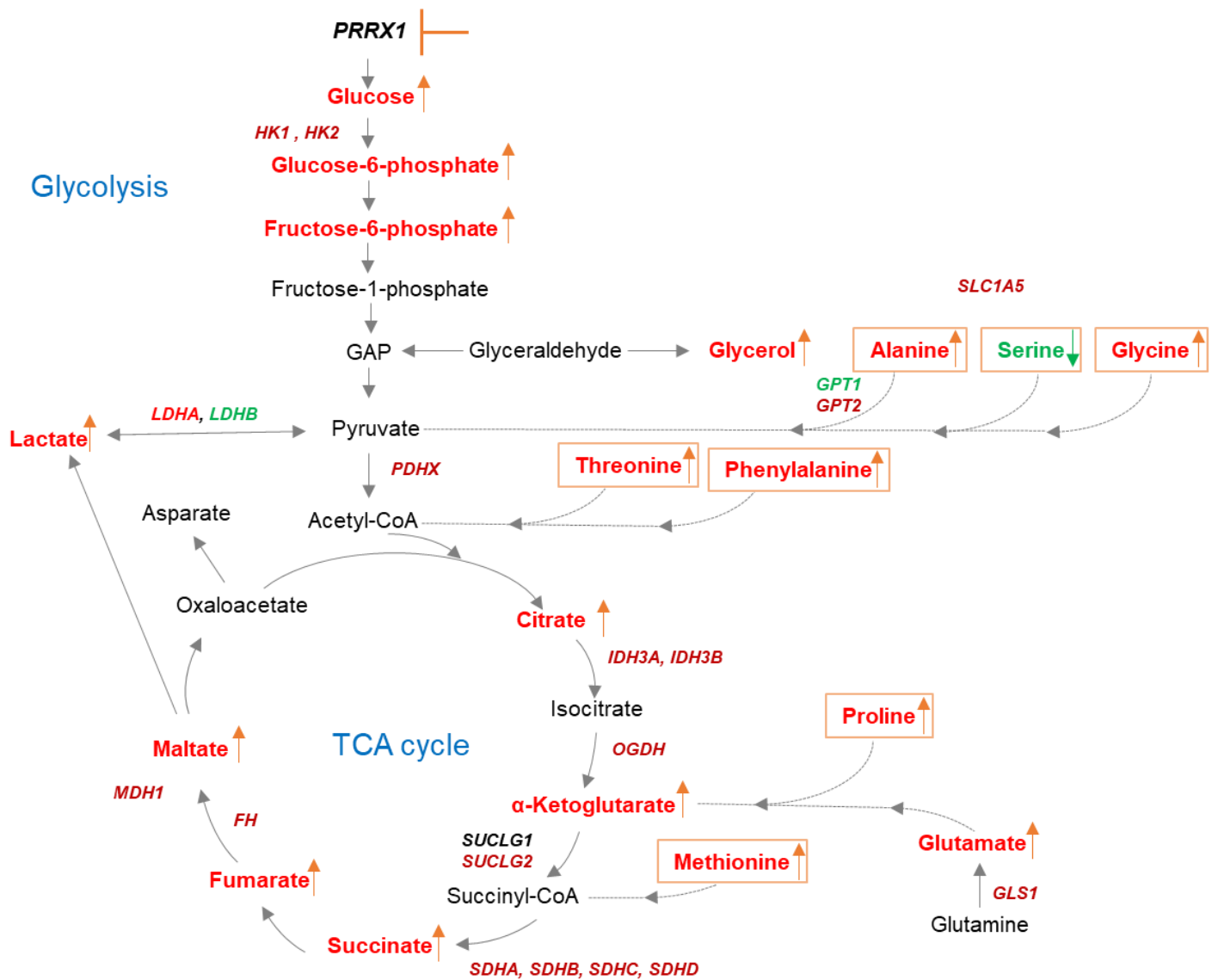


Figure 15A. Summary of metabolic changes after loss of *PRRX1* in HUH7 cells. Red = upregulation, green = downregulation, italics = genes, bold = dysregulated metabolites.

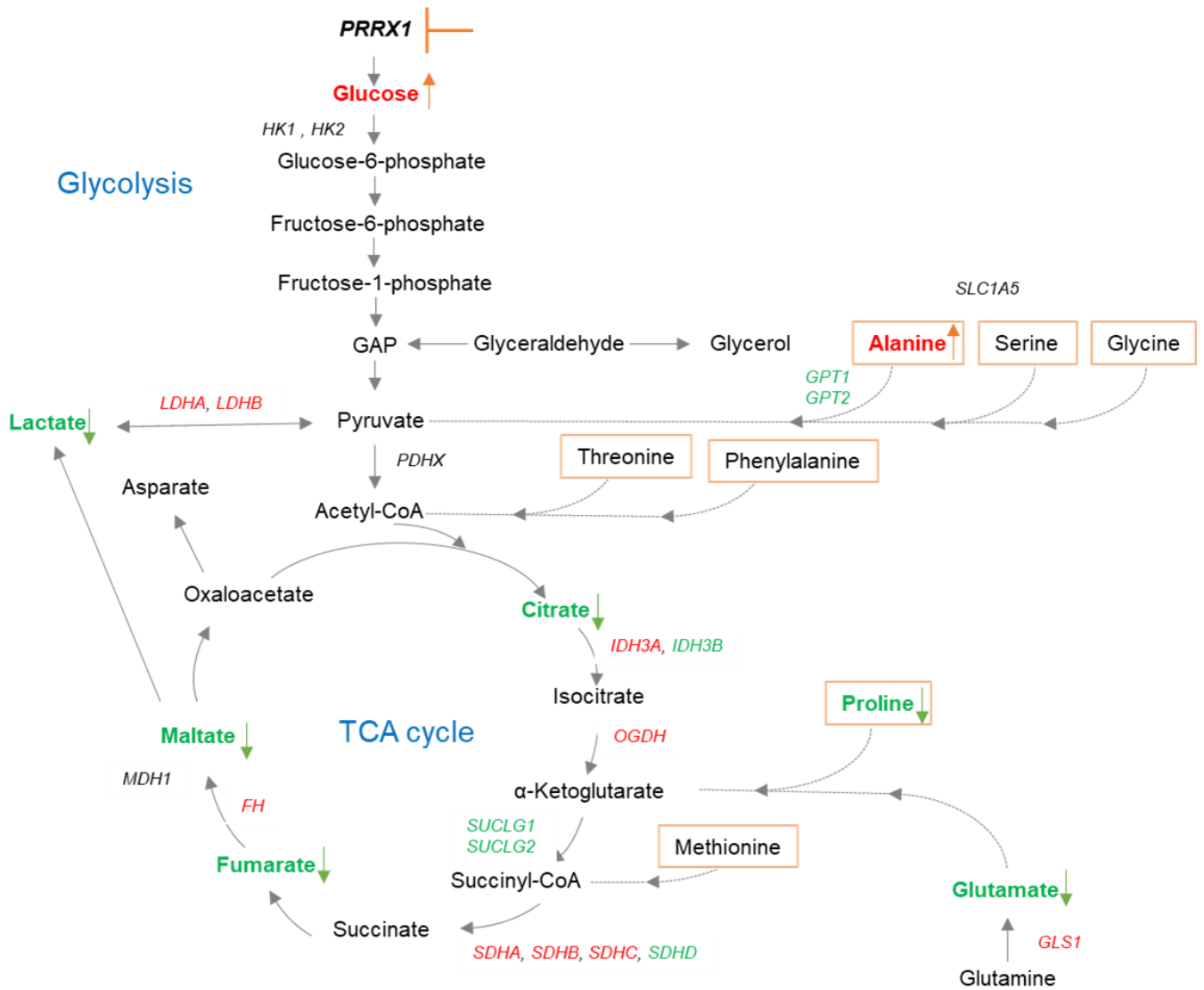


Figure 15B. Summary of metabolic changes after loss of *PRRX1* in HLF cells. Red = upregulation, green = downregulation, italics = genes, bold = dysregulated metabolites.

4.3.2.4 Alterations of ATP level

ATP is an organic compound that ensures energy to perform numerous processes in living cells (Bonora et al., 2012). ATP gives energy for processes in the cells by donating phosphate groups, following by the formation of either adenosine diphosphate (ADP) or adenosine monophosphate (AMP). ATP is produced with less efficiency by glycolysis (2 ATP invested and 4 ATP won, net yield 2 ATP) and with higher efficiency in the TCA cycle (the total energy balance of glucose degradation under aerobic conditions is +32 ATP per glucose molecule). As *PRRX1* influences glycolysis and TCA cycle, the aim was to proof whether *PRRX1* subsequently affects

the energy state of HCC cells. Therefore, *PRRX1* was knocked down in epithelial HUH7 and mesenchymal HLF cell lines. Subsequently, ATP level were measured using a luciferase-based assay in the cells 48 h after knockdown and data was normalized to protein concentration. Interestingly, in contrast to higher metabolite levels as measured by metabolomics in slower growing epithelial HUH7 cells, loss of *PRRX1* reduced the amount of available ATP by 40 % ($P < 0.01$) (**Figure 16**). Contradictory, faster growing mesenchymal HLF cells also showed 36 % ($P < 0.05$) reduction of ATP level in concert with reduced metabolites in TCA cycle (**Figure 16**). To conclude, reduction of *PRRX1* affects changes in ATP level by its reduction in HUH7 and HLF cell lines. Interestingly, *PRRX1* showed significant impact on metabolites of the TCA cycle, which are sources of ATPs under aerobic condition. In HUH7 cells, increased level of many metabolites from the TCA cycle was observed, while in HLF cells a tendency to their reduction was monitored. In any scenario, in both cell lines, a reduction of *PRRX1* leads to a reduction of ATP.

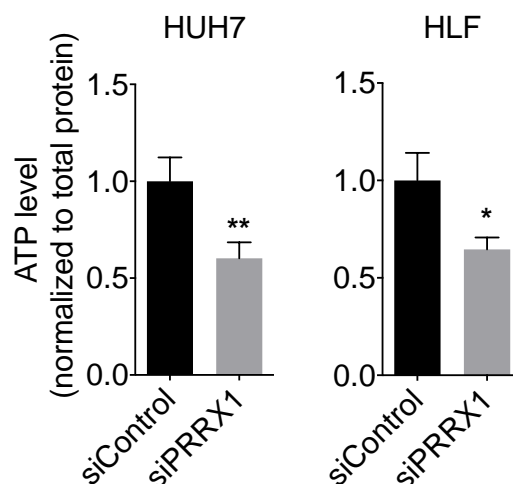


Figure 16. *PRRX1* and ATP level. ATP assay as measured 48 h after knockdown of *PRRX1*. Bars indicate mean \pm SD, n = 4 per group

4.3.3 *PRRX1* and fatty acid metabolism

4.3.3.1 Gene expression level

Alterations in lipid metabolism, and specifically the synthesis of fatty acids, could be additional aspects of metabolic reprogramming in cancer cells. Even more, in precancerous diseased livers, steatosis is a frequently observed. In this context, *in silico* analysis identified *PRRX1* as a factor involved in fatty acid metabolism. Thus, the aim was to measure whether *PRRX1* influences expression of genes involved in fatty

acid metabolism and regulation of total fatty acid levels in HCC cells. Therefore, *PRRX1* was knocked down in HUH7 and HLF cells and 48 h later, RNA and cell extracts were collected for gene expression analysis and measurement of cellular fatty acid levels. The results prove a correlation between *PRRX1* and expression of genes related to fatty acids (shown in **Figure 17A**) as well as changes in fatty acids upon loss of *PRRX1*, especially in HUH7 cells.

Acetyl-CoA carboxylase alpha / beta (*ACACA* and *ACACB*), acyl-CoA synthetase long chain family member 5 (*ACSL5*) and fatty acid synthase (*FASN*) were altered upon *PRRX1* modulation. Reduction of *PRRX1* induced *ACACA* (in HUH7 by 1.90 fold, $P < 0.0001$; in HLF by 1.44 fold, $P < 0.01$) and reduced *ACACB* (in HUH7 by 65 %, $P < 0.01$; in HLF by 48 %, $P < 0.01$). This might affect the carboxylation of acetyl-CoA to malonyl-CoA and *de novo* fatty acid biosynthesis. Further, *ACSL5* was tremendously increased by 5.93 fold in HUH7 ($P < 0.0001$) and 3.40 fold in HLF cells ($P < 0.01$), which might influence degradation of fatty acids. Moreover, reduction of *PRRX1* led to a significant induction of *FASN* in HUH7 (3.60 fold, $P < 0.01$) and HLF (1.19 fold, $P < 0.05$), which might influence the conversion of acetyl-CoA and malonyl-CoA to the 16-carbon fatty acid palmitate. Moreover, carnitine palmitoyltransferase 2 (*CPT2*) was significantly increased (2.34 fold, $P < 0.0001$) upon reduction of *PRRX1* in HUH7 and not significantly changed in HLF cells. This alteration might influence oxidation of long-chain fatty acids in the mitochondria of HUH7 cells.

Taken together, *in silico* analysis identified *PRRX1* as a factor involved in fatty acid metabolism and this connection was further confirmed *in vitro* in HCC cell lines. The reduction of *PRRX1* caused upregulation of genes regulating fatty acid biosynthesis and oxidation, given that *PRRX1* plays a role in those processes in tested HUH7 and HLF cell lines. This observation is consistent with what has been found in previous *in silico* work.

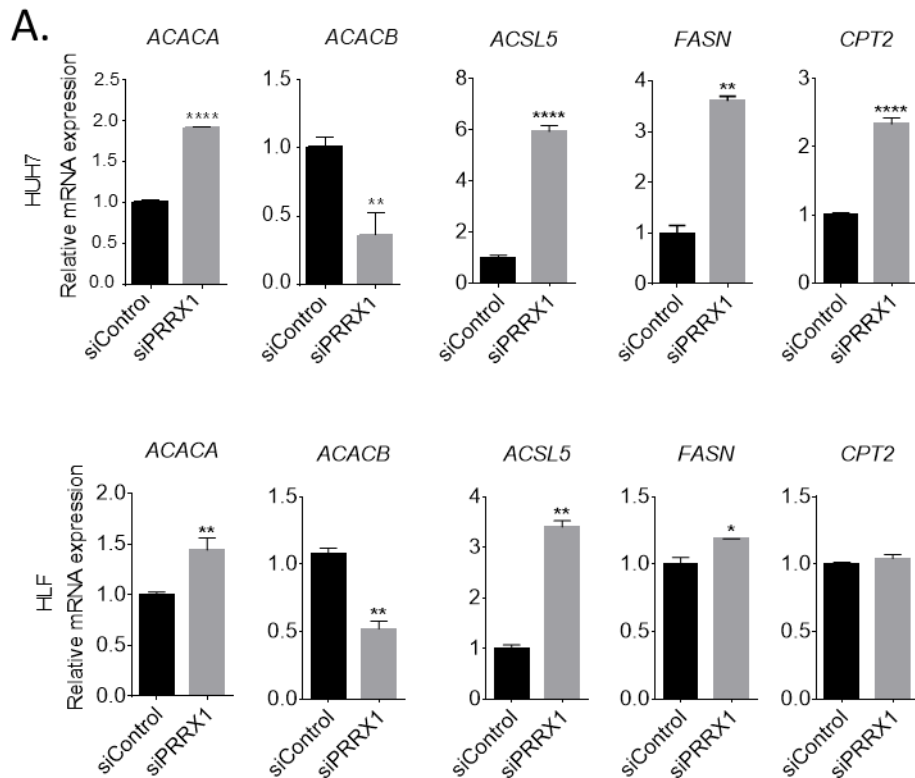
4.3.3.2 Total fatty acid / metabolites

Fatty acids are essential for cells, partially because they are used for membrane biosynthesis and provide an important energy source during conditions of metabolic stress. Due to *in silico* prediction and measurement of expression of genes related to fatty acids, the level of fatty acids were measured in HCC cells upon modulation of *PRRX1*. Therefore, the lipid fraction of cell samples collected (chapter 4.3.5) was used for analysis of long-chain fatty acids and cholesterol to determine whether *PRRX1*

plays a role in synthesis and metabolism. In general, a reduction of *PRRX1* caused a tendency to increased levels of fatty acids in HUH7 cells and decreased levels in HLF (**Figure 17B**), but many values did not reach significance, especially in HLF cells. Palmitic acid (16:0) is the most common saturated acid (Parisi, Li, & Atilla-Gokcumen, 2017), while palmitoleic acid (16:1) is a unique monounsaturated fatty acid that is formed nearly only through desaturation of palmitic acid (Duckett, Volpi-Lagrecia, Alende, & Long, 2014). The physiological role of palmitic acid is the preservation of a definite tissue concentration and repartition in different lipid classes, which requires a fine regulation of its metabolism (Carta, Murru, Banni, & Manca, 2017). Interestingly, reduction of *PRRX1* did not affect palmitic acid in both, HUH7 and HLF cells. Nevertheless, increased palmitoleic acid (desaturated palmitic acid) levels were observed in HUH7 (1.62 fold, $P = 0.006$), while a tendency to decreased levels in HLF cells ($P = 0.18$) was found. Palmitoleic acid is important for several cellular processes, i.e. fat synthesis and storage, cell differentiation and proliferation, portrays the different roles in cells, which might be affected by *PRRX1*. Then, elaidic acid (C18:1n:9t), also termed trans-oleic acid, an unsaturated fatty acid, was significantly increased (1.31 fold, $P = 0.01$) in HUH7 cells and but not changed in HLF ($P = 0.30$) upon *PRRX1* knockdown. This lipid is typically integrated in the plasma membrane of cells and has been shown to induce glucose-regulated protein (GRP), an endoplasmic reticulum chaperone protein whose expression is induced during oxidative stress (Cassagno et al., 2005), indicating that elaidic acid promotes ROS accumulation, and *PRRX1* might play a role in this process. Interestingly, the cis form of elaidic acid - oleic acid (C18:1n:9c), is a more prooxidative factor. It has been also documented that erucic acid (cis-13-docosenoic, C22:1n:9, a monounsaturated fatty acid) was very rapidly transformed into oleic acid in the liver (Hopf, Hopf, Kober, Kaltenbach, & Riemann, 1975). The level of erucic acid was increased in HUH7 (1.34 fold, $P = 0.008$) and decreased in HLF cells (reduced by 32%, $P = 0.02$), nevertheless the level of oleic acid was not affected by *PRRX1* in both HUH7 and HLF cells. Moreover, eicosanoic (arachidic acid, C20:0), eicosenoic (gondoic acid, C20:1n-9), eicosadienoic (C20:2) acids were increased in HUH7 cells (1.67 fold, $P = 0.03$; 1.48 fold $P = 0.04$; 1.38 fold, $P = 0.04$, respectively), but not in HLF, which showed only a tendency to decreased eicosenoic acid levels. Then, the saturated behenic acid (docosanoic acid, C22:0) was significantly increased in HLF (1.12 fold, $P = 0.01$) cells and showed also a tendency to upregulation in HUH7. Lignoceric acid (tetracosanoic acid, C24:0) belongs to very

long chain fatty acids and did not change in HUH7 but was significantly decreased in HLF (reduced by 24%, $P = 0.005$). Measured fatty acids are important parts of membrane integrity, are used as energy sources and play a role in energy storage, which suggests that *PRRX1* might affect those processes. Other analyzed fatty acids with shorter chains were not affected by *PRRX1* in HUH7 cells. Interestingly, in HLF cells *PRRX1* affected only three measured very long chain fatty acids, but had no effect on shorter chain fatty acids as well. With regard to cholesterol, whose incorporation in membranes reduces fluidity and consequently inhibits metastasis by limiting the morphological changes and motility of the cells (Zhao et al., 2016), no effects of *PRRX1* were documented.

In summary, the reduction of *PRRX1* showed a negative correlation with levels of distinct fatty acids in HUH7 cells. Its reduced expression led to increased synthesis of several analyzed fatty acids involved in e.g., cell membrane stabilization, being energy sources and storages in HUH7 cells. In contrast, in poorly differentiated HLF cells levels of a few fatty acids were significantly changed upon loss of *PRRX1*. Besides of that, a general trend towards downregulation was observed for most measured metabolites. The slight changes observed in HLF cells might be due to a general lower expression level of *PRRX1* in those cells and also a lower efficiency of *PRRX1* knockdown. Loss of *PRRX1* affected very long chain fatty acids by downregulation (eurucic and lignoceric acids), except behenic acid, but did not affect several other important fatty acids. Nevertheless, those analyses showed that *PRRX1* takes part in fatty acid metabolism of HCC cells. Its effect is more pronounced in well-differentiated HUH7 (negative correlation) than in poorly differentiated HLF (positive correlation) cells, which might be connected to differences in metabolic gene expression profiling and metabolites level in those cell lines.



B.

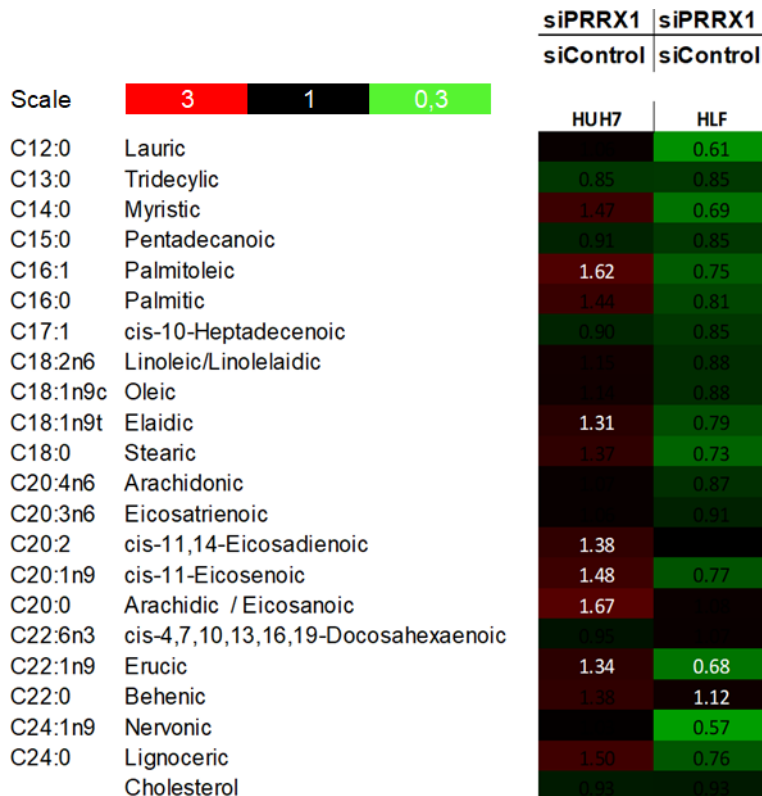


Figure 17. Alteration in fatty acids in HCC cells. (A) Expression of indicated targets in HUH7 and HLF cells 48 h after *PRRX1* knockdown. Normalized to expression in cells transfected with non-targeted siControl. **(B)** The heatmap of changes in level of fatty acids in HUH7 and HLF cells 48 h after *PRRX1* knock down. White numbers for $P < 0.05$; black not significant. Experiment was performed in triplicates.

5 DISCUSSION

5.1 *PRRX1* expression in HCC

PRRX1 expression and its role in HCC is not well described. Previously, *PRRX1* expression regulation has been investigated in breast, colorectal and pancreatic cancer (Ocana et al., 2012), (Reichert et al., 2013), (Takahashi et al., 2013). Then, Hirata and Fan with colleagues investigated the expression of *PRRX1* in HCC (Hirata et al., 2015), (Fan et al., 2017), but in a small set of patients samples. Therefore, in this study, the bioinformatics analysis of a large cohort covering > 1.400 HCC tumour samples was performed to resolve the expression pattern of *PRRX1* in HCC. *PRRX1* is frequently upregulated or not changed, but no downregulation was found in human HCC cohorts, suggesting that its function is significant in HCC. These findings are in line with data from Hirata.

Additionally, HCC cell lines provide evidence of variable *PRRX1* level, with a notable low expression in HLF. Nevertheless, *PRRX1* level did not clearly enable discrimination of well from poorly differentiated HCC cell lines unlike we and others have shown for other proteins, e.g. caveolin-1, albumin, alpha fetoprotein, SMADs, and WNT signaling targets (Yuzugullu et al., 2009), (Cokakli et al., 2009), (Dzieran et al., 2013), (Meyer et al., 2013). Furthermore, the expression pattern of *PRRX1* isoforms, *PRRX1a* and *PRRX1b*, is not known in human patient samples. However, in HCC cell lines, this study now provides information. Except for SNU398, in the HCC cell lines tested in this study, *PRRX1b* isoform is expressed higher than *PRRX1a*. Future studies are required to determine the ratio in human patients, as functional differences were described, e.g., in pancreatic cancer overexpression of *PRRX1a* caused the induction of genes involved in cell migration, whereas *PRRX1b* was involved in regulation of cell cycle processes (Reichert et al., 2013). Furthermore, the knockdown of *PRRX1b* inhibited proliferation as well as migratory and invasive capabilities of triple negative (does not have estrogen, progesteron and human epidermal growth factor receptors) breast cancer cell lines, showing the importance of future analyses of *PRRX1* isoform expression in human samples.

5.2 TGF- β as regulator of *PRRX1* expression

As *PRRX1* was previously linked to EMT (Mitchell et al., 2006) and TGF- β is the major EMT mediator (Ungefroren, 2019), a potential connection of those factors in HCC was studied. TGF- β triggers *PRRX1* expression in all four tested HCC cell lines. HUH7 cells showed stronger induction after TGF- β treatment compared to the HLF cell line, though basal expression level is relatively high compared to HLF. Similarly, Ocana et al. described *PRRX1* as a TGF- β target in MDCK cells, and Hardin et al. in human thyroid cancer cell lines as TGF- β induced expression of *PRRX1* in those cells (Ocana et al., 2012), (Hardin et al., 2014). A positive correlation was found for expression of *PRRX1* and TGF- β 1-3 as well as their receptors in human HCC samples. Interestingly, this observation is supported by data describing a positive feedback loop between TGF- β and *PRRX1*, because *PRRX1* overexpression led to increased expression of TGF- β 2 and TGF- β 3 in preadipocytes (Du et al., 2013). As consequence, induction of *PRRX1* may increase TGF- β signaling, or even modulate signaling by different TGF- β isoforms (TGF- β 1, -2, and -3). Thus, the mechanisms of *PRRX1* regulation by TGF- β (s) need further investigation.

5.3 The functions of *PRRX1* in HCC

Information about functions of *PRRX1* in HCC is scarce. *In silico* prediction revealed a direct functional correlation between *PRRX1* and stroma remodeling, i.e. the extracellular matrix, modulation of signal transduction activities, reorganization of the cytoskeleton and changes in adhesion - all processes which are related to cancer. The exact role of *PRRX1* in controlling the predicted processes needs empirical validation, especially given that the knockdown of *PRRX1* induced pro-cancer activities, but that its high expression in human tumors had marginal clinicopathological correlation. In this work, and consistent with the previous report by Hirata and colleagues (Hirata et al., 2015), *PRRX1* level did not correlate with several clinical parameters (tumour size, BCLC and TNM staging, ALT and AFP). However, Hirata et al. found in the same cohort as analyzed here, that high *PRRX1* expression predicted significantly longer OS. In this study, only a trend was observed (not significant). This discrepancy may be attributed to differences in the number of samples used for the OS analysis. They analyzed 146 samples with high *PRRX1* and 96 with low *PRRX1* expression, while here were analyzed 111 and 110 samples, respectively. It is not clear why a higher

number of HCC patients was available at the time Hirata et al. conducted the study, probably they collected data from the two platforms (GPL571, GPL3921), thus they got higher number of samples in HCC group, but they do not provide this information in their work. The study by Fan et al. (Fan et al., 2017) also points to a favorable outcome with high *PRRX1* (determined by immunohistochemistry), as low expression correlated with vascular invasion, intrahepatic and distant metastasis as well as advanced tumour stage. Thus, based on the pattern of association with clinical parameters observed by others and here, *PRRX1* can be considered as a tumour suppressor in HCC. Interestingly, Takahashi and colleagues reported contradictory results for patients with colon cancer, where they showed poor OS for patients with high expressed *PRRX1* in cancer cells (Takahashi et al., 2013), which suggests distinct functions of *PRRX1* in different types of cancer.

In previous studies, *PRRX1* had been described as EMT gene (Ocana et al., 2012), (Reichert et al., 2013), (Takano et al., 2016) and prior studies linked *ZEB1* with unfavourable clinical outcome in HCC (T. Wan et al., 2017), (Hashiguchi et al., 2013). Interestingly, EMT genes *ZEB1/2* were identified as specific candidates that together with *PRRX1* impact on clinical OS outcome. *PRRX1* is significantly correlating with *ZEB1/2* in several HCC cohorts analyzed. Whereas none of the three genes independently predicted overall survival in the datasets, high *PRRX1* and either low *ZEB1* or high *ZEB2* expression predicted a better OS, but no other clinicopathological variables were affected. Noteworthy, no study yet describes whether *PRRX1* and *ZEB1/2* expression are interdependent. Thus, *in vitro* *ZEB1/2* expression was measured in HCC cells upon knockdown of *PRRX1*. A reduction confirmed a causal correlation between *PRRX1* and *ZEB1/2*, and most pronounced for *ZEB1*. In addition, the expression of other EMT targets was measured. As indicted by alterations in EMT markers, the epithelial phenotype of HUH7 was stabilized upon reduction of *PRRX1* expression (except of *SNAI1* - its expression was not decreased as hypothesized). In this context, Ocana et al. showed in their previous breast cancer study that *PRRX1* overexpression induces EMT related transcription factors, but not *SNAI1* (Ocana et al., 2012). A contradictory effect of reduced *PRRX1* was shown in mesenchymal HLF cells. Those cells did change expression of the epithelial marker *CDH1* upon *PRRX1* knockdown. Nevertheless, in this cell line, a tendency was found towards a decrease of mesenchymal markers (except *SNAI1*). Thus, *PRRX1* is able to modulate expression of EMT related factors.

Furthermore, cell migration was analyzed upon reduction of *PRRX1* as a connection has been shown before. For instance, Reichert et al. reported increased cell migration upon *PRRX1* overexpression in pancreatic cancer cells (Reichert et al., 2013), while Fan et al. showed increased migration upon loss of *PRRX1* in HCC cell lines HEPG2 and SMMC7721 (Fan et al., 2017). However, when tested in other cell lines in this work, migration was increased in HUH7 and reduced in HLF cells. Noteworthy, the differentiated cell line HUH7 migrated more after the loss of *PRRX1*, but at the same time the epithelial phenotype was stabilized, as indicated by alterations in EMT markers. In contrast, mesenchymal HLF cells migrated less, but did not change expression of the epithelial marker *CDH1* upon *PRRX1* knockdown. Nevertheless, in this cell line, a tendency was found towards a decrease of mesenchymal markers (except *SNAI1*). Thus, *PRRX1* is a factor that influences migration and modulates expression of EMT markers in HCC. However, the phenotypical observations are not entirely reflected by the expression analyses. This could be due to a more complex control of cell behaviour involving other crucial proteins. To summarize, in HCC, *PRRX1* could be considered as a new key regulator of plasticity processes.

PRRX1 influences cancer cell proliferation. Lv et al. reported decreased cell proliferation upon silencing of *PRRX1b* in the MDA-MB-231 cell line (Lv et al., 2016). In contrast, in this study we observed an increased proliferation upon *PRRX1* knockdown (except in SNU398, which showed no change), which supports the conclusion of a growth-suppressive function of *PRRX1* in HCC. The observation of a proliferation phenotype, even in the cells with comparatively low basal *PRRX1* (i.e. HLF), raises another possibility that certain functions of *PRRX1* are conserved in the different HCC cell lines regardless of basal expression. Nevertheless, HLF cells showed a reduction of proliferation markers upon knockdown. In addition to that, these cells showed higher level of caspase 3 activities, which is not surprising for fast growing poorly-differentiated cells – increased proliferation rates could relate to elevated apoptosis. Further, in contradiction to the study in colon cancer (Takahashi et al., 2013) and similar to the report of Ocana et al., the reduction of *PRRX1* led to higher capacity to form colonies. This effect was most pronounced in SNU398 cells. Then, considering the *PRRX1* isoforms, most HCC cells expressed more *PRRX1b* isoform than *PRRX1a*. The exception was SNU398, which showed no change in proliferation after *PRRX1* knockdown, but high induction to form cell colonies. Thus, it could be speculated that *PRRX1a*, rather than *PRRX1b* is involved in proliferation in HCC. Further functional

studies will be required to clearly resolve the conditions under which *PRRX1* may exert specific functions in HCC and the exact contribution of the isoform ratio.

Furthermore, *in silico* analysis predicted that *PRRX1* likely acts by repressing metabolic events in HCC. The data suggested a strong connection to amino acid and fatty acid metabolism. Before, the link between *PRRX1* and metabolism in cancer was not well understood. In this study, we could show that *PRRX1* regulates gene expression of prominent targets involved in the TCA cycle, glutaminolysis, as well as sugar and lipid metabolism in HCC cell lines. Based on this, *PRRX1* should be considered as an important factor in HCC metabolism. Interestingly, the knockdown of *PRRX1* promoted the Warburg effect in HCC cells as glucose turnover and lactate output were increased. In concert with that, the expression of key factors in glucose metabolism were induced upon the loss of *PRRX1*. Noteworthy, a recent genome-wide association study (GWAS) by Timmons et al. (Timmons et al., 2018) reports on a pattern that links type II diabetes sensitivity with gene expression patterns. The authors showed that *PRRX1* is positively linked with insulin sensitivity, supporting the finding that *PRRX1* is linked to glucose metabolism. Furthermore, the pentose phosphate pathway plays an important role in regulating cancer cell growth by giving to the cells not only ribose-5-phosphate, but also NADPH for detoxification of intracellular reactive oxygen species, reductive biosynthesis, and ribose biogenesis (Harris et al., 2015). It is known that cancer cells prefer glycolysis to generate energy, however, metabolites profiling as well as a gene expression analysis upon loss of the *PRRX1* suggested not only induction of glycolysis, but also the TCA cycle in HUH7 cells. Interestingly, despite the induction of both processes, ATP level were reduced upon *PRRX1* knockdown. This contradiction needs further investigations. In contrast, HLF cells showed induction in glycolysis, but reduction in TCA cycle activity, indicating that these cells utilize mainly glycolysis to produce energy. Surprisingly, also here, total ATP level were decreased upon reducing *PRRX1*. Thus, *PRRX1* affected changes of ATP level in HUH7 and HLF cells are independent of TCA cycle alterations.

Amino acids, metabolites closely related to the TCA cycle and energy production, are also affected by *PRRX1*. In agreement with results of the *in silico* analysis, except serine, which is decreased by reduction of *PRRX1*, altered amino acid levels negatively correlated with *PRRX1* expression in HUH7 cells. Then, alterations in free fatty acid metabolism are frequently observed in cancer cells (Santos & Schulze, 2012). Jiang and colleagues reported a significant association of high *PRRX1* expression with high

free fatty acids levels in salivary adenoid cystic carcinoma patients (Y. P. Jiang et al., 2020). In contrast, but in agreement with *in silico* data, in this work, a reduction of *PRRX1* showed a negative association with increased levels of fatty acids in HUH7 cells. Observed alterations in amino acids and fatty acids levels indicated another energy sources for cancer cells upon loss of *PRRX1*. Those observations reflect a tumour suppressive function, even though more studies are required to validate the role of *PRRX1* in cell metabolism.

Evidence from prior studies in colon, breast, and pancreatic cancer support that *PRRX1* has context-dependent functions – i.e. it can have a tumour promoter function or act as tumour suppressor. The experimental data with cell lines and dataset analyses of patient samples support the conclusion of a tumour suppressor function of *PRRX1* in HCC.

6 SUMMARY

This study demonstrates the expression and functions of *PRRX1* in human HCC. Among the most remarkable observations is the observation of a frequent upregulation. Further, TGF- β regulates *PRRX1* expression. *PRRX1* has anti-tumour functions, both in advanced HCC stages based on patients' OS data and in experimental observations. *PRRX1* correlated with EMT transcription factors, especially with *ZEB1/2* (with respect to patients' survival outcome). *PRRX1* can be considered as a new key regulator of plasticity processes involved in liver cancer. Finally, novel functions of *PRRX1* in modulating metabolism were identified, i.e. a suppression of the Warburg effect and regulation of TCA cycle metabolites, amino acids as well as fatty acids. The results of my thesis show that *PRRX1* plays significant roles in the devastating human disease HCC, and the new information on *PRRX1* functions will enable further in-depth mechanistic studies on the relevance of *PRRX1* in human liver cancer, including its crosstalk with *ZEB1/2* and importance in cancer metabolism. Further studies can yield to stratification of specific patient's cohorts where *PRRX1* or *PRRX1* downstream effects contribute to disease progression and hence could be used in improving the identification of patients' subsets for therapeutic intervention.

7 REFERENCES

- Abdel-Misih, S. R., & Bloomston, M. (2010). Liver anatomy. *Surg Clin North Am*, 90(4), 643-653. doi:10.1016/j.suc.2010.04.017
- Abu El Maaty, M. A., Alborzina, H., Khan, S. J., Buttner, M., & Wolf, S. (2017). 1,25(OH)2D3 disrupts glucose metabolism in prostate cancer cells leading to a truncation of the TCA cycle and inhibition of TXNIP expression. *Biochim Biophys Acta Mol Cell Res*, 1864(10), 1618-1630. doi:10.1016/j.bbamcr.2017.06.019
- Amann, T., Maegdefrau, U., Hartmann, A., Agaimy, A., Marienhagen, J., Weiss, T. S., . . . Hellerbrand, C. (2009). GLUT1 expression is increased in hepatocellular carcinoma and promotes tumorigenesis. *Am J Pathol*, 174(4), 1544-1552. doi:10.2353/ajpath.2009.080596
- Bai, P. S., Xia, N., Sun, H., & Kong, Y. (2017). Pleiotrophin, a target of miR-384, promotes proliferation, metastasis and lipogenesis in HBV-related hepatocellular carcinoma. *J Cell Mol Med*, 21(11), 3023-3043. doi:10.1111/jcmm.13213
- Bakin, A. V., Tomlinson, A. K., Bhowmick, N. A., Moses, H. L., & Arteaga, C. L. (2000). Phosphatidylinositol 3-kinase function is required for transforming growth factor beta-mediated epithelial to mesenchymal transition and cell migration. *J Biol Chem*, 275(47), 36803-36810. doi:10.1074/jbc.M005912200
- Barrett, T., Wilhite, S. E., Ledoux, P., Evangelista, C., Kim, I. F., Tomashevsky, M., . . . Soboleva, A. (2013). NCBI GEO: archive for functional genomics data sets--update. *Nucleic Acids Res*, 41(Database issue), D991-995. doi:10.1093/nar/gks1193
- Barton, D. E., Foellmer, B. E., Du, J., Tamm, J., Derynck, R., & Francke, U. (1988). Chromosomal mapping of genes for transforming growth factors beta 2 and beta 3 in man and mouse: dispersion of TGF-beta gene family. *Oncogene Res*, 3(4), 323-331. Retrieved from <https://www.ncbi.nlm.nih.gov/pubmed/3226728>
- Bonora, M., Patergnani, S., Rimessi, A., De Marchi, E., Suski, J. M., Bononi, A., . . . Pinton, P. (2012). ATP synthesis and storage. *Purinergic Signal*, 8(3), 343-357. doi:10.1007/s11302-012-9305-8
- Bradner, J. E., Hnisz, D., & Young, R. A. (2017). Transcriptional Addiction in Cancer. *Cell*, 168(4), 629-643. doi:10.1016/j.cell.2016.12.013
- Bruix, J., & Colombo, M. (2014). Hepatocellular carcinoma: current state of the art in diagnosis and treatment. *Best Pract Res Clin Gastroenterol*, 28(5), 751. doi:10.1016/j.bpg.2014.08.010
- Bruix, J., Qin, S., Merle, P., Granito, A., Huang, Y. H., Bodoky, G., . . . Investigators, R. (2017). Regorafenib for patients with hepatocellular carcinoma who progressed on sorafenib treatment (RESORCE): a randomised, double-blind, placebo-controlled, phase 3 trial. *Lancet*, 389(10064), 56-66. doi:10.1016/S0140-6736(16)32453-9
- Budhu, A., Roessler, S., Zhao, X., Yu, Z., Forgues, M., Ji, J., . . . Wang, X. W. (2013). Integrated metabolite and gene expression profiles identify lipid biomarkers associated with progression of hepatocellular carcinoma and patient outcomes. *Gastroenterology*, 144(5), 1066-1075 e1061. doi:10.1053/j.gastro.2013.01.054
- Cairns, R. A., Harris, I. S., & Mak, T. W. (2011). Regulation of cancer cell metabolism. *Nat Rev Cancer*, 11(2), 85-95. doi:10.1038/nrc2981

- Calvisi, D. F., Wang, C., Ho, C., Ladu, S., Lee, S. A., Mattu, S., . . . Evert, M. (2011). Increased lipogenesis, induced by AKT-mTORC1-RPS6 signaling, promotes development of human hepatocellular carcinoma. *Gastroenterology*, *140*(3), 1071-1083. doi:10.1053/j.gastro.2010.12.006
- Carta, G., Murru, E., Banni, S., & Manca, C. (2017). Palmitic Acid: Physiological Role, Metabolism and Nutritional Implications. *Front Physiol*, *8*, 902. doi:10.3389/fphys.2017.00902
- Cassagno, N., Palos-Pinto, A., Costet, P., Breilh, D., Darmon, M., & Berard, A. M. (2005). Low amounts of trans 18:1 fatty acids elevate plasma triacylglycerols but not cholesterol and alter the cellular defence to oxidative stress in mice. *Br J Nutr*, *94*(3), 346-352. doi:10.1079/bjn20051512
- Chaerkady, R., Harsha, H. C., Nalli, A., Gucek, M., Vivekanandan, P., Akhtar, J., . . . Thuluvath, P. J. (2008). A quantitative proteomic approach for identification of potential biomarkers in hepatocellular carcinoma. *J Proteome Res*, *7*(10), 4289-4298. doi:10.1021/pr800197z
- Chan, S. L., & Chan, A. W. (2015). Development of Serum DHCR24 Antibody as a Marker for Hepatocellular Carcinoma: The End of the Beginning. *EBioMedicine*, *2*(6), 497-498. doi:10.1016/j.ebiom.2015.05.020
- Chapnick, D. A., Warner, L., Bernet, J., Rao, T., & Liu, X. (2011). Partners in crime: the TGFbeta and MAPK pathways in cancer progression. *Cell Biosci*, *1*, 42. doi:10.1186/2045-3701-1-42
- Cheng, G., Zhong, M., Kawaguchi, R., Kassai, M., Al-Ubaidi, M., Deng, J., . . . Sun, H. (2014). Identification of PLXDC1 and PLXDC2 as the transmembrane receptors for the multifunctional factor PEDF. *Elife*, *3*, e05401. doi:10.7554/eLife.05401
- Cokakli, M., Erdal, E., Nart, D., Yilmaz, F., Sagol, O., Kilic, M., . . . Atabey, N. (2009). Differential expression of Caveolin-1 in hepatocellular carcinoma: correlation with differentiation state, motility and invasion. *BMC Cancer*, *9*, 65. doi:10.1186/1471-2407-9-65
- De Matteis, S., Ragusa, A., Marisi, G., De Domenico, S., Casadei Gardini, A., Bonafe, M., & Giudetti, A. M. (2018). Aberrant Metabolism in Hepatocellular Carcinoma Provides Diagnostic and Therapeutic Opportunities. *Oxid Med Cell Longev*, *2018*, 7512159. doi:10.1155/2018/7512159
- Dewidar, B., Meyer, C., Dooley, S., & Meindl-Beinker, A. N. (2019). TGF-beta in Hepatic Stellate Cell Activation and Liver Fibrogenesis-Updated 2019. *Cells*, *8*(11). doi:10.3390/cells8111419
- Di Tommaso, L., Franchi, G., Park, Y. N., Fiamengo, B., Destro, A., Morengi, E., . . . Roncalli, M. (2007). Diagnostic value of HSP70, glypican 3, and glutamine synthetase in hepatocellular nodules in cirrhosis. *Hepatology*, *45*(3), 725-734. doi:10.1002/hep.21531
- Diepenbruck, M., & Christofori, G. (2016). Epithelial-mesenchymal transition (EMT) and metastasis: yes, no, maybe? *Curr Opin Cell Biol*, *43*, 7-13. doi:10.1016/j.ceb.2016.06.002
- Dimri, M., & Satyanarayana, A. (2020). Molecular Signaling Pathways and Therapeutic Targets in Hepatocellular Carcinoma. *Cancers (Basel)*, *12*(2). doi:10.3390/cancers12020491
- Dooley, S., Hamzavi, J., Ciucan, L., Godoy, P., Ilkavets, I., Ehnert, S., . . . Mertens, P. R. (2008). Hepatocyte-specific Smad7 expression attenuates TGF-beta-mediated fibrogenesis and protects against liver damage. *Gastroenterology*, *135*(2), 642-659. doi:10.1053/j.gastro.2008.04.038

- Dooley, S., & ten Dijke, P. (2012). TGF-beta in progression of liver disease. *Cell Tissue Res*, 347(1), 245-256. doi:10.1007/s00441-011-1246-y
- Dooley, S., Weng, H., & Mertens, P. R. (2009). Hypotheses on the role of transforming growth factor-beta in the onset and progression of hepatocellular carcinoma. *Dig Dis*, 27(2), 93-101. doi:10.1159/000218340
- Dor, I., Namba, M., & Sato, J. (1975). Establishment and some biological characteristics of human hepatoma cell lines. *Gan*, 66(4), 385-392. Retrieved from <https://www.ncbi.nlm.nih.gov/pubmed/52570>
- Drucker, C., Parzefall, W., Teufelhofer, O., Grusch, M., Ellinger, A., Schulte-Hermann, R., & Grasl-Kraupp, B. (2006). Non-parenchymal liver cells support the growth advantage in the first stages of hepatocarcinogenesis. *Carcinogenesis*, 27(1), 152-161. doi:10.1093/carcin/bgi202
- Du, B., Cawthorn, W. P., Su, A., Doucette, C. R., Yao, Y., Hemati, N., . . . MacDougald, O. A. (2013). The transcription factor paired-related homeobox 1 (Prrx1) inhibits adipogenesis by activating transforming growth factor-beta (TGFbeta) signaling. *J Biol Chem*, 288(5), 3036-3047. doi:10.1074/jbc.M112.440370
- Du, B., & Shim, J. S. (2016). Targeting Epithelial-Mesenchymal Transition (EMT) to Overcome Drug Resistance in Cancer. *Molecules*, 21(7). doi:10.3390/molecules21070965
- Duckett, S. K., Volpi-Lagrec, G., Alende, M., & Long, N. M. (2014). Palmitoleic acid reduces intramuscular lipid and restores insulin sensitivity in obese sheep. *Diabetes Metab Syndr Obes*, 7, 553-563. doi:10.2147/DMSO.S72695
- Dzieran, J., Fabian, J., Feng, T., Coulouarn, C., Ilkavets, I., Kyselova, A., . . . Meindl-Beinker, N. M. (2013). Comparative analysis of TGF-beta/Smad signaling dependent cytotaxis in human hepatocellular carcinoma cell lines. *PLoS One*, 8(8), e72252. doi:10.1371/journal.pone.0072252
- Ell, B., & Kang, Y. (2013). MicroRNAs as regulators of tumor-associated stromal cells. *Oncotarget*, 4(12), 2166-2167. doi:10.18632/oncotarget.1625
- Fabregat, I., Moreno-Caceres, J., Sanchez, A., Dooley, S., Dewidar, B., Giannelli, G., . . . Consortium, I.-L. (2016). TGF-beta signalling and liver disease. *FEBS J*, 283(12), 2219-2232. doi:10.1111/febs.13665
- Fan, M., Shen, J., Liu, H., Wen, Z., Yang, J., Yang, P., . . . Lu, K. (2017). Downregulation of PRRX1 via the p53-dependent signaling pathway predicts poor prognosis in hepatocellular carcinoma. *Oncol Rep*, 38(2), 1083-1090. doi:10.3892/or.2017.5785
- Fattovich, G., Stroffolini, T., Zagni, I., & Donato, F. (2004). Hepatocellular carcinoma in cirrhosis: incidence and risk factors. *Gastroenterology*, 127(5 Suppl 1), S35-50. doi:10.1053/j.gastro.2004.09.014
- Feitelson, M. A., Sun, B., Satiroglu Tufan, N. L., Liu, J., Pan, J., & Lian, Z. (2002). Genetic mechanisms of hepatocarcinogenesis. *Oncogene*, 21(16), 2593-2604. doi:10.1038/sj.onc.1205434
- Ferrarini, A., Di Poto, C., He, S., Tu, C., Varghese, R. S., Kara Balla, A., . . . Ransom, H. W. (2019). Metabolomic Analysis of Liver Tissues for Characterization of Hepatocellular Carcinoma. *J Proteome Res*, 18(8), 3067-3076. doi:10.1021/acs.jproteome.9b00185
- Fransvea, E., Angelotti, U., Antonaci, S., & Giannelli, G. (2008). Blocking transforming growth factor-beta up-regulates E-cadherin and reduces migration and invasion of hepatocellular carcinoma cells. *Hepatology*, 47(5), 1557-1566. doi:10.1002/hep.22201

- Gao, J., Aksoy, B. A., Dogrusoz, U., Dresdner, G., Gross, B., Sumer, S. O., . . . Schultz, N. (2013). Integrative analysis of complex cancer genomics and clinical profiles using the cBioPortal. *Sci Signal*, 6(269), p11. doi:10.1126/scisignal.2004088
- Ghouri, Y. A., Mian, I., & Rowe, J. H. (2017). Review of hepatocellular carcinoma: Epidemiology, etiology, and carcinogenesis. *J Carcinog*, 16, 1. doi:10.4103/jcar.JCar_9_16
- Giannelli, G., Koudelkova, P., Dituri, F., & Mikulits, W. (2016). Role of epithelial to mesenchymal transition in hepatocellular carcinoma. *J Hepatol*, 65(4), 798-808. doi:10.1016/j.jhep.2016.05.007
- Gomaa, A. I., Khan, S. A., Toledano, M. B., Waked, I., & Taylor-Robinson, S. D. (2008). Hepatocellular carcinoma: epidemiology, risk factors and pathogenesis. *World J Gastroenterol*, 14(27), 4300-4308. doi:10.3748/wjg.14.4300
- Gressner, A. M., Weiskirchen, R., Breitkopf, K., & Dooley, S. (2002). Roles of TGF-beta in hepatic fibrosis. *Front Biosci*, 7, d793-807. Retrieved from <https://www.ncbi.nlm.nih.gov/pubmed/11897555>
- Hanahan, D., & Weinberg, R. A. (2011). Hallmarks of cancer: the next generation. *Cell*, 144(5), 646-674. doi:10.1016/j.cell.2011.02.013
- Hardin, H., Guo, Z., Shan, W., Montemayor-Garcia, C., Asioli, S., Yu, X. M., . . . Lloyd, R. V. (2014). The roles of the epithelial-mesenchymal transition marker PRRX1 and miR-146b-5p in papillary thyroid carcinoma progression. *Am J Pathol*, 184(8), 2342-2354. doi:10.1016/j.ajpath.2014.04.011
- Harris, I. S., Treloar, A. E., Inoue, S., Sasaki, M., Gorrini, C., Lee, K. C., . . . Mak, T. W. (2015). Glutathione and thioredoxin antioxidant pathways synergize to drive cancer initiation and progression. *Cancer Cell*, 27(2), 211-222. doi:10.1016/j.ccell.2014.11.019
- Hartsough, M. T., & Mulder, K. M. (1995). Transforming growth factor beta activation of p44mapk in proliferating cultures of epithelial cells. *J Biol Chem*, 270(13), 7117-7124. doi:10.1074/jbc.270.13.7117
- Hashiguchi, M., Ueno, S., Sakoda, M., Iino, S., Hiwatashi, K., Minami, K., . . . Natsugoe, S. (2013). Clinical implication of ZEB-1 and E-cadherin expression in hepatocellular carcinoma (HCC). *BMC Cancer*, 13, 572. doi:10.1186/1471-2407-13-572
- Heldin, C. H., Landstrom, M., & Moustakas, A. (2009). Mechanism of TGF-beta signaling to growth arrest, apoptosis, and epithelial-mesenchymal transition. *Curr Opin Cell Biol*, 21(2), 166-176. doi:10.1016/j.ceb.2009.01.021
- Heldin, C. H., & Moustakas, A. (2012). Role of Smads in TGFbeta signaling. *Cell Tissue Res*, 347(1), 21-36. doi:10.1007/s00441-011-1190-x
- Hirata, H., Sugimachi, K., Takahashi, Y., Ueda, M., Sakimura, S., Uchi, R., . . . Mimori, K. (2015). Downregulation of PRRX1 Confers Cancer Stem Cell-Like Properties and Predicts Poor Prognosis in Hepatocellular Carcinoma. *Ann Surg Oncol*, 22 Suppl 3, S1402-1409. doi:10.1245/s10434-014-4242-0
- Hopf, R., Hopf, M., Kober, G., Kaltenbach, M., & Riemann, H. (1975). [Proceedings: Value of radiological findings and EG in the thoracic diagnosis of primary myocardial diseases]. *Z Kardiol*, Suppl 2, 32. Retrieved from <https://www.ncbi.nlm.nih.gov/pubmed/128238>
- Huang, Q., Tan, Y., Yin, P., Ye, G., Gao, P., Lu, X., . . . Xu, G. (2013). Metabolic characterization of hepatocellular carcinoma using nontargeted tissue metabolomics. *Cancer Res*, 73(16), 4992-5002. doi:10.1158/0008-5472.CAN-13-0308

- Huang, W. (2017). MicroRNAs: Biomarkers, Diagnostics, and Therapeutics. *Methods Mol Biol*, 1617, 57-67. doi:10.1007/978-1-4939-7046-9_4
- Ishizawa, T., Hasegawa, K., Aoki, T., Takahashi, M., Inoue, Y., Sano, K., . . . Makuuchi, M. (2008). Neither multiple tumors nor portal hypertension are surgical contraindications for hepatocellular carcinoma. *Gastroenterology*, 134(7), 1908-1916. doi:10.1053/j.gastro.2008.02.091
- Ito, N., Kawata, S., Tamura, S., Shirai, Y., Kiso, S., Tsushima, H., & Matsuzawa, Y. (1995). Positive correlation of plasma transforming growth factor-beta 1 levels with tumor vascularity in hepatocellular carcinoma. *Cancer Lett*, 89(1), 45-48. doi:10.1016/0304-3835(95)90156-6
- Javelaud, D., & Mauviel, A. (2004). Mammalian transforming growth factor-betas: Smad signaling and physio-pathological roles. *Int J Biochem Cell Biol*, 36(7), 1161-1165. doi:10.1016/S1357-2725(03)00255-3
- Jelkmann, W. (2001). The role of the liver in the production of thrombopoietin compared with erythropoietin. *Eur J Gastroenterol Hepatol*, 13(7), 791-801. doi:10.1097/00042737-200107000-00006
- Jhunjunwala, S., Jiang, Z., Stawiski, E. W., Gnad, F., Liu, J., Mayba, O., . . . Zhang, Z. (2014). Diverse modes of genomic alteration in hepatocellular carcinoma. *Genome Biol*, 15(8), 436. doi:10.1186/s13059-014-0436-9
- Jiang, J., Zheng, M., Zhang, M., Yang, X., Li, L., Wang, S. S., . . . Liang, X. H. (2019). PRRX1 Regulates Cellular Phenotype Plasticity and Dormancy of Head and Neck Squamous Cell Carcinoma Through miR-642b-3p. *Neoplasia*, 21(2), 216-229. doi:10.1016/j.neo.2018.12.001
- Jiang, Y. P., Tang, Y. L., Wang, S. S., Wu, J. S., Zhang, M., Pang, X., . . . Liang, X. H. (2020). PRRX1-induced epithelial-to-mesenchymal transition in salivary adenoid cystic carcinoma activates the metabolic reprogramming of free fatty acids to promote invasion and metastasis. *Cell Prolif*, 53(1), e12705. doi:10.1111/cpr.12705
- Kalluri, R., & Weinberg, R. A. (2009). The basics of epithelial-mesenchymal transition. *J Clin Invest*, 119(6), 1420-1428. doi:10.1172/JCI39104
- Kelman, Z. (1997). PCNA: structure, functions and interactions. *Oncogene*, 14(6), 629-640. doi:10.1038/sj.onc.1200886
- Kim, J. W., Gao, P., Liu, Y. C., Semenza, G. L., & Dang, C. V. (2007). Hypoxia-inducible factor 1 and dysregulated c-Myc cooperatively induce vascular endothelial growth factor and metabolic switches hexokinase 2 and pyruvate dehydrogenase kinase 1. *Mol Cell Biol*, 27(21), 7381-7393. doi:10.1128/MCB.00440-07
- Kim, M. N., Kim, S. U., Kim, B. K., Park, J. Y., Kim, D. Y., Ahn, S. H., . . . Han, K. H. (2015). Increased risk of hepatocellular carcinoma in chronic hepatitis B patients with transient elastography-defined subclinical cirrhosis. *Hepatology*, 61(6), 1851-1859. doi:10.1002/hep.27735
- Kim, Y. H., Jeong, D. C., Pak, K., Han, M. E., Kim, J. Y., Liangwen, L., . . . Oh, S. O. (2017). SLC2A2 (GLUT2) as a novel prognostic factor for hepatocellular carcinoma. *Oncotarget*, 8(40), 68381-68392. doi:10.18632/oncotarget.20266
- King, A., Selak, M. A., & Gottlieb, E. (2006). Succinate dehydrogenase and fumarate hydratase: linking mitochondrial dysfunction and cancer. *Oncogene*, 25(34), 4675-4682. doi:10.1038/sj.onc.1209594
- Kinoshita, A., Onoda, H., Fushiya, N., Koike, K., Nishino, H., & Tajiri, H. (2015). Staging systems for hepatocellular carcinoma: Current status and future perspectives. *World J Hepatol*, 7(3), 406-424. doi:10.4254/wjh.v7.i3.406

- Knowles, B. B., Howe, C. C., & Aden, D. P. (1980). Human hepatocellular carcinoma cell lines secrete the major plasma proteins and hepatitis B surface antigen. *Science*, *209*(4455), 497-499. doi:10.1126/science.6248960
- Koh, W. P., Robien, K., Wang, R., Govindarajan, S., Yuan, J. M., & Yu, M. C. (2011). Smoking as an independent risk factor for hepatocellular carcinoma: the Singapore Chinese Health Study. *Br J Cancer*, *105*(9), 1430-1435. doi:10.1038/bjc.2011.360
- Krupp, M., Itzel, T., Maass, T., Hildebrandt, A., Galle, P. R., & Teufel, A. (2013). CellLineNavigator: a workbench for cancer cell line analysis. *Nucleic Acids Res*, *41*(Database issue), D942-948. doi:10.1093/nar/gks1012
- Kudo, M., Finn, R. S., Qin, S., Han, K. H., Ikeda, K., Piscaglia, F., . . . Cheng, A. L. (2018). Lenvatinib versus sorafenib in first-line treatment of patients with unresectable hepatocellular carcinoma: a randomised phase 3 non-inferiority trial. *Lancet*, *391*(10126), 1163-1173. doi:10.1016/S0140-6736(18)30207-1
- Latchman, D. S. (1997). Transcription factors: an overview. *Int J Biochem Cell Biol*, *29*(12), 1305-1312. doi:10.1016/s1357-2725(97)00085-x
- Lauby-Secretan, B., Scoccianti, C., Loomis, D., Grosse, Y., Bianchini, F., Straif, K., & International Agency for Research on Cancer Handbook Working, G. (2016). Body Fatness and Cancer--Viewpoint of the IARC Working Group. *N Engl J Med*, *375*(8), 794-798. doi:10.1056/NEJMSr1606602
- Lebrun, J. J. (2012). The Dual Role of TGFbeta in Human Cancer: From Tumor Suppression to Cancer Metastasis. *ISRN Mol Biol*, *2012*, 381428. doi:10.5402/2012/381428
- Lee, M. K., Pardoux, C., Hall, M. C., Lee, P. S., Warburton, D., Qing, J., . . . Derynck, R. (2007). TGF-beta activates Erk MAP kinase signalling through direct phosphorylation of ShcA. *EMBO J*, *26*(17), 3957-3967. doi:10.1038/sj.emboj.7601818
- Li, M. O., Wan, Y. Y., Sanjabi, S., Robertson, A. K., & Flavell, R. A. (2006). Transforming growth factor-beta regulation of immune responses. *Annu Rev Immunol*, *24*, 99-146. doi:10.1146/annurev.immunol.24.021605.090737
- Liberti, M. V., & Locasale, J. W. (2016). The Warburg Effect: How Does it Benefit Cancer Cells? *Trends Biochem Sci*, *41*(3), 211-218. doi:10.1016/j.tibs.2015.12.001
- Liu, H., Espinoza-Lewis, R. A., Chen, C., Hu, X., Zhang, Y., & Chen, Y. (2012). The role of Shox2 in SAN development and function. *Pediatr Cardiol*, *33*(6), 882-889. doi:10.1007/s00246-012-0179-x
- Liu, J., Yu, Z., Xiao, Y., Meng, Q., Wang, Y., & Chang, W. (2018). Coordination of FOXA2 and SIRT6 suppresses the hepatocellular carcinoma progression through ZEB2 inhibition. *Cancer Manag Res*, *10*, 391-402. doi:10.2147/CMAR.S150552
- Llovet, J. M., Ricci, S., Mazzaferro, V., Hilgard, P., Gane, E., Blanc, J. F., . . . Group, S. I. S. (2008). Sorafenib in advanced hepatocellular carcinoma. *N Engl J Med*, *359*(4), 378-390. doi:10.1056/NEJMoa0708857
- Llovet, J. M., Villanueva, A., Lachenmayer, A., & Finn, R. S. (2015). Advances in targeted therapies for hepatocellular carcinoma in the genomic era. *Nat Rev Clin Oncol*, *12*(7), 408-424. doi:10.1038/nrclinonc.2015.103
- Lund, P., Schubert, D., Niketeghad, F., & Schirmacher, P. (2004). Autocrine inhibition of chemotherapy response in human liver tumor cells by insulin-like growth factor-II. *Cancer Lett*, *206*(1), 85-96. doi:10.1016/j.canlet.2003.10.018
- Lv, Z. D., Yang, Z. C., Liu, X. P., Jin, L. Y., Dong, Q., Qu, H. L., . . . Wang, H. B. (2016). Silencing of Prrx1b suppresses cellular proliferation, migration,

- invasion and epithelial-mesenchymal transition in triple-negative breast cancer. *J Cell Mol Med*, 20(9), 1640-1650. doi:10.1111/jcmm.12856
- Malfettone, A., Soukupova, J., Bertran, E., Crosas-Molist, E., Lastra, R., Fernando, J., . . . Fabregat, I. (2017). Transforming growth factor-beta-induced plasticity causes a migratory stemness phenotype in hepatocellular carcinoma. *Cancer Lett*, 392, 39-50. doi:10.1016/j.canlet.2017.01.037
- Mancarella, S., Krol, S., Crovace, A., Leporatti, S., Dituri, F., Frusciante, M., & Giannelli, G. (2019). Validation of Hepatocellular Carcinoma Experimental Models for TGF-beta Promoting Tumor Progression. *Cancers (Basel)*, 11(10). doi:10.3390/cancers11101510
- Maroni, L., Haibo, B., Ray, D., Zhou, T., Wan, Y., Meng, F., . . . Alpini, G. (2015). Functional and structural features of cholangiocytes in health and disease. *Cell Mol Gastroenterol Hepatol*, 1(4), 368-380. doi:10.1016/j.jcmgh.2015.05.005
- Marrero, J. A., Kulik, L. M., Sirlin, C. B., Zhu, A. X., Finn, R. S., Abecassis, M. M., . . . Heimbach, J. K. (2018). Diagnosis, Staging, and Management of Hepatocellular Carcinoma: 2018 Practice Guidance by the American Association for the Study of Liver Diseases. *Hepatology*, 68(2), 723-750. doi:10.1002/hep.29913
- Martin, J. F., & Olson, E. N. (2000). Identification of a prx1 limb enhancer. *Genesis*, 26(4), 225-229. Retrieved from <https://www.ncbi.nlm.nih.gov/pubmed/10748458>
- Massague, J. (2008). TGFbeta in Cancer. *Cell*, 134(2), 215-230. doi:10.1016/j.cell.2008.07.001
- Massague, J. (2012). TGFbeta signalling in context. *Nat Rev Mol Cell Biol*, 13(10), 616-630. doi:10.1038/nrm3434
- Matsumoto, K., & Nakamura, T. (1996). Emerging multipotent aspects of hepatocyte growth factor. *J Biochem*, 119(4), 591-600. doi:10.1093/oxfordjournals.jbchem.a021283
- Meindl-Beinker, N. M., Matsuzaki, K., & Dooley, S. (2012). TGF-beta signaling in onset and progression of hepatocellular carcinoma. *Dig Dis*, 30(5), 514-523. doi:10.1159/000341704
- Meyer, C., Dzieran, J., Liu, Y., Schindler, F., Munker, S., Muller, A., . . . Dooley, S. (2013). Distinct dedifferentiation processes affect caveolin-1 expression in hepatocytes. *Cell Commun Signal*, 11(1), 6. doi:10.1186/1478-811X-11-6
- Michelotti, G. A., Machado, M. V., & Diehl, A. M. (2013). NAFLD, NASH and liver cancer. *Nat Rev Gastroenterol Hepatol*, 10(11), 656-665. doi:10.1038/nrgastro.2013.183
- Mitchell, J. M., Hicklin, D. M., Doughty, P. M., Hicklin, J. H., Dickert, J. W., Jr., Tolbert, S. M., . . . Kern, M. J. (2006). The Prx1 homeobox gene is critical for molar tooth morphogenesis. *J Dent Res*, 85(10), 888-893. doi:10.1177/154405910608501003
- Mittal, S., & El-Serag, H. B. (2013). Epidemiology of hepatocellular carcinoma: consider the population. *J Clin Gastroenterol*, 47 Suppl, S2-6. doi:10.1097/MCG.0b013e3182872f29
- Moses, H. L., Roberts, A. B., & Derynck, R. (2016). The Discovery and Early Days of TGF-beta: A Historical Perspective. *Cold Spring Harb Perspect Biol*, 8(7). doi:10.1101/cshperspect.a021865
- Nakabayashi, H., Taketa, K., Miyano, K., Yamane, T., & Sato, J. (1982). Growth of human hepatoma cells lines with differentiated functions in chemically defined

- medium. *Cancer Res*, 42(9), 3858-3863. Retrieved from <https://www.ncbi.nlm.nih.gov/pubmed/6286115>
- Niitsu, Y., Urushizaki, Y., Koshida, Y., Terui, K., Mahara, K., Kohgo, Y., & Urushizaki, I. (1988). Expression of TGF-beta gene in adult T cell leukemia. *Blood*, 71(1), 263-266. Retrieved from <https://www.ncbi.nlm.nih.gov/pubmed/2891388>
- Norris, R. A., & Kern, M. J. (2001). The identification of Prx1 transcription regulatory domains provides a mechanism for unequal compensation by the Prx1 and Prx2 loci. *J Biol Chem*, 276(29), 26829-26837. doi:10.1074/jbc.M100239200
- Nwosu, Z. C., Battello, N., Rothley, M., Pioronska, W., Sitek, B., Ebert, M. P., . . . Dooley, S. (2018). Liver cancer cell lines distinctly mimic the metabolic gene expression pattern of the corresponding human tumours. *J Exp Clin Cancer Res*, 37(1), 211. doi:10.1186/s13046-018-0872-6
- Nwosu, Z. C., Megger, D. A., Hammad, S., Sitek, B., Roessler, S., Ebert, M. P., . . . Dooley, S. (2017). Identification of the Consistently Altered Metabolic Targets in Human Hepatocellular Carcinoma. *Cell Mol Gastroenterol Hepatol*, 4(2), 303-323 e301. doi:10.1016/j.jcmgh.2017.05.004
- Nwosu, Z. C., Pioronska, W., Battello, N., Zimmer, A. D., Dewidar, B., Han, M., . . . Dooley, S. (2020). Severe metabolic alterations in liver cancer lead to ERK pathway activation and drug resistance. *EBioMedicine*, 54, 102699. doi:10.1016/j.ebiom.2020.102699
- Ocana, O. H., Corcoles, R., Fabra, A., Moreno-Bueno, G., Acloque, H., Vega, S., . . . Nieto, M. A. (2012). Metastatic colonization requires the repression of the epithelial-mesenchymal transition inducer Prrx1. *Cancer Cell*, 22(6), 709-724. doi:10.1016/j.ccr.2012.10.012
- Parisi, L. R., Li, N., & Atilla-Gokcumen, G. E. (2017). Very Long Chain Fatty Acids Are Functionally Involved in Necroptosis. *Cell Chem Biol*, 24(12), 1445-1454 e1448. doi:10.1016/j.chembiol.2017.08.026
- Park, J. G., Lee, J. H., Kang, M. S., Park, K. J., Jeon, Y. M., Lee, H. J., . . . et al. (1995). Characterization of cell lines established from human hepatocellular carcinoma. *Int J Cancer*, 62(3), 276-282. doi:10.1002/ijc.2910620308
- Paudyal, B., Paudyal, P., Oriuchi, N., Tsushima, Y., Nakajima, T., & Endo, K. (2008). Clinical implication of glucose transport and metabolism evaluated by 18F-FDG PET in hepatocellular carcinoma. *Int J Oncol*, 33(5), 1047-1054. Retrieved from <https://www.ncbi.nlm.nih.gov/pubmed/18949368>
- Pazgan-Simon, M., Simon, K. A., Jarowicz, E., Rotter, K., Szymanek-Pasternak, A., & Zuwala-Jagiello, J. (2018). Hepatitis B virus treatment in hepatocellular carcinoma patients prolongs survival and reduces the risk of cancer recurrence. *Clin Exp Hepatol*, 4(3), 210-216. doi:10.5114/ceh.2018.78127
- Pineiro-Carrero, V. M., & Pineiro, E. O. (2004). Liver. *Pediatrics*, 113(4 Suppl), 1097-1106. Retrieved from <https://www.ncbi.nlm.nih.gov/pubmed/15060205>
- Pollard, P. J., Briere, J. J., Alam, N. A., Barwell, J., Barclay, E., Wortham, N. C., . . . Tomlinson, I. P. (2005). Accumulation of Krebs cycle intermediates and over-expression of HIF1alpha in tumours which result from germline FH and SDH mutations. *Hum Mol Genet*, 14(15), 2231-2239. doi:10.1093/hmg/ddi227
- Pons, F., Varela, M., & Llovet, J. M. (2005). Staging systems in hepatocellular carcinoma. *HPB (Oxford)*, 7(1), 35-41. doi:10.1080/13651820410024058
- Poon, R. T., Ho, J. W., Tong, C. S., Lau, C., Ng, I. O., & Fan, S. T. (2004). Prognostic significance of serum vascular endothelial growth factor and endostatin in patients with hepatocellular carcinoma. *Br J Surg*, 91(10), 1354-1360. doi:10.1002/bjs.4594

- Pope, E. D., 3rd, Kimbrough, E. O., Vemireddy, L. P., Surapaneni, P. K., Copland, J. A., 3rd, & Mody, K. (2019). Aberrant lipid metabolism as a therapeutic target in liver cancer. *Expert Opin Ther Targets*, 23(6), 473-483. doi:10.1080/14728222.2019.1615883
- Refolo, M. G., Messa, C., Guerra, V., Carr, B. I., & D'Alessandro, R. (2020). Inflammatory Mechanisms of HCC Development. *Cancers (Basel)*, 12(3). doi:10.3390/cancers12030641
- Reichert, M., Takano, S., von Burstin, J., Kim, S. B., Lee, J. S., Ihida-Stansbury, K., . . . Rustgi, A. K. (2013). The Prrx1 homeodomain transcription factor plays a central role in pancreatic regeneration and carcinogenesis. *Genes Dev*, 27(3), 288-300. doi:10.1101/gad.204453.112
- Rhodes, D. R., Kalyana-Sundaram, S., Mahavisno, V., Varambally, R., Yu, J., Briggs, B. B., . . . Chinnaiyan, A. M. (2007). OncoPrint 3.0: genes, pathways, and networks in a collection of 18,000 cancer gene expression profiles. *Neoplasia*, 9(2), 166-180. doi:10.1593/neo.07112
- Roayaie, S., Jibara, G., Tabrizian, P., Park, J. W., Yang, J., Yan, L., . . . Sherman, M. (2015). The role of hepatic resection in the treatment of hepatocellular cancer. *Hepatology*, 62(2), 440-451. doi:10.1002/hep.27745
- Safran, M., Dalah, I., Alexander, J., Rosen, N., Iny Stein, T., Shmoish, M., . . . Lancet, D. (2010). GeneCards Version 3: the human gene integrator. *Database (Oxford)*, 2010, baq020. doi:10.1093/database/baq020
- Sahin, A. A., Ro, J. Y., Brown, R. W., Ordonez, N. G., Cleary, K. R., el-Naggar, A. K., . . . Ayala, A. G. (1994). Assessment of Ki-67-derived tumor proliferative activity in colorectal adenocarcinomas. *Mod Pathol*, 7(1), 17-22. Retrieved from <https://www.ncbi.nlm.nih.gov/pubmed/8159647>
- Santos, C. R., & Schulze, A. (2012). Lipid metabolism in cancer. *FEBS J*, 279(15), 2610-2623. doi:10.1111/j.1742-4658.2012.08644.x
- Sanyal, A. J., Chalasani, N., Kowdley, K. V., McCullough, A., Diehl, A. M., Bass, N. M., . . . Nash, C. R. N. (2010). Pioglitazone, vitamin E, or placebo for nonalcoholic steatohepatitis. *N Engl J Med*, 362(18), 1675-1685. doi:10.1056/NEJMoa0907929
- Schulze, K., Nault, J. C., & Villanueva, A. (2016). Genetic profiling of hepatocellular carcinoma using next-generation sequencing. *J Hepatol*, 65(5), 1031-1042. doi:10.1016/j.jhep.2016.05.035
- Shah, N., & Sukumar, S. (2010). The Hox genes and their roles in oncogenesis. *Nat Rev Cancer*, 10(5), 361-371. doi:10.1038/nrc2826
- Shang, L., Hosseini, M., Liu, X., Kisseleva, T., & Brenner, D. A. (2018). Human hepatic stellate cell isolation and characterization. *J Gastroenterol*, 53(1), 6-17. doi:10.1007/s00535-017-1404-4
- Shetty, S., Lalor, P. F., & Adams, D. H. (2018). Liver sinusoidal endothelial cells - gatekeepers of hepatic immunity. *Nat Rev Gastroenterol Hepatol*, 15(9), 555-567. doi:10.1038/s41575-018-0020-y
- Shindoh, J., & Vauthey, J. N. (2014). Staging of biliary tract and primary liver tumors. *Surg Oncol Clin N Am*, 23(2), 313-322. doi:10.1016/j.soc.2013.11.003
- Sia, D., Jiao, Y., Martinez-Quetglas, I., Kuchuk, O., Villacorta-Martin, C., Castro de Moura, M., . . . Llovet, J. M. (2017). Identification of an Immune-specific Class of Hepatocellular Carcinoma, Based on Molecular Features. *Gastroenterology*, 153(3), 812-826. doi:10.1053/j.gastro.2017.06.007
- Sia, D., Villanueva, A., Friedman, S. L., & Llovet, J. M. (2017). Liver Cancer Cell of Origin, Molecular Class, and Effects on Patient Prognosis. *Gastroenterology*, 152(4), 745-761. doi:10.1053/j.gastro.2016.11.048

- Stickel, F. (2015). Alcoholic cirrhosis and hepatocellular carcinoma. *Adv Exp Med Biol*, 815, 113-130. doi:10.1007/978-3-319-09614-8_7
- Sugiyama, M., Hasegawa, H., Ito, S., Sugiyama, K., Maeda, M., Aoki, K., . . . Senga, T. (2015). Paired related homeobox 1 is associated with the invasive properties of glioblastoma cells. *Oncol Rep*, 33(3), 1123-1130. doi:10.3892/or.2014.3681
- Sun, H. W., Yu, X. J., Wu, W. C., Chen, J., Shi, M., Zheng, L., & Xu, J. (2016). GLUT1 and ASCT2 as Predictors for Prognosis of Hepatocellular Carcinoma. *PLoS One*, 11(12), e0168907. doi:10.1371/journal.pone.0168907
- Takahashi, Y., Sawada, G., Kurashige, J., Uchi, R., Matsumura, T., Ueo, H., . . . Mimori, K. (2013). Paired related homoeobox 1, a new EMT inducer, is involved in metastasis and poor prognosis in colorectal cancer. *Br J Cancer*, 109(2), 307-311. doi:10.1038/bjc.2013.339
- Takano, S., Reichert, M., Bakir, B., Das, K. K., Nishida, T., Miyazaki, M., . . . Rustgi, A. K. (2016). Prrx1 isoform switching regulates pancreatic cancer invasion and metastatic colonization. *Genes Dev*, 30(2), 233-247. doi:10.1101/gad.263327.115
- Tang, Y., Lu, Y., Cheng, Y., Luo, L., Cai, L., Peng, B., . . . Pan, M. (2019). Pre-metastatic niche triggers SDF-1/CXCR4 axis and promotes organ colonisation by hepatocellular circulating tumour cells via downregulation of Prrx1. *J Exp Clin Cancer Res*, 38(1), 473. doi:10.1186/s13046-019-1475-6
- Taniguchi, H., Fujimoto, A., Kono, H., Furuta, M., Fujita, M., & Nakagawa, H. (2018). Loss-of-function mutations in Zn-finger DNA-binding domain of HNF4A cause aberrant transcriptional regulation in liver cancer. *Oncotarget*, 9(40), 26144-26156. doi:10.18632/oncotarget.25456
- ten Berge, D., Brouwer, A., Korving, J., Martin, J. F., & Meijlink, F. (1998). Prx1 and Prx2 in skeletogenesis: roles in the craniofacial region, inner ear and limbs. *Development*, 125(19), 3831-3842. Retrieved from <https://www.ncbi.nlm.nih.gov/pubmed/9729491>
- Thiery, J. P., Acloque, H., Huang, R. Y., & Nieto, M. A. (2009). Epithelial-mesenchymal transitions in development and disease. *Cell*, 139(5), 871-890. doi:10.1016/j.cell.2009.11.007
- Timmons, J. A., Atherton, P. J., Larsson, O., Sood, S., Blokhin, I. O., Brogan, R. J., . . . Kraus, W. E. (2018). A coding and non-coding transcriptomic perspective on the genomics of human metabolic disease. *Nucleic Acids Res*, 46(15), 7772-7792. doi:10.1093/nar/gky570
- Trefts, E., Gannon, M., & Wasserman, D. H. (2017). The liver. *Curr Biol*, 27(21), R1147-R1151. doi:10.1016/j.cub.2017.09.019
- Tseng, P. L., Wu, W. H., Hu, T. H., Chen, C. W., Cheng, H. C., Li, C. F., . . . Chang, W. T. (2018). Decreased succinate dehydrogenase B in human hepatocellular carcinoma accelerates tumor malignancy by inducing the Warburg effect. *Sci Rep*, 8(1), 3081. doi:10.1038/s41598-018-21361-6
- Tsochatzis, E. A., Bosch, J., & Burroughs, A. K. (2014). Liver cirrhosis. *Lancet*, 383(9930), 1749-1761. doi:10.1016/S0140-6736(14)60121-5
- Tu, S., Huang, W., Huang, C., Luo, Z., & Yan, X. (2019). Contextual Regulation of TGF-beta Signaling in Liver Cancer. *Cells*, 8(10). doi:10.3390/cells8101235
- Ungefroren, H. (2019). TGF-beta Signaling in Cancer: Control by Negative Regulators and Crosstalk with Proinflammatory and Fibrogenic Pathways. *Cancers (Basel)*, 11(3). doi:10.3390/cancers11030384

- Vescovo, T., Refolo, G., Vitagliano, G., Fimia, G. M., & Piacentini, M. (2016). Molecular mechanisms of hepatitis C virus-induced hepatocellular carcinoma. *Clin Microbiol Infect*, 22(10), 853-861. doi:10.1016/j.cmi.2016.07.019
- Villanueva, A. (2019). Hepatocellular Carcinoma. *N Engl J Med*, 380(15), 1450-1462. doi:10.1056/NEJMra1713263
- Villanueva, A., Hoshida, Y., Battiston, C., Tovar, V., Sia, D., Alsinet, C., . . . Llovet, J. M. (2011). Combining clinical, pathology, and gene expression data to predict recurrence of hepatocellular carcinoma. *Gastroenterology*, 140(5), 1501-1512 e1502. doi:10.1053/j.gastro.2011.02.006
- Walker, M., El-Serag, H. B., Sada, Y., Mittal, S., Ying, J., Duan, Z., . . . Kanwal, F. (2016). Cirrhosis is under-recognised in patients subsequently diagnosed with hepatocellular cancer. *Aliment Pharmacol Ther*, 43(5), 621-630. doi:10.1111/apt.13505
- Wan, J., Zhou, X., Cui, J., Zou, Z., Xu, Y., & You, D. (2013). Role of complement 3 in TNF-alpha-induced mesenchymal transition of renal tubular epithelial cells in vitro. *Mol Biotechnol*, 54(1), 92-100. doi:10.1007/s12033-012-9547-2
- Wan, T., Zhang, T., Si, X., & Zhou, Y. (2017). Overexpression of EMT-inducing transcription factors as a potential poor prognostic factor for hepatocellular carcinoma in Asian populations: A meta-analysis. *Oncotarget*, 8(35), 59500-59508. doi:10.18632/oncotarget.18352
- Warburg, O. (1956). On respiratory impairment in cancer cells. *Science*, 124(3215), 269-270. Retrieved from <https://www.ncbi.nlm.nih.gov/pubmed/13351639>
- Weiss, A., & Attisano, L. (2013). The TGFbeta superfamily signaling pathway. *Wiley Interdiscip Rev Dev Biol*, 2(1), 47-63. doi:10.1002/wdev.86
- Wilkes, M. C., Mitchell, H., Penheiter, S. G., Dore, J. J., Suzuki, K., Edens, M., . . . Leof, E. B. (2005). Transforming growth factor-beta activation of phosphatidylinositol 3-kinase is independent of Smad2 and Smad3 and regulates fibroblast responses via p21-activated kinase-2. *Cancer Res*, 65(22), 10431-10440. doi:10.1158/0008-5472.CAN-05-1522
- Xie, L., Law, B. K., Chytil, A. M., Brown, K. A., Aakre, M. E., & Moses, H. L. (2004). Activation of the Erk pathway is required for TGF-beta1-induced EMT in vitro. *Neoplasia*, 6(5), 603-610. doi:10.1593/neo.04241
- Yamada, Y., Nomura, N., Yamada, K., Matsuo, M., Suzuki, Y., Sameshima, K., . . . Wakamatsu, N. (2014). The spectrum of ZEB2 mutations causing the Mowat-Wilson syndrome in Japanese populations. *Am J Med Genet A*, 164A(8), 1899-1908. doi:10.1002/ajmg.a.36551
- Yang, L., Roh, Y. S., Song, J., Zhang, B., Liu, C., Loomba, R., & Seki, E. (2014). Transforming growth factor beta signaling in hepatocytes participates in steatohepatitis through regulation of cell death and lipid metabolism in mice. *Hepatology*, 59(2), 483-495. doi:10.1002/hep.26698
- Yi, K., Kim, H., Chung, Y., Ahn, H., Sim, J., Wi, Y. C., . . . Oh, Y. H. (2016). Clinicopathologic Correlations of E-cadherin and Prrx-1 Expression Loss in Hepatocellular Carcinoma. *J Pathol Transl Med*, 50(5), 327-336. doi:10.4132/jptm.2016.06.22
- Yue, J., & Mulder, K. M. (2001). Transforming growth factor-beta signal transduction in epithelial cells. *Pharmacol Ther*, 91(1), 1-34. doi:10.1016/s0163-7258(01)00143-7
- Yuzugullu, H., Benhaj, K., Ozturk, N., Senturk, S., Celik, E., Toyly, A., . . . Ozturk, M. (2009). Canonical Wnt signaling is antagonized by noncanonical Wnt5a in hepatocellular carcinoma cells. *Mol Cancer*, 8, 90. doi:10.1186/1476-4598-8-90

- Zaidi, N., Lupien, L., Kuemmerle, N. B., Kinlaw, W. B., Swinnen, J. V., & Smans, K. (2013). Lipogenesis and lipolysis: the pathways exploited by the cancer cells to acquire fatty acids. *Prog Lipid Res*, 52(4), 585-589. doi:10.1016/j.plipres.2013.08.005
- Zhao, W., Prijic, S., Urban, B. C., Tisza, M. J., Zuo, Y., Li, L., . . . Chang, J. T. (2016). Candidate Antimetastasis Drugs Suppress the Metastatic Capacity of Breast Cancer Cells by Reducing Membrane Fluidity. *Cancer Res*, 76(7), 2037-2049. doi:10.1158/0008-5472.CAN-15-1970
- Zucman-Rossi, J., Villanueva, A., Nault, J. C., & Llovet, J. M. (2015). Genetic Landscape and Biomarkers of Hepatocellular Carcinoma. *Gastroenterology*, 149(5), 1226-1239 e1224. doi:10.1053/j.gastro.2015.05.061

8 RESUME

Personal Information

Name: Weronika Piorońska
Date of birth: 27.05.1992
Nationality: Polish
Place of birth: Kościan, Poland

Education

Since December 2016 Doctoral student, Department of Medicine II, Section Molecular Hepatology, Medical Faculty Mannheim, University of Heidelberg, Germany

October 2014 - July 2016 Master's degree (MSc), Molecular Biology – Department of Biology, Adam Mickiewicz University in Poznań, Poland;

Master thesis: The influence of amine derivatives of purine alkaloids on human erythrocytes *in vitro*

October 2011 - July 2014 Bachelor's degree (BSc), Experimental biology – Department of Biology, Adam Mickiewicz University in Poznań, Poland;

Bachelor thesis: Erythrocytes as model cells in studies of the biological activity of chemical compounds used in biology and medicine

Publications

1. **Piorońska W**, Nwosu ZC, Han M, Büttner M, Ebert MP, Dooley S, Meyer C. Dysregulated *Paired related homeobox 1* impacts on hepatocellular carcinoma phenotypes (*Research Article – in revision*)
2. Nwosu ZC, **Piorońska W**, Battello N, Zimmer AD, Dewidar B, Han M, Pereira S, Blagojevic B, Castven D, Charlestin V, Holenya P, Lothead J, De La Torre C, Gretz N, Sajjakulnukit P, Zhang L, Ward MH, Marquardt JU, di Magliano MP, Lyssiotis CA, Sleeman J, Wöfl S, Ebert MP, Meyer C, Hofmann U, Dooley S.

Severe metabolic alterations in liver cancer lead to ERK pathway activation and drug resistance. *EBioMedicine*. 2020 Apr 21;54:102699.

3. Han M, **Piorońska W**, Wang S, Nwosu ZC, Sticht C, Wang S, Gao Y, Ebert MP, Dooley S, Meyer C. Hepatocyte caveolin-1 modulates metabolic gene profiles and functions in non-alcoholic fatty liver disease. *Cell Death Dis*. 2020 Feb 6;11(2):104
4. Han M, Nwosu ZC, **Piorońska W**, Ebert MP, Dooley S, Meyer C. Caveolin-1 Impacts on TGF- β Regulation of Metabolic Gene Signatures in Hepatocytes. *Front Physiol*. 2020 Jan 31;10:1606.
5. Nwosu ZC, Battello N, Rothley M, **Piorońska W**, Sitek B, Ebert MP, Hofmann U, Sleeman J, Wöfl S, Meyer C, Megger DA, Dooley S. Liver cancer cell lines distinctly mimic the metabolic gene expression pattern of the corresponding human tumours. *J Exp Clin Cancer Res*. 2018 Sep 3;37(1):211
6. Jasiewicz B, Sierakowska A, Jankowski W, Hoffmann M, **Piorońska W**, Górnicka A, Bielawska A, Bielawski K, Mrówczyńska L. Antioxidant and cytotoxic activity of new di- and polyamine caffeine analogues. *Free Radic Res*. 2018 Jun; 52(6): 724-736

Abstracts in scientific conference proceedings

1. **Piorońska W**, Nwosu ZC, Han M, Ebert MP, Dooley S, Meyer C: *PRRX1* as mediator of TGF β effects in HCC. Workshop: Primary Liver Cancer – Emerging Concepts and Novel Treatments FALK 2020, 13-14 February 2020, Mainz, Germany (**Poster of distinction**)
2. Li Y, Ayvaz S, **Piorońska W**, Meyer C, Nwosu ZC, Fan W, Dooley S: Decreased ECM1 expression is consistent in HCC and correlates with overall survival. Workshop: Primary Liver Cancer – Emerging Concepts and Novel Treatments FALK 2020, 13-14 February 2020, Mainz, Germany

3. **Piorońska W**, Nwosu ZC, Ebert MP, Dooley S, Meyer C: PRRX1 cooperate with ZEB1/ZEB2 in hepatocellular carcinoma. *Z Gastroenterol* 2019; 57(01): e68 GASL 2019, 22 - 23 February 2019, Heidelberg, Germany
4. Nwosu ZC, **Piorońska W**, Ebert MP, Meyer C, Dooley S: Glutamine deprivation link impaired metabolism to ERK pathway activation and drug resistance in liver cancer. *Z Gastroenterol* 2019; 57(01): e49 GASL 2019, 22 - 23 February 2019, Heidelberg, Germany
5. **Piorońska W**, Nwosu ZC, Ebert MP, Dooley S, Meyer C: Expression and functions of PRRX1 in hepatocellular carcinoma. *Z Gastroenterol* 2018; 56(08): 309 – 309 DGVS 2018, 12 - 15 September, Munich, Germany
6. Han M, Nwosu Z, **Pioronska W**, Ebert M, Dooley S, Meyer C: Hepatocyte-specific caveolin-1 in non-alcoholic steatohepatitis mouse model. EASL NAFLD Summit 2018, 20 - 22 September, Geneva, Switzerland
7. Nwosu ZC, **Piorońska W**, Meyer C, Megger D, Dooley S: Liver cancer cell lines distinctly reflect the metabolic gene expression pattern observed in clinical microarrays. EASL HCC Summit 2018, 01 - 03 March, Geneva, Switzerland

Research grant

7.900€ from “The Foundations and Awards” 2020 of the Medical Faculty Heidelberg for the project: “Regulation of *PRRX1* expression in hepatocellular carcinoma”.

9 ACKNOWLEDGEMENTS

I would not have been able to write and finish this thesis without the guidance, help and support of many kind people that I met over the course of this study.

I would like to thank Professor Dr. Steven Dooley for accepting me in his research group and his guidance to get the best out of my work. Without his mentorship and funding support, the completion of my thesis would not have been possible.

I will never forget and always appreciate opportunity that I got from Dr. Christoph Meyer to move here from Poland and work on this project. He got the funding from Wilhelm Sander Stiftung and backed me with trust and encouragement to work on this project. I am very grateful for his support, kindness, patience, and for vivid discussions.

I thank Dr. Mei Han for helping me during my first days in this group. I am also grateful for everything that Dr. Zeribe Nwosu taught me. I thank him for his 24/7 willingness to help to find solution for any scientific problem. I want to thank Dr. Sai Wang and Yujia Li for taking care and supporting me in the lab and outside lab anytime I encountered other personal issues. They two are like Angels. Moreover, I thank Kerry Gould and Vanessa Nalewaja for their help with organising the orders of needed stuff for this project, for their open ears and help in de-stressing by participating with me in Zumba evenings. I also want to say „thank you” to other people I met in the AG Dooley group during my work (Dr. Seddik Hammad, Dr. Anne Dropmann, Dr. Honglei Weng, Lin Tao, Rilü Feng, Yueni Li, George Gao, Sophie Alex, Verena Stephan, Monika Hurt, not to forget Dr. Yan Gao, Dr. Xiadong Yuan, Fernando Leonardi and Christof Dormann). You all helped to create a beautiful atmosphere for work in this lab.

I thank the staff of the Zentrum für Medizinische Forschung, Mannheim, for their support with glucose and lactate assay, and Dr. Michael Büttner at the Metabolomics Core, University of Heidelberg, for support with GC/MS-based metabolite analyses.

I would like to thank my polish friends (Marta Taberska, Hiacynta Światała and Ada Szypuła) for providing mental support and friendship even though we very rarely met in person. I also thank Adrian Solomon for believing in me and motivating me.

I thank my aunt Danuta Wyrzykiewicz for giving me a roof over my head, when I just started this project and recognized how difficult it is to find an apartment around.

I especially thank my lovely parents. My hard-working Mama Jolanta Piorońska and Tata Grzegorz Pioroński have sacrificed their comfort to give me the opportunity to educate the way I wished and provided unconditional love and care. I love them so much, and I would not have made it this far without them and their support.